

NASA CR-163, 627

JPL PUBLICATION 80-58



NASA-CR-163627  
19800024940

# Analytic Theory of Orbit Contraction and Ballistic Entry Into Planetary Atmospheres

James Michael Longuski  
Jet Propulsion Laboratory

Nguyen Xuan Vinh  
The University of Michigan

September 1, 1980

SEP 1 1980

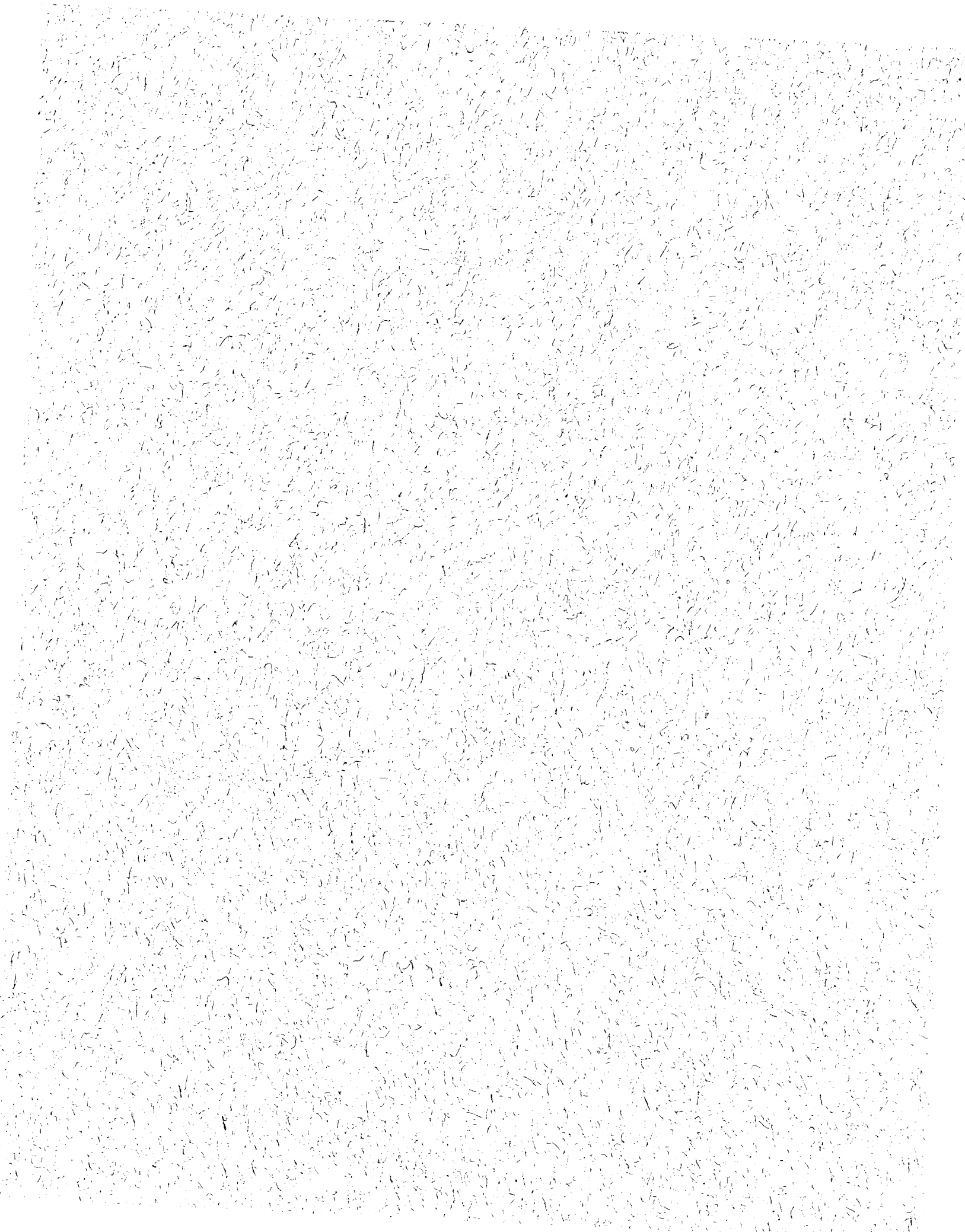
OCT 29 1980

Prepared for  
**Langley Research Center**  
Hampton, Virginia  
by  
**Jet Propulsion Laboratory**  
California Institute of Technology  
Pasadena, California

LANGLEY RESEARCH CENTER  
LIBRARY, NASA  
HAMPTON, VIRGINIA



NF01965



JPL PUBLICATION 80-58

# Analytic Theory of Orbit Contraction and Ballistic Entry Into Planetary Atmospheres

James Michael Longuski  
Jet Propulsion Laboratory

Nguyen Xuan Vinh  
The University of Michigan

September 1, 1980

Prepared for  
**Langley Research Center**  
Hampton, Virginia  
by  
**Jet Propulsion Laboratory**  
California Institute of Technology  
Pasadena, California

N80-33448#

The research described in this publication was carried out at The University of Michigan, and was partially funded under NASA Grant NSG 1448.

## LIST OF MAIN DEFINITIONS

The notation for orbital elements is standard. Figure 2-1 presents the nomenclature of the coordinate system. In addition, the following are the main definitions used:

### Contraction of Orbit

$$x = \beta ae = ae/H = \text{semi-major axis} \times \text{eccentricity/scale height}$$

$$z = a/a_o = \text{ratio of semi-major axis to initial semi-major axis}$$

### Ballistic Entry

$$\left. \begin{aligned} Z &= \frac{\rho S C_D}{2m} \sqrt{\frac{r}{\beta}} \\ u &= V^2 \cos^2 \gamma / gr \end{aligned} \right\} \text{Modified Chapman Variables}$$

$$v = V^2 / gr = \text{dimensionless velocity squared}$$

$$Y = 2Z$$

$$\Phi = -\sqrt{\beta r} \sin \gamma$$

$$X = -\text{Log } v$$

$$\bar{Y} = 2Z / \sqrt{\beta r}$$

$$\bar{\Phi} = -\sin \gamma$$

$$\eta = -2Z / \sqrt{\beta r} \sin \gamma_i$$

$$\bar{S} = \sin \gamma_i / \sin \gamma$$

$$\bar{v}_i = v_i e^{\eta_i}$$

where

$\rho$  = atmospheric density

$S$  = reference surface area of space vehicle

$C_D$  = drag coefficient of space vehicle

$m$  = mass of space vehicle

$r$  = radial distance from center of planet to space vehicle

$\beta$  =  $1/H$  = inverse scale height of atmosphere

$V$  = absolute velocity of space vehicle

$\gamma$  = flight path angle

$g$  = gravitational acceleration at radial distance  $r$

## ABSTRACT

A space object traveling through an atmosphere is governed by two forces: aerodynamic and gravitational. On this premise, equations of motion are derived to provide a set of universal entry equations applicable to all regimes of atmospheric flight from orbital motion under the dissipative force of drag through the dynamic phase of reentry, and finally to the point of contact with the planetary surface.

Rigorous mathematical techniques, such as averaging, Poincaré's method of small parameters, and Lagrange's expansion, are applied to obtain a highly accurate, purely analytic theory for orbit contraction and ballistic entry into planetary atmospheres.

The theory has a wide range of applications to modern problems including orbit decay of artificial satellites, atmospheric capture of planetary probes, atmospheric grazing, and ballistic reentry of manned and unmanned space vehicles.



## CONTENTS

### CHAPTER

1. INTRODUCTION . . . . .	1
2. THE UNIVERSAL EQUATIONS FOR ORBIT DECAY AND REENTRY . . . . .	6
2.1 Forces on a Satellite in Orbit . . . . .	6
2.2 The Universal Equations of Motion . . . . .	9
2.3 Satellite Motion in a Rotating Atmosphere . . . . .	11
3. THE VARIATIONAL EQUATIONS FOR ORBIT CONTRACTION . . . . .	18
3.1 The Osculating Orbit . . . . .	18
3.2 The Variational Equations . . . . .	20
4. THE THEORY OF ORBIT DECAY . . . . .	24
4.1 The Average Equations for Orbit Decay . . . . .	24
4.2 The Basic Equation for Orbit Contraction . . . . .	27
4.3 Integration by Poincaré's Method of Small Parameters . . . . .	31
4.4 The Parametric Solution of the Orbital Elements . . . . .	38
4.5 Explicit Formulas for the Orbital Elements . . . . .	40
4.6 The Contraction of Highly Eccentric Orbits . . . . .	46
4.7 The Contraction of Nearly Circular Orbits . . . . .	49
4.8 The Contraction of Circular Orbits . . . . .	50
4.9 The Orientation of the Orbit During Decay . . . . .	52

5. TIME IN ORBIT . . . . .	70
5.1 The Time Equation . . . . .	70
5.2 Integration of the Time Equation . . . . .	72
5.3 Approximate Integration of the Unknown Integrals . . . . .	74
6. BALLISTIC ENTRY . . . . .	82
6.1 The Ballistic Entry Equations . . . . .	82
6.2 Entry from Circular Orbit . . . . .	86
6.3 Entry from Nearly Circular Orbits . . . . .	94
6.4 Ballistic Entry at Moderate and Large Initial Flight Path Angles . . . . .	103
6.5 Applications of the Ballistic Entry Theories . . . . .	114
7. CONCLUSIONS AND RECOMMENDATIONS . . . . .	126
REFERENCES . . . . .	131

## LIST OF FIGURES

2-1	Nomenclature . . . . .	16
2-2	Aerodynamic Forces . . . . .	17
4-1	Variations of $z$ as Function of $x/x_0$ . . . . .	58
4-2	Variations of $(r_{p_0} - r_p)/H$ as Function of $x/x_0$ . . . . .	59
4-3	Variations of $(r_{a_0} - r_a)/H$ as Function of $x/x_0$ . . . . .	60
4-4	Variations of $r_p/r_{p_0}$ as Function of $x/x_0$ . . . . .	61
4-5	Variations of $r_a/r_{a_0}$ as Function of $x/x_0$ . . . . .	62
4-6	Variations of $T/T_0$ as Function of $x/x_0$ . . . . .	63
4-7	Variations of $z$ as Function of $e$ . . . . .	64
4-8	Variations of $(r_{p_0} - r_p)/H$ as Function of $e$ . . . . .	65
4-9	Variations of $(r_{a_0} - r_a)/H$ as Function of $e$ . . . . .	66
4-10	Variations of $r_p/r_{p_0}$ as Function of $e$ . . . . .	67
4-11	Variations of $r_a/r_{a_0}$ as Function of $e$ . . . . .	68
4-12	Variations of $T/T_0$ as Function of $e$ . . . . .	69
6-1	Variations of $G$ 's as Function of $v$ . . . . .	120
6-2	Variations of $-\gamma$ as Function of $v$ . . . . .	121
6-3	Variations of $\text{Log}(Z/Z_0)$ as Function of $v$ . . . . .	122
6-4	Variations of $G$ 's as Function of $v$ . . . . .	123
6-5	Variations of $-\gamma$ as Function of $v$ . . . . .	124
6-6	Variations of $\text{Log}(Z/Z_0)$ as Function of $v$ . . . . .	125



## CHAPTER 1

### INTRODUCTION

Since earliest recorded times man has always been fascinated by the motions of objects in the sky. This natural curiosity resulted in the development of astronomy as the first science which in turn acted as a catalyst for the advancement of mathematics. Many of the classical scholars such as Ptolemy, Copernicus, Kepler and Newton were both astronomers and mathematicians, and all of them made important contributions to a field now known as celestial mechanics.

Although Newton foresaw the possibility of artificial satellites and even computed the decay due to a resisting medium, it has only been in recent times that man has had sufficient knowledge of the atmosphere to develop adequate theories of satellites in low orbits. With empirical data from the first artificial satellites, King-Hele (1964) was able to publish a monograph presenting a large step in sophistication of analytic theories. He, and others, were primarily interested in applying classical celestial mechanics techniques in studying the slowly varying orbital elements of the osculating orbit, under the perturbation of atmospheric drag. Since the original

artificial satellites were not intended for recovery, the researchers confined their theories to the prediction of the satellite's orbital motion until its eventual burn-up in the Earth's atmosphere.

With the advent of manned space exploration and recoverable space probes, it became necessary to develop accurate theories of the entry phase, during which the altitude, velocity, deceleration, and the heating rate all vary rapidly. Space dynamicists such as Chapman, Loh and Yaroshevskii produced analytic theories to describe the reentry of ballistic and lifting spacecraft. In these analyses strong physical assumptions were made and soon the equations of the reentry scientists became very different from those of the celestial mechanics scholars.

At the University of Michigan the theories of King-Hele, Chapman, Loh and Yaroshevskii have been reviewed with an aim of achieving greater generality and flexibility in application. Vinh and Brace (1974) removed Chapman's restrictive assumptions by introducing modified Chapman variables which can be applied to three dimensional entry trajectories. Since the problem of orbit decay and the problem of reentry deal with the same physical phenomenon, namely, flight of a space object in an atmosphere, they must obey the same equations. Vinh, Busemann and Culp (1975) developed the set of exact universal entry equations

applicable to spacecraft in all regimes of flight from orbital motion, entry phase, glide and touchdown. The theses of Brace (1974) and Bletsos (1976) clearly demonstrate the superiority of the more general approaches. The purpose of this report is to illustrate the application of the universal entry equations to orbit decay, as well as ballistic entry into a planetary atmosphere and to present rigorous mathematical analyses of the resulting math models. In order to provide a firm foundation the simplest cases were assumed in the math model: exponential atmosphere, constant  $\beta$  or  $\beta r$ , and spherical rotating planet. However, the techniques can be extended to include the effects of varying scale height and oblate atmosphere. The report is organized into chapters as follows.

In Chapter 2 the universal entry equations are derived from aerodynamic equations of motion. Next, the perturbation equations for satellite motion in a rotating atmosphere are deduced from the universal equations. Then, in Chapter 3, the variational equations for orbit decay are derived by applying the averaging technique to the perturbation equations. The solutions of these equations are presented in Chapter 4 as the theory of orbit decay. Poincaré's method of small parameters is applied to the basic nonlinear first order differential equation for contraction of orbits of small and moderate eccentricity and exact solutions are obtained for the first

five order terms to find the semi-major axis and eccentricity in parametric form. Lagrange's expansion is used to obtain the semi-major axis as a function of eccentricity. For highly eccentric orbits, the governing differential equation is derived directly from the basic equation and solved in closed form parametrically. First order solutions are found for the other orbital elements, giving the orientation of the orbit. Solutions are also derived for circular and nearly circular orbits. For the main effect of orbit contraction, a uniformly valid, mathematically rigorous theory for all eccentricities,  $0 < e < 1$ , is presented.

In Chapter 5 the problem of time in orbit is considered. Difficulties arise in obtaining exact integrals, but an approximate method gives excellent numerical results. The time solution is used for the time at any point during the orbit decay, as well as for the maximum lifetime of the satellite for the assumed atmospheric model.

In Chapter 6 a higher order theory for ballistic entry is developed by applying Poincaré's method to a system of nonlinear differential equations. The problem is divided into three separate cases: entry from circular orbit, entry at small initial flight path angles and entry at moderate and large flight path angles. The second order solution of the first case gives a significant improvement over

the Yaroshevskii solution which enters as the zero order term.

Similarly, the solution to the third case shows marked improvement over the classical solution of Chapman, again entering as the zero order term. The second case bridges the gap between the first and third cases and provides adequate numerical results.

In Chapter 7 conclusions are drawn and recommendations for future research are made.

CHAPTER 2  
THE UNIVERSAL EQUATIONS FOR ORBIT DECAY  
AND REENTRY

2.1 Forces on a Satellite in Orbit

Only two forces will be considered to effect the motion of a space object in an atmosphere: gravitational and aerodynamic. It is assumed that the planet is spherical with uniform mass distribution, so that the gravitational force is an inverse square force of attraction with acceleration

$$g(r) = \frac{\mu}{r^2} \quad (2-1)$$

where  $r$  is the radial distance from the center of the planet and  $\mu$  is a positive constant which, for two-body relative motion is  $G(M+m)$  where  $G$  is Newton's universal gravitational constant,  $M$  is the mass of the planet and  $m$  is the mass of the spacecraft. The atmospheric force is in the form of drag,  $D_A$ , which acts in a direction opposite to the velocity  $\vec{V}_A$  relative to the ambient air

$$D_A = \frac{1}{2} \rho S C_D V_A^2 \quad (2-2)$$

where  $C_D$  is the drag coefficient for a reference area  $S$  and  $\rho$  is the

atmospheric density. The atmospheric density is assumed to vary exponentially with altitude

$$\rho = \rho_{p_0} e^{\beta(r_{p_0} - r)} \quad (2-3)$$

where  $\rho_{p_0}$  is the density at the initial periapsis,  $r_{p_0}$ , and  $\beta$  is a constant

$$\beta = \frac{1}{H} \quad (2-4)$$

where  $H$  is the scale height. For simplicity, it is assumed that there is no lift force.

These forces represent perhaps the most elementary of realistic models. The emphasis will be to provide a pure mathematical treatment of the orbit decay problem which will serve as a firm foundation for the development of more sophisticated solutions which include oblateness of the atmosphere and variation of scale height, as well as other important features.

The equations of motion are written with respect to an inertial reference frame with the origin at the center of the planet. In Fig. 2-1,  $\vec{V}$  is the absolute velocity of the satellite

$$\vec{V} = \vec{V}_A + \vec{V}_e \quad (2-5)$$

where  $\vec{V}_e$  is the velocity at the point  $M$ , of the ambient air relative to the planet center. If  $\vec{\omega}$  is the angular velocity of the rotating

atmosphere, then

$$V_e = rw \cos \phi \quad (2-6)$$

where  $\phi$  is the latitude of the point M.

If  $\psi'$  is the angle between  $\vec{V}_e$  and  $\vec{V}$ , then by the cosine rule

$$V_A^2 = V^2 + V_e^2 - 2 V V_e \cos \psi' \quad (2-7)$$

The heading angle,  $\psi$ , is the angle between  $\vec{V}_e$  and the projection  $\vec{V}_H$  of  $\vec{V}$  on the horizontal plane and is related to the latitude  $\phi$  and the inclination  $i$  of the orbital plane by the well-known relation

$$\cos \psi \cos \phi = \cos i \quad (2-8)$$

The flight path angle,  $\gamma$ , is the angle between  $\vec{V}_H$  and  $\vec{V}$  and is related to  $\psi$  and  $\psi'$  by

$$\cos \psi' = \cos \psi \cos \gamma \quad (2-9)$$

Near periapsis, where the aerodynamic drag is most effective, the satellite travels in a nearly horizontal direction and hence  $\gamma$  is small, allowing the approximation

$$V_e \cos \psi' = V_e \cos \psi \cos \gamma \approx rw \cos \phi \cos \psi = rw \cos i \quad (2-10)$$

Substituting Eqs. (2-6) and (2-10) into Eq. (2-7) gives

$$V_A^2 = V^2 \left( 1 - \frac{2rw}{V} \cos i + \frac{r^2 w^2}{V^2} \cos \phi \right) \quad (2-11)$$

The rotation of the atmosphere is so slow that the term  $w^2$  can be

neglected. For the small term  $rw/V$ , it is appropriate to use an average value. King-Hele suggested using the average value at perigee  $r_{p_0}/V_{p_0}$  to replace  $r/V$ . Since the inclination  $i$  usually varies by less than  $0.3^\circ$  during a satellite's lifetime, it may be taken equal to its initial value  $i_0$ . The result is King-Hele's expression (King-Hele, 1964)

$$V_A^2 = f V^2 \quad (2-12)$$

with the slightly different average constant

$$f = \left( 1 - \frac{2r_{p_0} w}{V_{p_0}} \cos i_0 \right) \quad (2-13)$$

Thus, in terms of the absolute speed, the drag force is

$$D_A = \frac{1}{2} \rho S f C_D V^2 \quad (2-14)$$

which acts opposite to the direction of the velocity  $\vec{V}_A$  of the satellite relative to the ambient air.

## 2.2 The Universal Equations of Motion

For the flight of an aerodynamic vehicle in a nonrotating atmosphere with a lift coefficient  $C_L$  and a drag coefficient  $C_D$ , it is customary to use the equations of motion with the notation of Fig. 2-1.

$$\begin{aligned}
\frac{dr}{dt} &= V \sin \gamma \\
\frac{d\theta}{dt} &= \frac{V \cos \gamma \cos \psi}{r \cos \phi} \\
\frac{d\phi}{dt} &= \frac{V \cos \gamma \sin \psi}{r} \\
\frac{dV}{dt} &= - \frac{\rho S C_D V^2}{2m} - g \sin \gamma \\
V \frac{d\gamma}{dt} &= \frac{\rho S C_L V^2 \cos \sigma}{2m} - \left( g - \frac{V^2}{r} \right) \cos \gamma \\
V \frac{d\psi}{dt} &= \frac{\rho S C_L V^2 \sin \sigma}{2m \cos \gamma} - \frac{V^2}{r} \cos \gamma \cos \psi \tan \phi
\end{aligned} \tag{2-15}$$

where the bank angle  $\sigma$  is defined as the angle between the local vertical plane containing the velocity and the plane containing the velocity and the aerodynamic force.

Using the modified Chapman variables

$$\begin{aligned}
u &= \frac{V^2 \cos^2 \gamma}{gr} \\
Z &= \frac{\rho S C_D}{2m} \sqrt{\frac{r}{\beta}}
\end{aligned} \tag{2-16}$$

and the dimensionless independent variable

$$s = \int_0^t \left( \frac{V}{r} \right) \cos \gamma dt \tag{2-17}$$

the exact universal equations for entry trajectories into a planetary

atmosphere assumed to be at rest are derived (Vinh et al., 1975)

$$\begin{aligned}
 \frac{dZ}{ds} &= -\beta r \left( -\frac{1}{\beta \rho} \frac{d\rho}{dr} - \frac{1}{2\beta r} + \frac{1}{2\beta^2} \frac{d\beta}{dr} \right) Z \tan \gamma \\
 \frac{du}{ds} &= -\frac{2\sqrt{\beta r} Zu}{\cos \gamma} \left( 1 + \frac{C_L}{C_D} \cos \sigma \tan \gamma + \frac{\sin \gamma}{2\sqrt{\beta r} Z} \right) \\
 \frac{d\gamma}{ds} &= \frac{\sqrt{\beta r} Z}{\cos \gamma} \left[ \frac{C_L}{C_D} \cos \sigma + \frac{\cos \gamma}{\sqrt{\beta r} Z} \left( 1 - \frac{\cos^2 \gamma}{u} \right) \right] \\
 \frac{d\theta}{ds} &= \frac{\cos \psi}{\cos \phi} \\
 \frac{d\phi}{ds} &= \sin \psi \\
 \frac{d\psi}{ds} &= \frac{\sqrt{\beta r} Z}{\cos^2 \gamma} \left( \frac{C_L}{C_D} \sin \sigma - \frac{\cos^2 \gamma \cos \psi \tan \phi}{\sqrt{\beta r} Z} \right).
 \end{aligned} \tag{2-18}$$

### 2.3 Satellite Motion in a Rotating Atmosphere

Next, the universal entry equations will be transformed to obtain the equations for satellite motion inside a rotating atmosphere.

Using the following relations from spherical trigonometry

$$\begin{aligned}
 \cos \phi \cos \psi &= \cos i \\
 \cos \phi \sin \psi &= \sin i \cos \alpha \\
 \cos \alpha &= \cos \phi \cos (\theta - \Omega)
 \end{aligned} \tag{2-19}$$

the last three equations of (2-18) are transformed to

$$\begin{aligned}
\frac{d\alpha}{ds} &= 1 - \frac{\sqrt{\beta r} Z \sin \alpha}{\tan i \cos^2 \gamma} \left( \frac{C_L}{C_D} \right) \sin \sigma \\
\frac{d\Omega}{ds} &= \frac{\sqrt{\beta r} Z \sin \alpha}{\sin i \cos^2 \gamma} \left( \frac{C_L}{C_D} \right) \sin \sigma \\
\frac{di}{ds} &= \frac{\sqrt{\beta r} Z \cos \alpha}{\cos^2 \gamma} \left( \frac{C_L}{C_D} \right) \sin \sigma
\end{aligned} \tag{2-20}$$

where  $\Omega$  is the longitude of the ascending node of the osculating plane and  $\alpha$  is the angle between the ascending node and the position vector.

For satellite motion in a rotating atmosphere there is a complication in that the drag force is modified by the factor  $f$  and is directed opposite to the velocity  $\vec{V}_A$ , not the absolute velocity  $\vec{V}$ . At the same time there is the simplification of no lift.

In Fig. (2-2) the aerodynamic force diagram used in deriving the equations of motion (2-15) is illustrated. In addition the velocity  $\vec{V}_A$  with respect to the ambient air, and the drag force  $\vec{D}_A$ , opposite in direction to  $\vec{V}_A$  are shown. For the present derivation the lift force  $\vec{L}$  is removed and the vector drag  $\vec{D}$  is replaced by  $\vec{D}_A$ . The force  $\vec{D}_A$  can be decomposed into one component in the orbital plane and one component normal to the orbital plane. Since  $\vec{V}_e$  is small,  $\vec{V}_A$  is nearly aligned to  $\vec{V}$  and the drag component in the orbital plane can be considered to be directly opposite to  $\vec{V}$ , with magnitude  $D_A$  as given by Eq. (2-14). The normal component

of the drag,  $\vec{D}_N$ , is found from the projection of

$$\vec{D}_A = -\frac{1}{2} \rho S f C_D V^2 \frac{\vec{V}_A}{V_A} \quad (2-21)$$

in the direction orthogonal to the orbital plane. Since  $\vec{V}$  is in the orbital plane and  $\vec{V} = \vec{V}_A + \vec{V}_e$ , the projection of  $\vec{V}_A$  on the normal to the orbital plane is the same as the projection of  $\vec{V}_e$  which has magnitude

$$\begin{aligned} V_e \sin \psi &= r w \cos \phi \sin \psi \\ &= r w \sin i \cos \alpha \end{aligned} \quad (2-22)$$

Thus, the vector  $\vec{D}_N$  has magnitude

$$D_N = \frac{1}{2} \rho S f C_D r w \sin i \cos \alpha \frac{V^2}{V_A} \quad (2-23)$$

From King-Hele's expression (2-12) it can be written as

$$D_N = \frac{\rho S f C_D V}{2f^{1/2}} r w \sin i \cos \alpha \quad (2-24)$$

and its direction is opposite to the vector  $L \sin \sigma$  in Fig. (2-2).

The final result of this analysis is that, in Eqs. (2-18) and (2-20) the  $C_D$  is replaced by the modified drag coefficient  $fC_D$ , the component  $C_L \cos \sigma$  is deleted and the component  $C_L \sin \sigma$  is replaced by

$$C_L \sin \sigma = -f^{1/2} C_D \left( \frac{r w}{V} \right) \sin i \cos \alpha \quad (2-25)$$

The modified Chapman variable  $Z$  is most effective in analyzing the entry phase of the vehicle. While the vehicle is still in orbit, it is used in the following form with constant  $\beta$

$$\sqrt{\beta r} Z = Z_o \left( \frac{r}{r_{p_o}} \right) e^{\beta (r_{p_o} - r)} \quad (2-26)$$

where the dimensionless constant  $Z_o$  is

$$Z_o = \frac{\rho_{p_o} S f C_D r_{p_o}}{2m} \quad (2-27)$$

Eqs. (18) and (19) are now rewritten introducing the equation for  $r/r_{p_o}$  to replace the equation for  $Z$ .

$$\frac{d}{ds} \left( \frac{r}{r_{p_o}} \right) = \left( \frac{r}{r_{p_o}} \right) \tan \gamma$$

$$\frac{du}{ds} = -u \tan \gamma - \frac{2 Z_o u}{\cos \gamma} \left( \frac{r}{r_{p_o}} \right) e^{\beta (r_{p_o} - r)}$$

$$\frac{d\gamma}{ds} = 1 - \frac{\cos^2 \gamma}{u}$$

$$\frac{d\alpha}{ds} = 1 + \frac{r_{p_o} w Z_o}{\sqrt{\mu f / r_{p_o}}} \left( \frac{r}{r_{p_o}} \right)^{5/2} \frac{\cos i \sin \alpha \cos \alpha}{u^{1/2} \cos \gamma} e^{\beta (r_{p_o} - r)}$$

$$\frac{d\Omega}{ds} = - \frac{r_{p_o} w Z_o}{\sqrt{\mu f / r_{p_o}}} \left( \frac{r}{r_{p_o}} \right)^{5/2} \frac{\sin \alpha \cos \alpha}{u^{1/2} \cos \gamma} e^{\beta (r_{p_o} - r)}$$

$$\frac{di}{ds} = - \frac{r_{p_o} w Z_o}{\sqrt{\mu f / r_{p_o}}} \left( \frac{r}{r_{p_o}} \right)^{5/2} \frac{\sin i \cos^2 \alpha}{u^{1/2} \cos \gamma} e^{\beta (r_{p_o} - r)} \quad (2-28)$$

Eqs. (2-28) bridge the gap between the satellite theory and the entry theory. As a matter of fact, they can be used to follow the motion of a vehicle subject to gravitational force and drag force of a rotating planet for its entire life in orbit until the end of its entry and contact with the planetary surface. The accuracy depends on the readjustment, for each layer of the atmosphere, of the "constant value"  $\beta$ . These equations are most useful for analyzing the last few revolutions and the entry phase. In Chapter 3 the entry variables  $r$ ,  $u$  and  $\gamma$  will be transformed into orbital elements and the variational equations of orbit decay will be derived.

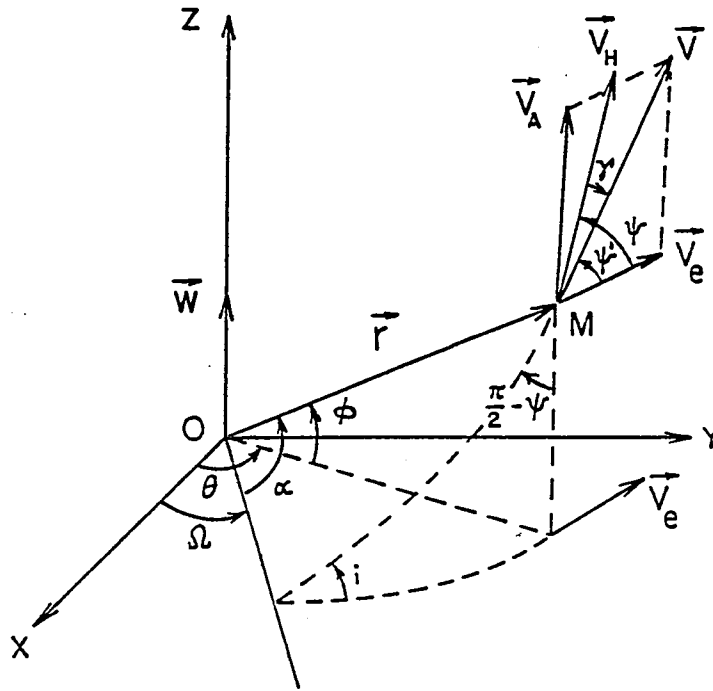


Fig. 2-1. Nomenclature.

The space vehicle  $M$  is located by the position vector  $\vec{r}$  and has absolute velocity  $\vec{V}$ .  $\vec{V}_H$  is the horizontal component of  $\vec{V}$  projected through the flight path angle  $\gamma$  while  $\vec{V}_A$  and  $\vec{V}_e$  are the velocity with respect to the ambient air and the absolute velocity of the atmosphere respectively.  $\vec{V}_H$  and  $\vec{V}_e$  are in the local horizontal plane and form an angle  $\psi$  which is called the heading angle.  $\theta$  and  $\phi$  are the longitude and latitude.  $\Omega$ , the longitude of the ascending node, and  $i$ , the inclination, are orbital elements of the osculating orbit.  $\vec{w}$  is the angular velocity of the atmosphere.

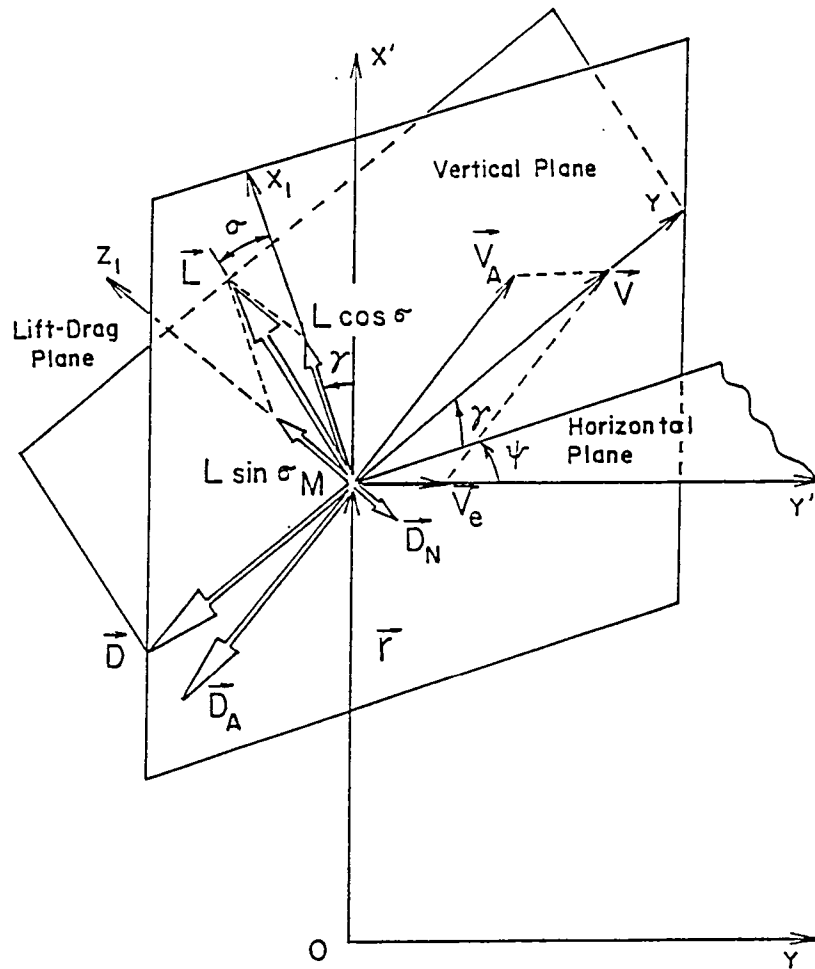


Fig. 2-2. Aerodynamic Forces.

In the derivation of the equations of motion for a rotating atmosphere, a lifting body with lift  $\vec{L}$ , bank angle  $\sigma$  and drag  $\vec{D}$  is compared with a nonlifting body with out of plane drag  $\vec{D}_A$ .

## CHAPTER 3

### THE VARIATIONAL EQUATIONS FOR ORBIT CONTRACTION

#### 3.1 The Osculating Orbit

The osculating orbit is the trajectory the vehicle would follow if the perturbing force (the drag) suddenly vanished. By setting  $Z_o = 0$  in Eqs. (2-28), the equations for the osculating orbit are found.

$$\begin{aligned}\frac{d}{ds} \left( \frac{r}{r_{p_o}} \right) &= \left( \frac{r}{r_{p_o}} \right) \tan \gamma \\ \frac{du}{ds} &= -u \tan \gamma \\ \frac{d\gamma}{ds} &= 1 - \frac{\cos^2 \gamma}{u} \\ \frac{d\alpha}{ds} &= 1 \\ \frac{d\Omega}{ds} &= 0 \\ \frac{di}{ds} &= 0\end{aligned}\tag{3-1}$$

Dividing the first of Eqs. (3-1) by the second and integrating

$$r = \frac{C_2}{u}\tag{3-2}$$

By taking the derivative of the second equation in (3-1) ,

$$\frac{d^2 u}{ds^2} + u = 1 \quad (3-3)$$

which has the solution

$$u = 1 + C_7 \cos(s - C_3) \quad (3-4)$$

Substituting Eq. (3-4) back into the  $\frac{du}{ds}$  equation, it is easy to show that

$$\cos^2 \gamma = \frac{u^2}{2u + C_7^2 - 1} \quad (3-5)$$

Changing the indices of the constants, the general integration is as follows:

$$\begin{aligned} \cos^2 \gamma &= \frac{u^2}{2u - C_1} \\ r &= \frac{C_2}{u} \\ u &= 1 + \sqrt{1 - C_1} \cos(s - C_3) \\ s &= \alpha + C_4 \\ \Omega &= C_5 \\ i &= C_6 \end{aligned} \quad (3-6)$$

Actually there are only 5 constants since  $s$  is equivalent to  $\alpha$ . The sixth constant of integration is found from the time equation (2-17). The first three constants of integration can be evaluated by taking the origin of time at the instant of passage through the periapsis.

$$\begin{aligned}\cos^2 \gamma &= \frac{u^2}{2u - (1 - e^2)} \\ u &= 1 + e \cos (\alpha - \omega) \\ r &= \frac{a(1 - e^2)}{1 + e \cos (\alpha - \omega)}\end{aligned}\quad (3-7)$$

These transformation equations provide the relation of the entry variables  $r$ ,  $u$  and  $\gamma$  and the orbital elements  $a$ , the semi-major axis,  $e$ , the eccentricity, and  $\omega$ , the argument of the periapsis.

### 3.2 The Variational Equations

While the vehicle is in orbit,  $Z_o$  is small, acting as a perturbation, and so the orbital elements actually vary slowly. Thus, the variation equations, or perturbation equations, can be obtained from Eqs. (3-7) by taking the derivatives and assuming that  $a$ ,  $e$  and  $\omega$  are varying quantities. First, the derivatives are taken with respect to  $s$  to obtain:

$$\begin{aligned}\frac{de}{ds} &= \frac{2Z_o u^2}{e \cos^3 \gamma} \left( \frac{\cos^2 \gamma}{u} - 1 \right) \left( \frac{r}{r_{p_o}} \right) e^{\beta (r_{p_o} - r)} \\ \frac{da}{ds} &= \frac{-2Z_o a u^2}{(1 - e^2) \cos^3 \gamma} \left( \frac{r}{r_{p_o}} \right) e^{\beta (r_{p_o} - r)}\end{aligned}$$

$$\frac{d\alpha}{ds} - \frac{d\omega}{ds} = \frac{u \tan \gamma}{\sqrt{e^2 - (u-1)^2}} + \frac{2Z_o u}{\cos \gamma \sqrt{e^2 - (u-1)^2}} \left\{ 1 + \frac{u(u-1)}{e^2 \cos^2 \gamma} \left( \frac{\cos^2 \gamma}{u} - 1 \right) \right\} \left( \frac{r}{r_{p_o}} \right) e^{\beta (r_{p_o} - r)} \quad (3-8)$$

Along with the last three equations of (2-28) this provides all the derivatives with respect to  $s$ . It is interesting to note from the first of Eqs. (3-8) that the eccentricity does not decrease continuously under the influence of atmospheric drag, but while decreasing secularly, it oscillates between maximum and minimum values as the flight path angle passes through minimum and maximum values respectively during each orbital period.

Finally, the variational equations will be put in terms of the more familiar eccentric anomaly  $E$  as the independent variable.

Since

$$r = a(1 - e \cos E) \quad (3-9)$$

and

$$\frac{dr}{dE} = ae \sin E \quad (3-10)$$

The differential relation between  $s$  and  $E$  is

$$\begin{aligned} \frac{ds}{dE} &= \frac{dr}{dE} \frac{ds}{dr} = \frac{e \sin E}{(1 - e \cos E) \tan \gamma} \\ &= \frac{\sqrt{1 - e^2}}{1 - e \cos E} \end{aligned} \quad (3-11)$$

From Eqs. (2-28), (3-8) and (3-11) the variational equations are obtained.

$$\begin{aligned}
 \frac{de}{dE} &= -2Z_o(1-e^2) \frac{a}{r_{p_o}} \cos E \left( \frac{1+e \cos E}{1-e \cos E} \right)^{1/2} e^{\beta(r_{p_o}-r)} \\
 \frac{da}{dE} &= -2Z_o \frac{a^2}{r_{p_o}} \frac{(1+e \cos E)^{3/2}}{(1-e \cos E)^{1/2}} e^{\beta(r_{p_o}-r)} \\
 \frac{d\alpha}{dE} - \frac{d\omega}{dE} &= \frac{\sqrt{1-e^2}}{1-e \cos E} \left[ 1 + \frac{2Z_o}{e} \left( \frac{a}{r_{p_o}} \right) \sin E (1-e \cos E)^{1/2} \right. \\
 &\quad \left. \times (1+e \cos E)^{1/2} e^{\beta(r_{p_o}-r)} \right] \\
 \frac{d\Omega}{dE} &= - \frac{r_{p_o} w Z_o}{\sqrt{\mu f / r_{p_o}} \sqrt{1-e^2}} \left( \frac{a}{r_{p_o}} \right)^{5/2} (1-e \cos E)^{5/2} \\
 &\quad \times (1+e \cos E)^{1/2} \sin \alpha \cos \alpha e^{\beta(r_{p_o}-r)} \\
 \frac{di}{dE} &= - \frac{r_{p_o} w Z_o}{\sqrt{\mu f / r_{p_o}} \sqrt{1-e^2}} \left( \frac{a}{r_{p_o}} \right)^{5/2} (1-e \cos E)^{5/2} \\
 &\quad \times (1+e \cos E)^{1/2} \sin i \cos^2 \alpha e^{\beta(r_{p_o}-r)}
 \end{aligned} \tag{3-12}$$

The variational equations apply to the space vehicle for the entire lifetime in orbit from the initial eccentric orbit until circularization and the onset of reentry. In Chapter 4 mathematically rigorous

analytic techniques will be employed in order to solve the problem of  
of the orbit decay phase.

## CHAPTER 4

### THE THEORY OF ORBIT DECAY

#### 4.1 The Average Equations for Orbit Decay

The variational equations (3-12) exhibit both oscillatory or periodic behavior and slowly varying secular behavior. The focus of this chapter is to solve for the slowly varying orbital elements of the osculating orbit and to avoid the periodic terms. Fortunately there is a rigorous method, the averaging technique (Bogoliubov and Mitropolsky, 1961), which allows the periodic terms to be replaced by the average value and which converges to the correct analytic solution as the independent variable goes to infinity. This is precisely the situation in the decaying process in which the satellite makes thousands of orbits during its lifetime. The beauty of the technique is that it circumvents the problem of computing the trajectory for each orbit which can cause numerical integration schemes to diverge over the long integration intervals.

In the variational equations (3-12) the radial distance will be written as

$$\begin{aligned} r &= a(1 - e \cos E) \\ r_{P_0} &= a_0(1 - e_0) \end{aligned} \tag{4-1}$$

so that the exponential function

$$\exp [ \beta (r_{p_o} - r) ] = \exp [ \beta (a_o - a - a_o e_o) + \beta a e \cos E ] \quad (4-2)$$

where  $a_o$  and  $e_o$  are the initial semi-major axis and initial eccentricity respectively. To facilitate the theory a new dimensionless variable  $x$  will be used to replace  $e$ .

$$x = \beta a e \quad (4-3)$$

Differentiating Eq. (4-3) gives

$$\frac{dx}{dE} = - \frac{2Z_o \beta a^2}{r_{p_o}} (e + \cos E) \left( \frac{1 + e \cos E}{1 - e \cos E} \right)^{1/2} e^{1/2} \beta (r_{p_o} - r) \quad (4-4)$$

Now it is evident that the  $x$  varies like  $e$  since  $x$  passes through stationary values when  $\cos E = -e$ , but, on the average, decreases with time.

The purpose of introducing the new variable  $x$  becomes clear after considering the  $n^{\text{th}}$  order modified Bessel function,  $I_n(x)$ , of the first kind

$$I_n(x) = \frac{1}{2\pi} \int_0^{2\pi} \cos nE \exp(x \cos E) dE$$

along with the relation

$$0 = \frac{1}{2\pi} \int_0^{2\pi} \sin nE \exp(x \cos E) dE. \quad (4-5)$$

The average equations from Eqs. (3-12) are

$$\begin{aligned}
\frac{da}{dE} &= -2Z_o \frac{a^2}{r_{p_o}} \exp\left[\beta(a_o - a - a_o e_o)\right] \\
&\times \frac{1}{2\pi} \int_0^{2\pi} \frac{(1 + e \cos E)^{3/2}}{(1 - e \cos E)^{1/2}} \exp(x \cos E) dE \\
\frac{dx}{dE} &= -\frac{2Z_o \beta a^2}{r_{p_o}} \exp\left[\beta(a_o - a - a_o e_o)\right] \\
&\times \frac{1}{2\pi} \int_0^{2\pi} (e + \cos E) \left(\frac{1 + e \cos E}{1 - e \cos E}\right)^{1/2} \exp(x \cos E) dE \\
\frac{d\omega}{dE} &= 0 \\
\frac{d\Omega}{dE} &= \frac{-r_{p_o} w Z_o}{\sqrt{\mu f / r_{p_o}} \sqrt{1 - e^2}} \left(\frac{a}{r_{p_o}}\right)^{5/2} \exp\left[\beta(a_o - a - a_o e_o)\right] \\
&\times \frac{1}{2\pi} \int_0^{2\pi} \sin \alpha \cos \alpha (1 - e \cos E)^{5/2} (1 + e \cos E)^{1/2} \exp(x \cos E) dE \\
\frac{1}{\sin i} \frac{di}{dE} &= \frac{-r_{p_o} w Z_o}{\sqrt{\mu f / r_{p_o}} \sqrt{1 - e^2}} \left(\frac{a}{r_{p_o}}\right)^{5/2} \exp\left[\beta(a_o - a - a_o e_o)\right] \\
&\times \frac{1}{2\pi} \int_0^{2\pi} \cos^2 \alpha (1 - e \cos E)^{5/2} (1 + e \cos E)^{1/2} \exp(x \cos E) dE
\end{aligned} \tag{4-6}$$

After setting  $\omega = \omega_o$ , it is apparent that the average equations

can be written as power series in  $e$ , for small  $e$ , with Bessel Function coefficients as functions of the dimensionless variable  $x$ .

#### 4.2 The Basic Equation for Orbit Contraction

The most dramatic and important effect of the dissipative force of atmospheric drag on the satellite's orbital path is the reduction of both the semi-major axis and the eccentricity. In general, the orbit contracts from an initial elliptical orbit to a nearly circular orbit so that  $e$  and  $x$  approach zero in the final stages of the decay. At this time the satellite is in the last few orbits and entry is imminent. The main purpose of this chapter is to provide a rigorous mathematical treatment of the orbit contraction problem.

For small eccentricity, the integrand of the first equation of (4-6) can be expanded in a power series in  $e$  and integrated to obtain

$$\frac{da}{dE} = - \frac{2Z_o a^2}{r_{p_o}} \exp \left[ \beta (a_o - a - a_o e_o) \right] \left\{ I_o + 2eI_1 + \frac{3}{4} e^2 (I_o + I_2) \right. \\ \left. + \frac{e^3}{4} (3I_1 + I_3) + \frac{e^4}{64} (21I_o + 28I_2 + 7I_4) + 0(e^5) \right\} \quad (4-7)$$

Following the same procedure for the  $x$  equation

$$\begin{aligned}
\frac{dx}{dE} = & \frac{-2Z_o \beta a^2}{r_{p_o}} \exp \left[ \beta (a_o - a - a_o e_o) \right] \left\{ I_1 + \frac{1}{2} e (3I_o + I_2) \right. \\
& + \frac{e^2}{8} (11I_1 + I_3) + \frac{e^3}{16} (7I_o + 8I_2 + I_4) \\
& \left. + \frac{e^4}{128} (78I_1 + 31I_3 + 3I_5) + 0(e^5) \right\} .
\end{aligned} \tag{4-8}$$

Let

$$z = \frac{a}{a_o} \tag{4-9}$$

be the dimensionless semi-major axis. Dividing Eq. (4-7) by Eq. (4-8) and expanding the ratio in a power series

$$\begin{aligned}
\beta a_o \frac{dz}{dx} = & y_o + \frac{e}{2} (4 - 3y_o^2 - y_o y_2) + \frac{e^2}{8} \left[ 2y_o (3y_o + y_2)^2 - 29y_o - 2y_2 - y_o y_3 \right] \\
& + \frac{e^3}{16} \left[ -32 + 113y_o^2 + 38y_o y_2 - y_o y_4 + 2y_2^2 + 6y_o^2 y_3 + 2y_o y_2 y_3 \right. \\
& \quad \left. - 2y_o (3y_o + y_2)^3 \right] \\
& + \frac{e^4}{128} \left[ 8y_o (3y_o + y_2)^4 - 8(3y_o + y_2)^2 (9y_o + y_2) - 12y_o (3y_o + y_2)^2 (11 + y_3) \right. \\
& \quad + 2y_o (11 + y_3)^2 + 8y_o (3y_o + y_2) (7y_o + 8y_2 + y_4) + 16(3y_o + y_2) (19 + y_3) \\
& \quad \left. - 12(y_o + y_2) (11 + y_3) - y_o (78 + 31y_3 + 3y_5) - 2(35y_o + 36y_2 + y_4) \right] \\
& + 0(e^5)
\end{aligned} \tag{4-10}$$

where the ratios of Bessel functions have been defined as

$$y_n = \frac{I_n}{I_1}, \quad n \neq 1 \quad (4-11)$$

The Bessel functions satisfy the recurrence formula

$$I_{n-1}(x) - I_{n+1}(x) = \frac{2n}{x} I_n(x) \quad (4-12)$$

so that any  $y_n(x)$  can be expressed in terms of  $y_0(x)$  and  $x$ . For example,

$$\begin{aligned} y_2 &= y_0 - \frac{2}{x} \\ y_3 &= 1 + \frac{8}{x^2} - \frac{4}{x} y_0 \\ y_4 &= -\frac{8}{x} - \frac{48}{x^3} + y_0 + 24 \frac{y_0}{x} \\ y_5 &= 1 + \frac{72}{x^2} + \frac{384}{x^4} - \frac{12}{x} y_0 - \frac{192}{x^3} y_0. \end{aligned} \quad (4-13)$$

Putting the eccentricity,  $e$ , in terms of  $z$  and  $x$

$$e = \epsilon \frac{x}{z} \quad (4-14)$$

where

$$\epsilon = \frac{1}{\beta a_0} \quad (4-15)$$

is a small quantity of order  $10^{-2}$  or less.

Thus, from Eqs. (4-10) - (4-15) the basic equation for orbit contraction is derived

$$\begin{aligned}
\frac{dz}{dx} = & \epsilon y_0 + \epsilon^2 \frac{x}{z} \left( 2 - 2y_0^2 + \frac{y_0}{x} \right) \\
& + \epsilon^3 \frac{x^2}{2z^2} \left( -8y_0 - 7 \frac{y_0^2}{x} + 8y_0^3 + \frac{1}{x} \right) \\
& + \epsilon^4 \frac{x^3}{2z^3} \left( -4 + 20y_0^2 - 10 \frac{y_0}{x} + 4 \frac{y_0}{x^3} - 5 \frac{y_0^2}{x} + 20 \frac{y_0^3}{x} \right. \\
& \qquad \qquad \qquad \left. - 16y_0^4 + \frac{1}{2} \right) \\
& + \epsilon^5 \frac{x^4}{4z^4} \left( 32y_0 - 96y_0^3 + 82 \frac{y_0^2}{x} - \frac{6}{x} - 17 \frac{y_0}{x^2} + \frac{3}{x^3} - 24 \frac{y_0^2}{x^3} \right. \\
& \qquad \qquad \qquad \left. + 49 \frac{y_0^3}{x} - 16 \frac{y_0}{x^4} - 104 \frac{y_0^4}{x} + 64y_0^5 \right) + 0(\epsilon^6) .
\end{aligned}
\tag{4-16}$$

The basic equation is a nonlinear differential equation with varying coefficients. The true nature of the equation was not recognized by King-Hele, who worked with Eq. (4-10) to the order  $e^3$ . In the form of Eq. (4-16) it is appropriate to apply Poincaré's method of small parameters. Since the parameter  $\epsilon$  is very small, to a higher order in  $\epsilon$ , the solution of the basic equation can be considered to be the exact solution of Eq. (4-10) truncated to the order  $e^4$  included.

### 4.3 Integration by Poincaré's Method of Small Parameters

Poincaré's method for integration (Poincaré, 1960) of a nonlinear differential equation containing a small parameter is a rigorous mathematical technique, proven to be convergent for small values of the parameter  $\epsilon$ . It has been used extensively in analytic work in celestial mechanics (Moulton, 1920).

The method begins by assuming a solution of  $z$  in the form

$$z = z_0 + \epsilon z_1 + \epsilon^2 z_2 + \epsilon^3 z_3 + \epsilon^4 z_4 + \epsilon^5 z_5 + \dots \quad (4-17)$$

After substituting Eq. (4-17) into the basic equation, Eq. (4-16), and equating coefficients of like powers in  $\epsilon$ , the following differential equations are obtained

$$\frac{dz_0}{dx} = 0$$

$$\frac{dz_1}{dx} = y_0$$

$$\frac{dz_2}{dx} = \frac{x}{z_0} \left( 2 + \frac{y_0}{x} - 2y_0^2 \right)$$

$$\frac{dz_3}{dx} = -\frac{xz_1}{z_0^2} \left( 2 + \frac{y_0}{x} - 2y_0^2 \right) + \frac{x^2}{2z_0^2} \left( \frac{1}{x} - 8y_0 - 7\frac{y_0^2}{x} + 8y_0^3 \right)$$

$$\begin{aligned}
\frac{dz_4}{dx} &= -\frac{x^2 z_1}{z_0^3} \left( \frac{1}{x} - 8y_0 - 7\frac{y_0^2}{x} + 8y_0^3 \right) + \frac{x}{z_0} \left( 2 + \frac{y_0}{x} - 2y_0^2 \right) \left( \frac{z_1^2}{z_0^2} - \frac{z_2}{z_0} \right) \\
&\quad + \frac{x^3}{2z_0^3} \left( -4 + \frac{1}{x} + 20y_0^2 - 10\frac{y_0}{x} + 4\frac{y_0}{x^3} - 5\frac{y_0^2}{x^2} + 20\frac{y_0^3}{x} - 16y_0^4 \right) \\
\frac{dz_5}{dx} &= \frac{x}{z_0} \left( 2\frac{z_1 z_2}{z_0^2} - \frac{z_1^3}{z_0^3} - \frac{z_3}{z_0} \right) \left( 2 - 2y_0^2 + \frac{y_0}{x} \right) \\
&\quad + \frac{x^2}{z_0^2} \left( \frac{3}{2}\frac{z_1^2}{z_0^2} - \frac{z_2}{z_0} \right) \left( -8y_0 - 7\frac{y_0^2}{x} + 8y_0^3 + \frac{1}{x} \right) \\
&\quad - \frac{3x^3 z_1}{2z_0^4} \left( -4 + 20y_0^2 - 10\frac{y_0}{x} + 4\frac{y_0}{x^3} - 5\frac{y_0^2}{x^2} + 20\frac{y_0^3}{x} - 16y_0^4 \right. \\
&\quad \quad \left. + \frac{1}{x^2} \right) + \frac{x^4}{4z_0^4} \left( 32y_0 - 96y_0^3 + 82\frac{y_0^2}{x} - \frac{6}{x} + \frac{3}{x^3} \right. \\
&\quad \quad \left. - 17\frac{y_0}{x^2} - 24\frac{y_0^2}{x^3} + 49\frac{y_0^3}{x^2} - 16\frac{y_0}{x^4} - 104\frac{y_0^4}{x} + 64y_0^5 \right)
\end{aligned} \tag{4-18}$$

with the initial conditions

$$z_0(x_0) = 1, z_1(x_0) = z_2(x_0) = \dots = 0. \tag{4-19}$$

The success of Poincare's method is not guaranteed; it depends on whether the integration of Eqs. (4-18) can be put in terms of known

functions.

In analyzing Eqs. (4-18), an important recurrence formula was discovered which greatly facilitates the integrations.

$$\int p(x) y_o^{n+1} dx = -\frac{p(x)}{n} y_o^n + \int p(x) y_o^{n-1} dx + \int \left[ \frac{p(x)}{x} + \frac{p'(x)}{n} \right] y_o^n dx \quad (4-20)$$

where  $n \neq 0$  and  $p(x)$  is an arbitrary function. The formula is derived by using the well-known relation

$$x I_n'(x) + n I_n(x) = x I_{n-1}(x) \quad (4-21)$$

so that for  $n = 1$

$$y_o = \frac{I_1'}{I_1} + \frac{1}{x} \quad (4-22)$$

and for  $n = 0$

$$I_o' = I_1(x) \quad (4-23)$$

Therefore, if  $y_o = I_o/I_1$

$$y_o' = \frac{I_o'}{I_1} - \frac{I_o I_1'}{I_1^2} = 1 + \frac{y_o}{x} - y_o^2 \quad (4-24)$$

Now consider

$$\int p(x) d\left(\frac{y_o^n}{n}\right) = \frac{p(x)}{n} y_o^n - \int \frac{p'(x)}{n} y_o^n dx$$

or

$$\int p(x) y_0^{n-1} y_0' dx = \int p(x) y_0^{n-1} \left( 1 + \frac{y_0}{x} - y_0^2 \right) dx$$

$$= \frac{p(x)}{n} y_0^n - \int \frac{p'(x)}{n} y_0^n dx .$$

Rearranging the equation gives Eq. (4-20).

Eqs. (4-18) can now be integrated with the initial conditions (4-19). The solution for  $z_0$  is simply

$$z_0(x) = 1 \quad (4-25)$$

From Eq. (4-22),

$$z_1 = \text{Log} \frac{x I_1(x)}{x_0 I_1(x_0)} \quad (4-26)$$

Since  $z_0 = 1$ , the  $z_2$  equation becomes

$$\frac{dz_2}{dx} = 2x + y_0 - 2xy_0^2$$

Integrating

$$z_2 = x^2 + \text{Log} x I_1(x) - 2 \int xy_0^2 dx . \quad (4-27)$$

Applying the recurrence formula (4-20) with  $p(x) = x$  and  $n = 1$ ,

$$\int xy_0^2 dx = \frac{1}{2} x^2 - xy_0 + 2 \text{Log} x I_1(x) \quad (4-28)$$

so that  $z_2$  with the initial conditions is

$$z_2 = 2xy_0(x) - 2x_0y_0(x_0) - 3 \operatorname{Log} \frac{xI_1(x)}{x_0I_1(x_0)} \quad (4-29)$$

The solution of  $z_3$ ,  $z_4$  and  $z_5$  are obtained in the same manner, but the integrations are much more laborious. The  $z_1(x)$  can be expressed in terms of two functions

$$A(x) = x \frac{I_0(x)}{I_1(x)} = xy_0(x), \quad z_1(x) = \operatorname{Log} \frac{xI_1(x)}{x_0I_1(x_0)} \quad (4-30)$$

The final solution is

$$\begin{aligned} z_0(x) &= 1 \\ z_1(x) &= \operatorname{Log} \frac{xI_1(x)}{x_0I_1(x_0)} \\ z_2(x) &= 2(A-A_0) - 3z_1 \\ z_3(x) &= \frac{7}{2}(x^2 - x_0^2) - \frac{13}{2}(A-A_0) - 2(A^2 - A_0^2) + 13z_1 - 2Az_1 + \frac{3}{2}z_1^2 \\ z_4(x) &= -\frac{35}{2}(x^2 - x_0^2) + \frac{71}{2}(A-A_0) + 3(A^2 - A_0^2) + \frac{8}{3}(A^3 - A_0^3) \\ &\quad + 4A_0(A - A_0) - 2(x^2A - x_0^2A_0) \\ &\quad - (69 + 6A_0 + 7x^2 - 19A - 4A^2)z_1 - \frac{35}{2}z_1^2 \\ &\quad - z_1^3 + 2Az_1^2 \end{aligned}$$

$$\begin{aligned}
z_5(x) = & z_1^2(162+6A_o) + \frac{41}{2} z_1^3 + \frac{3}{4} z_1^4 \\
& + z_1(437 - \frac{21}{2} x_o^2 + \frac{143}{2} A_o + 6A_o^2) - 2z_1^3 A - 6z_1^2 A^2 \\
& - \frac{69}{2} z_1^2 A + \frac{21}{2} z_1^2 x^2 - 8A^3 z_1 - 21A^2 z_1 + 6x^2 A z_1 \\
& + A z_1 ( - \frac{343}{2} - 8A_o) + \frac{147}{2} x^2 z_1 \\
& + \frac{3}{4} (x^4 - x_o^4) + (14A_o + \frac{885}{8})(x^2 - x_o^2) \\
& + (7x_o^2 - 39A_o - 4A_o^2 - \frac{441}{2})(A - A_o) \\
& - \frac{23}{2} x^2 A + \frac{23}{2} x_o^2 A_o + (-\frac{97}{8} - 8A_o)(A^2 - A_o^2) \\
& + 4x^2 A^2 - 4x_o^2 A_o^2 + 2A^3 - 2A_o^3 - 4A^4 + 4A_o^4 \quad . \quad (4-31)
\end{aligned}$$

The semi-major axis of the orbit under contraction is given as a function of the parameter  $x$ .

$$\frac{a}{a_o} = 1 + \epsilon z_1(x) + \epsilon^2 z_2(x) + \epsilon^3 z_3(x) + \epsilon^4 z_4(x) + \epsilon^5 z_5(x) \quad (4-32)$$

The accuracy of this solution has been tested by numerically integrating the basic equation (4-16) and comparing with Eq. (4-32). The expansions used to obtain the basic nonlinear equation are only valid for small and moderate values of eccentricity. To be exact, expansions in elliptic motion apply to eccentricities which are less than

0.663. Above this value, the series are no longer absolutely convergent. However, in the accuracy test it was found that the analytic solution was always greater than the numerical integration with a maximum error of approximately  $\epsilon e_o^5 / 5(1 - e_o^2)$  for  $0.1 \leq e_o \leq 0.99$ . It is interesting to note that even as  $e_o \rightarrow 1$ , which is outside the region of strict mathematical validity, the maximum error is less than  $1/10 \beta r_{p_o}$  (of the order  $10^{-3}$ ). The reason for this extended range is that as  $e_o \rightarrow 1$ ,  $a_o \rightarrow \infty$  and the parameter  $\epsilon \rightarrow 0$ . This important result prompted investigation of the asymptotic expansion of the basic nonlinear equation and the development of a closed form theory for orbit contraction for large eccentricity which is presented in Section 4.6. For small values of eccentricity the solution is extremely accurate. For example, when  $e_o = 0.1$  and  $\epsilon = 0.008$ , Eqs. (4-31) and (4-32) provide 7 digits of accuracy, while for the same case King-Hele's heuristic solution gives only 4 digits of accuracy. Thus, the present solution provides a major improvement in that it is much more accurate and that it is uniformly valid for all eccentricities,  $(0 < e \leq e_o)$ .

#### 4.4 The Parametric Solution of the Orbital Elements

The solution for the semi-major axis is given as a function of  $x$  by Eqs. (4-32) and (4-31) and is plotted against  $x/x_0$  in Fig. (4-1). Initially the solution is nearly linear with the slope in the figure approximately equal to  $e_0$ , but near the end as  $x$  and  $e$  approach zero, it exhibits rapid decay. This explains the difficulty encountered by King-Hele and why he treated the problem in separate phases in his analytic integration.

The eccentricity can be recovered from Fig. (4-1) using

$$\frac{e}{e_0} = \frac{1}{z} \left( \frac{x}{x_0} \right) \quad . \quad (4-33)$$

From the parametric solutions of the semi-major axis  $a$  and the eccentricity  $e$  it is easy to find expressions for the periapsis, the apoapsis and the period.

The drop in scale height of the periapsis is obtained from

$$\frac{r_{P_0} - r_P}{H} = \beta \left[ r_{P_0} - a(1-e) \right] = \beta a_0 - \beta a_0 e_0 + \beta a e - \beta a_0 (1 + \epsilon z_1 + \dots)$$

or

$$\frac{r_{P_0} - r_P}{H} = (x - x_0) - (z_1 + \epsilon z_2 + \epsilon^2 z_3 + \epsilon^3 z_4 + \epsilon^4 z_5) \quad (4-34)$$

Similarly, the other quantities of interest can be written in parametric form.

The drop in scale height of the apoapsis is

$$\frac{r_{a_o} - r_a}{H} = x_o - x - (z_1 + \epsilon z_2 + \dots + \epsilon^4 z_5) \quad (4-35)$$

The ratio of periapsis to initial periapsis is

$$\frac{r_p}{r_{p_o}} = \frac{z - \epsilon x}{1 - e_o} \quad (4-36)$$

The ratio of apoapsis to initial apoapsis is

$$\frac{r_a}{r_{a_o}} = \frac{z + \epsilon x}{1 + e_o} \quad (4-37)$$

The orbital period is

$$\frac{T}{T_o} = \left( \frac{a}{a_o} \right)^{3/2} = z^{3/2}(x) \quad (4-38)$$

Eqs. (4-34) - (4-38) are plotted in Figs. (4-2) - (4-6) as functions of  $x/x_o$ . The parameters used are the initial eccentricity  $e_o$  and the initial periapsis distance  $r_{p_o}$ , or equivalently the dimensionless small parameter  $1/\beta r_{p_o}$ . Then

$$\epsilon = \frac{(1 - e_o)}{\beta r_{p_o}} \quad (4-39)$$

which tends toward zero as  $e_o \rightarrow 1$ . By using the three values

$\frac{1}{\beta r_{p_0}} = 0.005, 0.01 \text{ and } 0.02$ , a wide range of periapsis heights are covered. In making these figures reference was made to the dependency of the accuracy on the initial parameters  $e_0$  and  $\frac{1}{\beta r_{p_0}}$  as mentioned in the previous section. The figures are plotted only for those values which provide imperceptible deviation from the exact solution.

#### 4.5 Explicit Formulas for the Orbital Elements

The solutions for the orbital elements have been obtained in parametric form, as functions of  $x$  in the previous section. In this section the elements will be obtained explicitly in terms of the eccentricity. One approach might be to eliminate  $x$  between the parametric equations. However, because of the transcendental nature of the solutions, this task is cumbersome. Fortunately, since  $\epsilon$  is small,  $x$  can be eliminated by applying Lagrange's expansion.

To derive the explicit expression for the semi-major axis in terms of the eccentricity,  $z$  must be written in a form suitable to Lagrange's expansion:

$$z = p + \epsilon \phi(z) \tag{4-40}$$

and since

$$x = \beta a e = \beta a_o c_o \left( \frac{a}{a_o} \right) \left( \frac{e}{e_o} \right) \quad (4-41)$$

it can be written as

$$x = \alpha z \quad (4-42)$$

with

$$\alpha = x_o \left( \frac{e}{e_o} \right) \quad (4-43)$$

so that  $\alpha$  is proportional to  $e$ . Then

$$\phi(z) = z_1(\alpha z) + \epsilon z_2(\alpha z) + \dots + \epsilon^4 z_5(\alpha z) \quad (4-44)$$

Lagrange's expansion of Eq. (4-40) is

$$z = p + \sum_{n=1}^{\infty} \frac{\epsilon^n}{n!} \left( \frac{d}{dp} \right)^{n-1} [\phi(p)]^n \quad (4-45)$$

where the expansion is carried out first and then  $p$  is set equal to 1 to give to the order of  $\epsilon^5$

$$z = 1 + \epsilon h_1(\alpha) + \epsilon^2 h_2(\alpha) + \epsilon^3 h_3(\alpha) + \epsilon^4 h_4(\alpha) + \epsilon^5 h_5(\alpha) \quad (4-46)$$

where

$$\begin{aligned}
h_1 &= z_1 \\
h_2 &= 2(A-A_0) + (A-3)z_1 \\
h_3 &= \frac{7}{2}(\alpha^2 - x_0^2) - (2A_0 + \frac{13}{2})(A-A_0) + (13+2\alpha^2 - 4A-A^2)z_1 \\
&\quad + \frac{1}{2}(3+\alpha^2 + A-A^2)z_1^2 \\
h_4 &= -\frac{1}{2}(\alpha^2 - x_0^2)(35+4A_0 - 7A) \\
&\quad + \frac{1}{6}(A-A_0)(213+42A_0 + 16A_0^2 + 12\alpha^2 - 9A+4A_0A - 8A^2) \\
&\quad - \frac{1}{2}z_1(138+25\alpha^2 - 46A-7A^2 - 2A^3) \\
&\quad - \frac{1}{2}z_1^2(35+7\alpha^2 - 6A^2 + \alpha^2A - A^3) \\
&\quad + 2(A-A_0)z_1(3+\alpha^2 + A-A^2) \\
&\quad - \frac{1}{6}z_1^3(6-\alpha^2 + 2\alpha^2A + 3A^2 - 2A^3) \\
h_5 &= -\frac{3}{4}(\alpha^2 - x_0^2)^2 + \frac{1}{8}(\alpha^2 - x_0^2)(885+68\alpha^2 - 92A-12A^2) \\
&\quad - (\alpha^2 - x_0^2)(A-A_0)(\frac{19}{2} + 4A_0 + 2A) \\
&\quad - (A-A_0)(\frac{441}{2} + \frac{33}{2}\alpha^2 + \frac{137}{4}A + 2\alpha^2A + \frac{9}{2}A^2 + 2A^3) \\
&\quad + (A-A_0)^2(\frac{409}{8} + 2\alpha^2 + 23A + 12A^2) - (A-A_0)^3(10 + \frac{40}{3}A) \\
&\quad + 4(A-A_0)^4 + \frac{7}{2}(\alpha^2 - x_0^2)z_1(3+\alpha^2 + A-A^2) \\
&\quad + z_1(437+88\alpha^2 + 2\alpha^4 - 154A - 5\alpha^2A - 22A^2 - 3A^3 - A^4) \\
&\quad - \frac{1}{2}(A-A_0)z_1(143+29\alpha^2 + 25A + 12\alpha^2A - 17A^2 - 12A^3)
\end{aligned}$$

$$\begin{aligned}
& + 2(A-A_0)^2 z_1 (3 + \alpha^2 + A - A^2) \\
& + \frac{1}{4} z_1^2 (648 + 133\alpha^2 + 4\alpha^4 - 96A + 14\alpha^2 A - 91A^2 - 4\alpha^2 A^2 - 10A^3) \\
& - (A-A_0) z_1^2 (6 - \alpha^2 + 2\alpha^2 A + 3A^2 - 2A^3) \\
& + \frac{1}{6} z_1^3 (123 + 4\alpha^2 - \alpha^4 - 6A + 18\alpha^2 A + 15A^2 + 2\alpha^2 A^2 - 18A^3 - A^4) \\
& + \frac{1}{24} z_1^4 (18 - \alpha^2 - 2\alpha^4 - 8\alpha^2 A - 3A^2 + 8\alpha^2 A^2 + 12A^3 - 6A^4) .
\end{aligned} \tag{4-47}$$

In the expressions for  $h_i(\alpha)$  the following definitions were used

$$A = \alpha y_0(\alpha) , \quad z_1 = \text{Log} \frac{\alpha I_1(\alpha)}{x_0 I_1(x_0)} . \tag{4-48}$$

Thus, Eqs. (4-46)-(4-48) provide an explicit expression of the variation of  $a/a_0$  as a function of  $e/e_0$  since  $\alpha = x_0(e/e_0)$ .

Following the approach of the previous section, the other orbital elements can be easily expressed in terms of  $e$  to obtain the drop in periapsis, the drop in apoapsis and the change in orbital period.

$$\frac{r_{p_0} - r_p}{H} = (\alpha - x_0) - (1-e)(h_1 + \epsilon h_2 + \epsilon^2 h_3 + \epsilon^3 h_4 + \epsilon^4 h_5) \tag{4-49}$$

$$\frac{r_{a_0} - r_a}{H} = (x_0 - \alpha) - (1+e)(h_1 + \epsilon h_2 + \epsilon^2 h_3 + \epsilon^3 h_4 + \epsilon^4 h_5) \tag{4-50}$$

$$\frac{r_p}{r_{p_0}} = \frac{(1 - \epsilon \alpha)}{(1 - e_0)} z(\alpha) \quad (4-51)$$

$$\frac{r_a}{r_{a_0}} = \frac{(1 + \epsilon \alpha)}{(1 + e_0)} z(\alpha) \quad (4-52)$$

$$\frac{T}{T_0} = z^{3/2}(\alpha) \quad (4-53)$$

The last expression, Eq. (4-53), provides a powerful method of verifying the assumption made on the atmosphere from two of the most accurately and easily measured orbital elements, namely, the period of revolution and the eccentricity.

Eqs. (4-46) and (4-49)-(4-53) are plotted in Figs. (4-7)-(4-12) respectively.

Fig. (4-7) plots the solution  $z = z(\alpha) = z(e/\epsilon)$  as a function of the eccentricity for several values of  $e_0$ . The range of validity is limited to  $0 < e_0 \leq 0.5$  since the  $z(\alpha)$  solution is not as accurate as the  $z(x)$  solution. It was found that  $z(\alpha)$  exceeds the numerical solution (found by integrating the basic nonlinear equation (4-16)) by a maximum value approximated by  $e_0^6/15(1-e_0)$ , which still gives 7 digits of accuracy for  $e_0 = 0.1$ , but diverges as  $e_0 \rightarrow 1$ . For  $e_0 = 0.5$  the error is imperceptible in the figure. The decay in the periapsis distance  $r_p$  versus the eccentricity for  $e_0 = 0.1$  and  $e_0 =$

0.4 is presented in Fig. (4-10). The ratio  $r_p / r_{p_0}$  remains nearly equal to one for a large portion of the decay process, but as  $e \rightarrow 0$  the drop in periapsis altitude increases rapidly. For small values of  $\frac{1}{\beta r_{p_0}}$  (0.005), which correspond to higher initial periapsis altitudes for fixed  $\beta$ , decay is much slower than for large values (0.02) as evident in the figure. The fractional error in this plot and in the others is kept to an imperceptible amount by considering the error formula mentioned earlier.

The decay in the apoapsis distance  $r_a$  versus the eccentricity for several values of  $e_0$  is presented in Fig. (4-11). It is evident that the ratio  $r_a / r_{a_0}$  decreases rapidly with the eccentricity. Initially the parameter  $\frac{1}{\beta r_{p_0}}$  seems to have little effect, but as the eccentricity approaches zero the larger values of  $\frac{1}{\beta r_{p_0}}$  yield more rapid decay.

Finally, the decay in the orbital period  $T$  as a function of the eccentricity is presented in Fig. (4-12). As pointed out by King-Hele, this functional relationship  $T = T(e, \epsilon)$  provides a powerful formula for testing the atmospheric parameter  $\epsilon$  since the orbital period and eccentricity can be accurately measured.

#### 4.6 The Contraction of Highly Eccentric Orbits

For the case of orbits with large eccentricities, King-Hele used an entirely different method from the following to derive the basic equation for orbit contraction. Using the present notation, his equation takes the following form

$$\frac{dz}{dx} = \epsilon \left( 1 + \frac{1}{2x} \right) - \frac{\epsilon^2}{z + \epsilon x} \quad (4-54)$$

This equation can be directly derived from the basic non-linear equation (4-16). Since  $x = \beta ae$ , when  $e \rightarrow 1$ ,  $a \rightarrow \infty$ ,  $x$  becomes very large and the asymptotic expansion for Bessel's ratio  $y_0(x)$  is

$$\begin{aligned} y_0 &= 1 + \frac{1}{2x} + \dots \\ y_0^2 &= 1 + \frac{1}{x} + \dots \end{aligned} \quad (4-55)$$

Substituting Eqs. (4-55) into Eq. (4-16) provides

$$\frac{dz}{dx} = \epsilon \left( 1 + \frac{1}{2x} \right) - \frac{\epsilon^2}{z} + \frac{\epsilon^3 x}{z^2} - \frac{\epsilon^4 x^2}{z^3} + \frac{\epsilon^5 x^3}{z^4} - \dots \quad (4-56)$$

which is immediately recognized as the development of Eq. (4-54).

King-Hele provides an approximate solution to the nonlinear equation (4-54) by assuming that on the right-hand side  $z$  is approximated by  $z = 1 - \epsilon(x_0 - x)$  and then integrating. In this

analysis, the exact solution will be given.

Using the transformation

$$z = \epsilon (x + q) \quad (4-57)$$

and changing the independent variable from  $x$  to  $q$  results in the

Bernoulli equation

$$\frac{dx}{dq} = 2x + \frac{4x^2}{q} \quad (4-58)$$

Substituting the change of variable

$$x = \frac{e^{2q}}{K(q)} \quad (4-59)$$

into Eq. (4-58) provides

$$\frac{dK}{dq} = - \frac{4e^{2q}}{q} \quad (4-60)$$

Upon integrating it is found that  $K$  can be expressed in terms of the exponential integral .

$$\begin{aligned} K &= -4 \int \frac{e^{2q}}{2q} d(2q) + C \\ &= -4 E_i(2q) + C \quad (4-61) \end{aligned}$$

Thus, the exact solution in parametric form is

$$x = \frac{e^{2(q-q_0)}}{\frac{1}{x_0} + 4e^{-2q_0} [E_i(2q_0) - E_i(2q)]} \quad (4-62)$$

along with Eq. (4-57) and the initial conditions

$$\begin{aligned} z(x_0) &= 1 \\ q_0 &= \frac{1}{\epsilon} - x_0 = \frac{(1-e_0)}{\epsilon} \end{aligned} \quad (4-63)$$

The exponential integral can be evaluated through its asymptotic form since the argument  $2q$  is large. In general, the exponential integral of the form

$$E_n(x) = \int e^x x^{n-1} dx \quad (4-64)$$

can be integrated by parts

$$E_n(x) = x^{n-1} e^x - (n-1) E_{n-1}$$

By repeated application of this formula, the asymptotic expansion for large  $x$  is deduced

$$E_n(x) = x^{n-1} e^x \left[ 1 - \frac{(n-1)}{x} + \frac{(n-1)(n-2)}{x^2} - \frac{(n-1)(n-2)(n-3)}{x^3} + \dots \right] \quad (4-65)$$

When  $n = 0$ , Eq. (4-64) becomes the exponential integral appearing in Eq. (4-62). Taking 6 terms of the series (Eq. (4-65)), for  $x > 50$ , the solution is identical to numerical values tabulated by Abramowitz and Stegun (1972).

Numerical computation has revealed that the analytic solution

$z(x)$  of the basic nonlinear equation (4-16) and the present solution  $z(q)$  of the asymptotic equation are in very close agreement. Even for  $e_0 = 0.99$  the two solutions are nearly identical except for very small values of  $x/x_0$ . This gives further testimony to the wide application of the solution  $z(x)$  of the basic nonlinear equation.

#### 4.7 The Contraction of Nearly Circular Orbits

For very small eccentricities,  $x$  is very small and the series expansion of  $y_0(x)$  for small  $x$  is

$$y_0 = \frac{2}{x} + \frac{1}{4}x - \frac{1}{96}x^3 + \frac{1}{1536}x^5 - \dots \quad (4-66)$$

The derivation is discussed in detail in Chapter 5. Substituting Eqs. (4-66) and (4-13) into Eq. (4-10) results in the following

$$\frac{1}{\epsilon} \frac{dz}{dx} = \frac{2}{x} \left( 1 - 3\frac{e}{x} + 9\frac{e^2}{x^2} - 27\frac{e^3}{x^3} + \dots \right) \quad (4-67)$$

Eq. (4-67) is recognized as the expansion of

$$\frac{1}{\epsilon} \frac{dz}{dx} = \frac{2}{x(1+3\frac{e}{x})} \quad (4-68)$$

Writing  $e = \frac{\epsilon x}{z}$ , the equation can be put in the form

$$\left(1 + 3 \frac{\epsilon}{z}\right) dz = \frac{2\epsilon}{x} dx$$

Upon integrating

$$z + 3\epsilon \text{Log } z = 1 + 2\epsilon \text{Log } \frac{x}{x_0} \quad (4-69)$$

a closed form parametric solution is obtained for very small values of eccentricity. It would be useful to have the explicit solution of the semi-major axis  $z$  in terms of the eccentricity. This is accomplished by using Lagrange's expansion as before, with

$$\phi(z) = 2 \text{Log } \frac{e}{e_0} - \text{Log } z .$$

Applying the expansion,

$$\begin{aligned} z(e/e_0) &= 1 + \epsilon 2 \text{Log } \frac{e}{e_0} (1 - \epsilon + \epsilon^2 - \epsilon^3 + \dots) \\ &= 1 + \frac{2\epsilon}{1+\epsilon} \text{Log } \frac{e}{e_0} \end{aligned} \quad (4-70)$$

provides the closed form solution of  $z$  as a function of eccentricity for very small values of eccentricity.

#### 4.8 The Contraction of Circular Orbits

For contraction of circular orbits, it is necessary to go back to the variational equations (3-12) and substitute  $e = 0$  into the  $\frac{da}{dE}$  equation. Since  $r = a$ , the equation becomes

$$\frac{dr}{dM} = - \frac{2Z_o r^2}{r_{p_o}} e^{\beta(r_{p_o} - r)} \quad (4-71)$$

where M is the mean anomaly. The equation can be rearranged to give

$$\frac{e^{\beta r}}{(\beta r)^2} d\beta r = - \frac{2Z_o}{\beta r_{p_o}} e^{\beta r_{p_o}} dM \quad (4-72)$$

The first integral is simply  $E_{-1}(\beta r)$ , as defined by Eq. (4-64) with  $n = -1$ . Assuming initial conditions  $r_{p_o}$  and  $M_o$  the integration provides

$$E_{-1}(\beta r) - E_{-1}(\beta r_{p_o}) = - 2\epsilon Z_o e^{\frac{1}{\epsilon}} [M - M_o] \quad (4-73)$$

The exact total time in circular orbit is found by setting the radial distance to the minimum final distance,  $r_f$ , at which the orbit can barely be maintained and by replacing the mean anomaly

M by  $\sqrt{\frac{\mu}{r^3}} t$  and the initial mean anomaly by zero

$$t_f = \frac{\sqrt{\frac{r_f^3}{\mu}}}{2\epsilon Z_o e^{1/\epsilon}} \left[ E_{-1}(\beta r_{p_o}) - E_{-1}(\beta r_f) \right] \quad (4-74)$$

#### 4.9 The Orientation of the Orbit During Decay

Due to the fact that oblateness has been ignored in the math model, it turns out that the argument of the periapsis,  $\omega$ , remains a constant

$$\omega = \omega_0 \quad (4-75)$$

from the third of Eqs. (4-6). This allows the replacement of  $\sin \alpha$  and  $\cos \alpha$  with terms in  $\sin E$  and  $\cos E$  in the last two variational equations for  $\Omega$ , the longitude of the ascending node, and  $i$ , the inclination of the orbit plane. This is done by using the well-known relations of true anomaly  $\alpha - \omega_0$  and eccentric anomaly  $E$

$$\begin{aligned} \cos (\alpha - \omega_0) &= \frac{\cos E - e}{1 - e \cos E} \\ \sin (\alpha - \omega_0) &= \frac{\sqrt{1 - e^2} \sin E}{1 - e \cos E} \end{aligned} \quad (4-76)$$

From Eqs. (4-76) it is easy to obtain

$$\begin{aligned} \cos \alpha &= \frac{(\cos \omega_0)(\cos E - e) - (\sin \omega_0) \sqrt{1 - e^2} \sin E}{1 - e \cos E} \\ \sin \alpha &= \frac{(\sin \omega_0)(\cos E - e) + (\cos \omega_0) \sqrt{1 - e^2} \sin E}{1 - e \cos E} \end{aligned} \quad (4-77)$$

The terms  $\sin \alpha$ ,  $\cos \alpha$  and  $\cos^2 \alpha$  are needed for the variational equations. In terms of eccentric anomaly, they are

$$\begin{aligned}
\sin \alpha \cos \alpha &= \frac{1}{(1-e \cos E)^2} \left\{ \cos \omega_o \sin \omega_o \left[ (\cos E - e)^2 + (e^2 - 1)(1 - \cos^2 E) \right] \right. \\
&\quad \left. + (2 \cos^2 \omega_o - 1) \left[ \sqrt{1 - e^2} \sin E (\cos E - e) \right] \right\} \\
\cos^2 \alpha &= \frac{1}{(1 - e \cos E)^2} \left\{ \cos^2 \omega_o (\cos E - e)^2 \right. \\
&\quad - 2 \cos \omega_o \sin \omega_o \sqrt{1 - e^2} \sin E (\cos E - e) \\
&\quad \left. + \sin^2 \omega_o (1 - e^2)(1 - \cos^2 E) \right\} \tag{4-78}
\end{aligned}$$

It is now clear that the average equations can be obtained in the same manner as in Section 4.1 by using Eqs. (4-5). Noting that the  $\sin E$  terms vanish, the average equations for  $\Omega$  and  $i$  become

$$\begin{aligned}
\frac{d\Omega}{dE} &= \frac{-r_{p_o} w Z_o}{\sqrt{\mu f / r_{p_o}} \sqrt{1-e^2}} \left(\frac{a}{r_{p_o}}\right)^{5/2} \exp\left[\beta(a_o - a - a_o e_o)\right] \\
&\quad \times \frac{1}{2\pi} \int_0^{2\pi} \cos \omega_o \sin \omega_o \\
&\quad \times (1-e \cos E)^{1/2} (1+e \cos E)^{1/2} \left[(\cos E - e)^2 + (e^2 - 1)(1 - \cos^2 E)\right] \\
&\quad \times \exp(x \cos E) dE \\
\frac{1}{\sin i} \frac{di}{dE} &= \frac{-r_{p_o} w Z_o}{\sqrt{\mu f / r_{p_o}} \sqrt{1-e^2}} \left(\frac{a}{r_{p_o}}\right)^{5/2} \exp\left[\beta(a_o - a - a_o e_o)\right] \\
&\quad \times \frac{1}{2\pi} \int_0^{2\pi} (1-e \cos E)^{1/2} (1+e \cos E)^{1/2} \\
&\quad \times \left[\cos^2 \omega_o (\cos E - e)^2 + \sin^2 \omega_o (1 - e^2)(1 - \cos^2 E)\right] \\
&\quad \times \exp(x \cos E) dE \tag{4-79}
\end{aligned}$$

Expanding to the first order in eccentricity and identifying the Bessel functions,  $I_n(x)$ , the average equations become:

$$\frac{d\Omega}{dE} = \frac{-r_{p_o} w Z_o}{\sqrt{\mu f / r_{p_o}} \sqrt{1-e^2}} \left( \frac{a}{r_{p_o}} \right)^{5/2} \exp \left[ \beta (a_o - a - a_o e_o) \right] \cos \omega_o \sin \omega_o$$

$$\times [I_2 - 2eI_1 + 0(e^2)]$$

$$\frac{d(\text{Log}(\tan \frac{i}{2}))}{dE} = \frac{-r_{p_o} w Z_o}{\sqrt{\mu f / r_{p_o}} \sqrt{1-e^2}} \left( \frac{a}{r_{p_o}} \right)^{5/2} \exp \left[ \beta (a_o - a - a_o e_o) \right]$$

$$\times \left\{ \frac{1}{2} I_o + \frac{1}{2} I_2 (\cos^2 \omega_o - \sin^2 \omega_o) - 2e \cos^2 \omega_o I_1 + 0(e^2) \right\}$$

(4-80)

Dividing both equations of (4-80) by the average  $\frac{dx}{dE}$  equation,

Eq. (4-8)

$$\frac{d\Omega}{dx} = \frac{\epsilon w}{2\sqrt{1-e^2}} \sqrt{\frac{a_o^3}{\mu f}} z^{1/2} \cos \omega_o \sin \omega_o$$

$$\times \frac{[I_2 - 2eI_1 + 0(e^2)]}{[I_1 + \frac{1}{2} e (3I_o + I_2) + 0(e^2)]}$$

$$\frac{d(\text{Log}(\tan \frac{i}{2}))}{dx} = \frac{\epsilon w}{2\sqrt{1-e^2}} \sqrt{\frac{a_o^3}{\mu f}} z^{1/2}$$

$$\times \frac{\left[ \frac{1}{2} I_o + \frac{1}{2} I_2 (\cos^2 \omega_o - \sin^2 \omega_o) - 2e \cos^2 \omega_o I_1 + 0(e^2) \right]}{\left[ I_1 + \frac{1}{2} e(3I_o + I_2) + 0(e^2) \right]} \quad (4-81)$$

Since the term  $\epsilon w$  is very small,  $\Omega$  and  $i$  vary slowly. For the present development, a first order analysis will be adequate. This implies setting  $e = 0$  in Eqs. (4-81).

$$\frac{d\Omega}{dx} = \frac{\epsilon w}{2} \sqrt{\frac{a_o^3}{\mu f}} \cos \omega_o \sin \omega_o y_2(x)$$

$$\frac{d(\text{Log}(\tan \frac{i}{2}))}{dx} = \frac{\epsilon w}{2} \sqrt{\frac{a_o^3}{\mu f}} \left[ \frac{1}{2} y_o + \frac{1}{2} (\cos^2 \omega_o - \sin^2 \omega_o) y_2 \right] \quad (4-82)$$

Substituting  $y_2 = y_o - \frac{2}{x}$  into Eqs. (4-82)

$$\frac{d\Omega}{dx} = \frac{\epsilon w}{2} \sqrt{\frac{a_o^3}{\mu f}} \cos \omega_o \sin \omega_o \left( y_o - \frac{2}{x} \right)$$

$$\frac{d(\text{Log}(\tan \frac{i}{2}))}{dx} = \frac{\epsilon w}{2} \sqrt{\frac{a_o^3}{\mu f}} \left[ \cos^2 \omega_o y_o - (\cos^2 \omega_o - \sin^2 \omega_o) \frac{1}{x} \right] \quad (4-83)$$

Finally, Eqs. (4-83) can be integrated from  $x_0$  to  $x$  with initial conditions  $\Omega_0$  and  $i_0$ .

$$\Omega = \Omega_0 + \frac{\epsilon w}{2} \sqrt{\frac{a_0^3}{\mu f}} \cos \omega_0 \sin \omega_0 \left[ z_1(x) - 2 \text{Log} \frac{x}{x_0} \right]$$

$$\text{Log} \left( \frac{\tan \frac{i}{2}}{\tan \frac{i_0}{2}} \right) = \frac{\epsilon w}{2} \sqrt{\frac{a_0^3}{\mu f}} \left[ \cos^2 \omega_0 z_1(x) - (\cos^2 \omega_0 - \sin^2 \omega_0) \text{Log} \frac{x}{x_0} \right] \quad (4-84)$$

where  $z_1(x)$  is defined by Eq. (4-26). Thus, first order solutions have been found in parametric form for the longitude of the ascending node,  $\Omega$ , and the inclination angle,  $i$ . For small eccentricities, Eqs. (4-84) indicate that  $\Omega$  varies very slightly, not only because  $w$  is small, but because as  $x \rightarrow 0$ ,  $z_1(x) \rightarrow 2 \text{Log} \frac{x}{x_0}$ . Similarly, for the inclination angle, it can be shown that for small  $x$

$$\tan \frac{i}{2} \approx \left( \frac{x}{x_0} \right)^\delta \tan \frac{i_0}{2}, \quad \text{where } \delta = \frac{\epsilon w}{2} \sqrt{\frac{a_0^3}{\mu f}}.$$

Since  $\delta$  is very small, the inclination of the orbit plane hardly changes during the lifetime of the satellite for nonzero values of  $x$ .

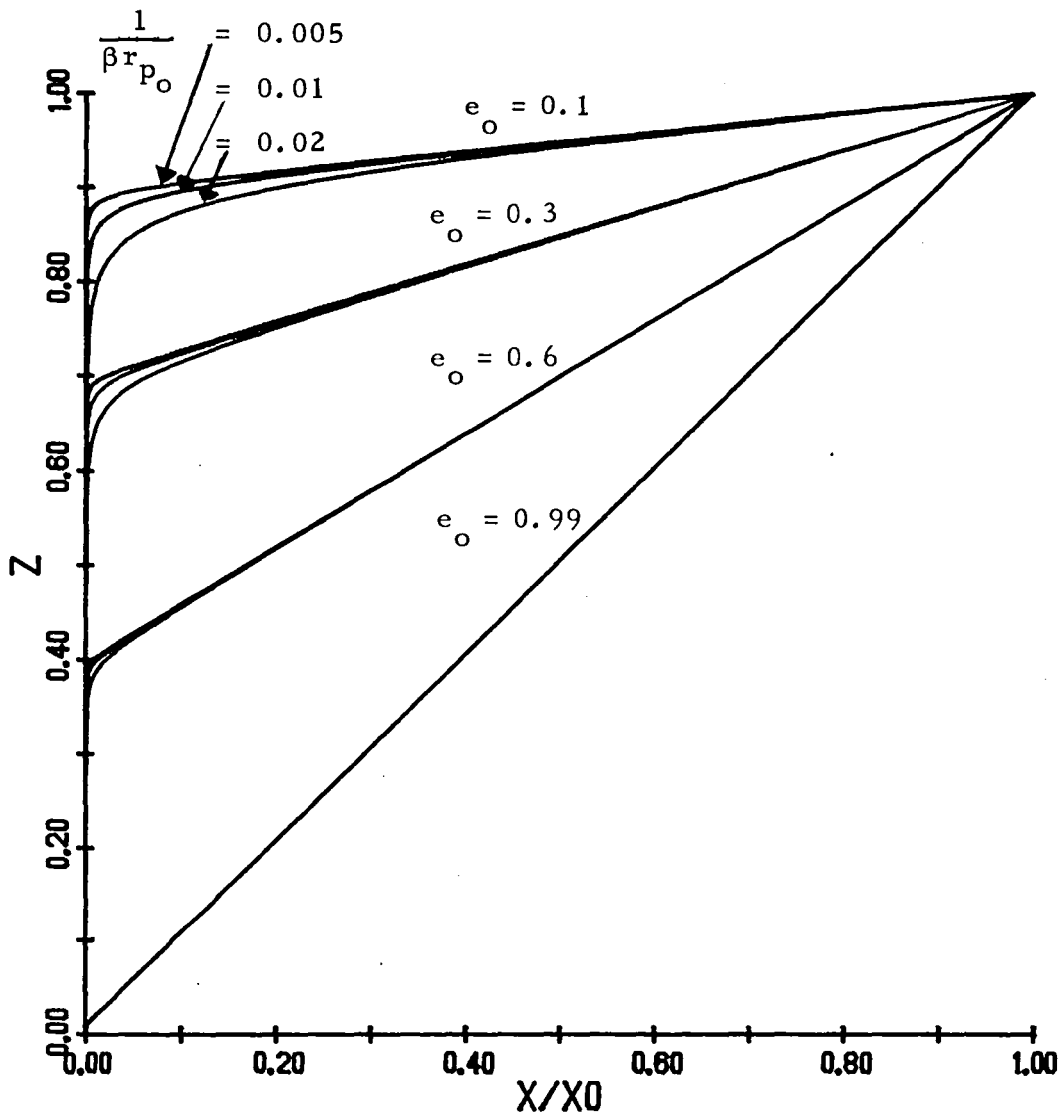


Fig. 4-1. Variations of  $z$  as Function of  $x/x_0$ .  
 $z$  = nondimensional semi-major axis =  $a/a_0$ ,  
 $e_0$  = initial eccentricity and  $x = \beta a e$ .  
The parametric solution  $z(x)$  is generated by  
Eqs. (4-32) and (4-31).

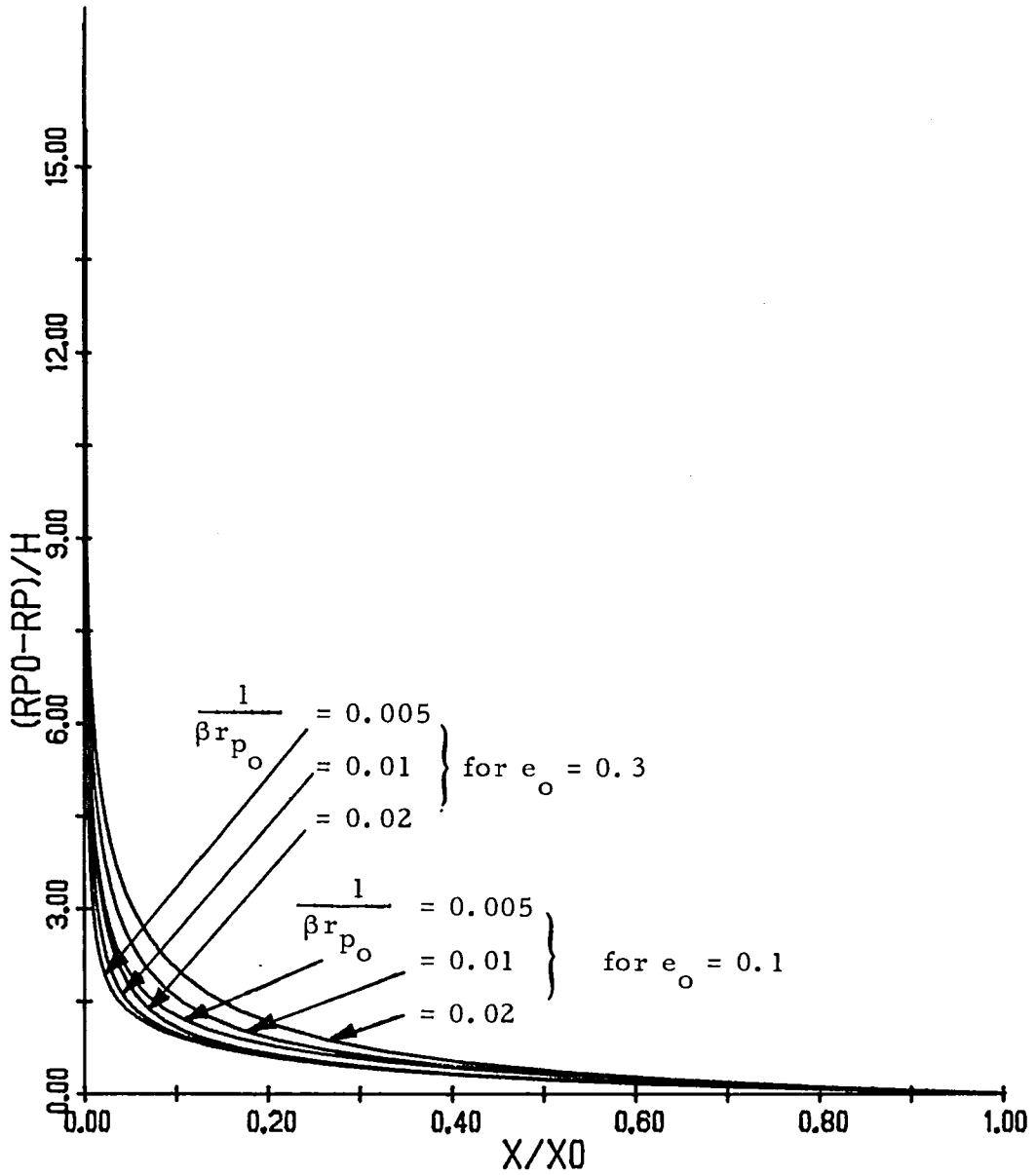


Fig. 4-2. Variations of  $(r_{p_0} - r_p)/H$  as Function of  $x/x_0$ .  
 $(r_{p_0} - r_p)/H$  = drop of periapsis in scale heights,  
 $e_0$  = initial eccentricity and  $x = \beta ae = ae/H$ .  
 The plot is generated from Eqs. (4-34) and (4-31).

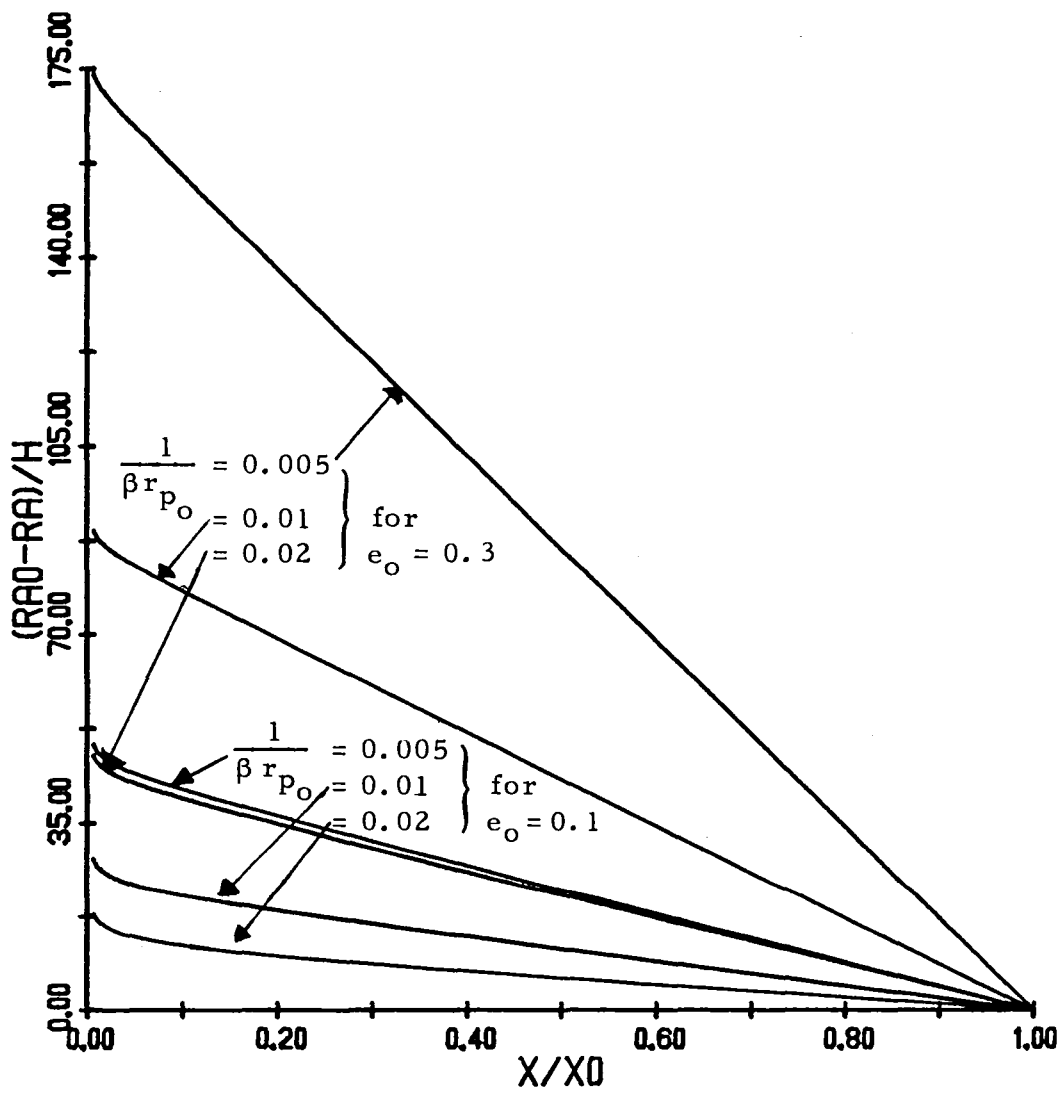


Fig. 4-3. Variations of  $(r_{a_0} - r_a)/H$  as Function of  $x/x_0$ .  
 $(r_{a_0} - r_a)/H$  = drop of apoapsis in scale heights,  
 $e_0$  = initial eccentricity and  $x = \beta a e = a e/H$ .  
 The plot is generated from Eqs. (4-35) and (4-31).

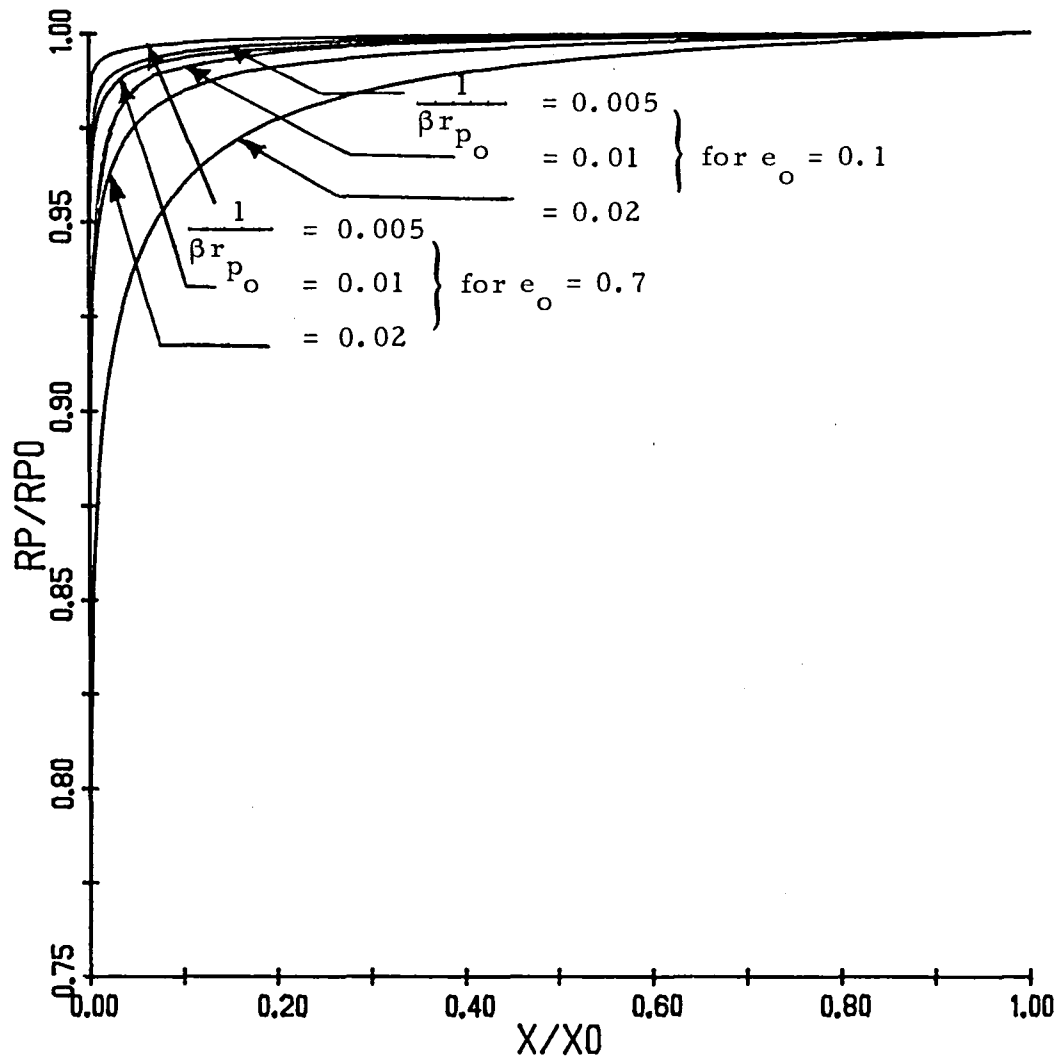


Fig. 4-4. Variations of  $r_p / r_{p_0}$  as Function of  $x/x_0$ .  
 $r_p / r_{p_0}$  = ratio of periapsis to initial periapsis,  
 $e_0$  = initial eccentricity and  $x = \beta a e_0$ .  
 The plot is generated from Eqs. (4-36), (4-32)  
 and (4-31).

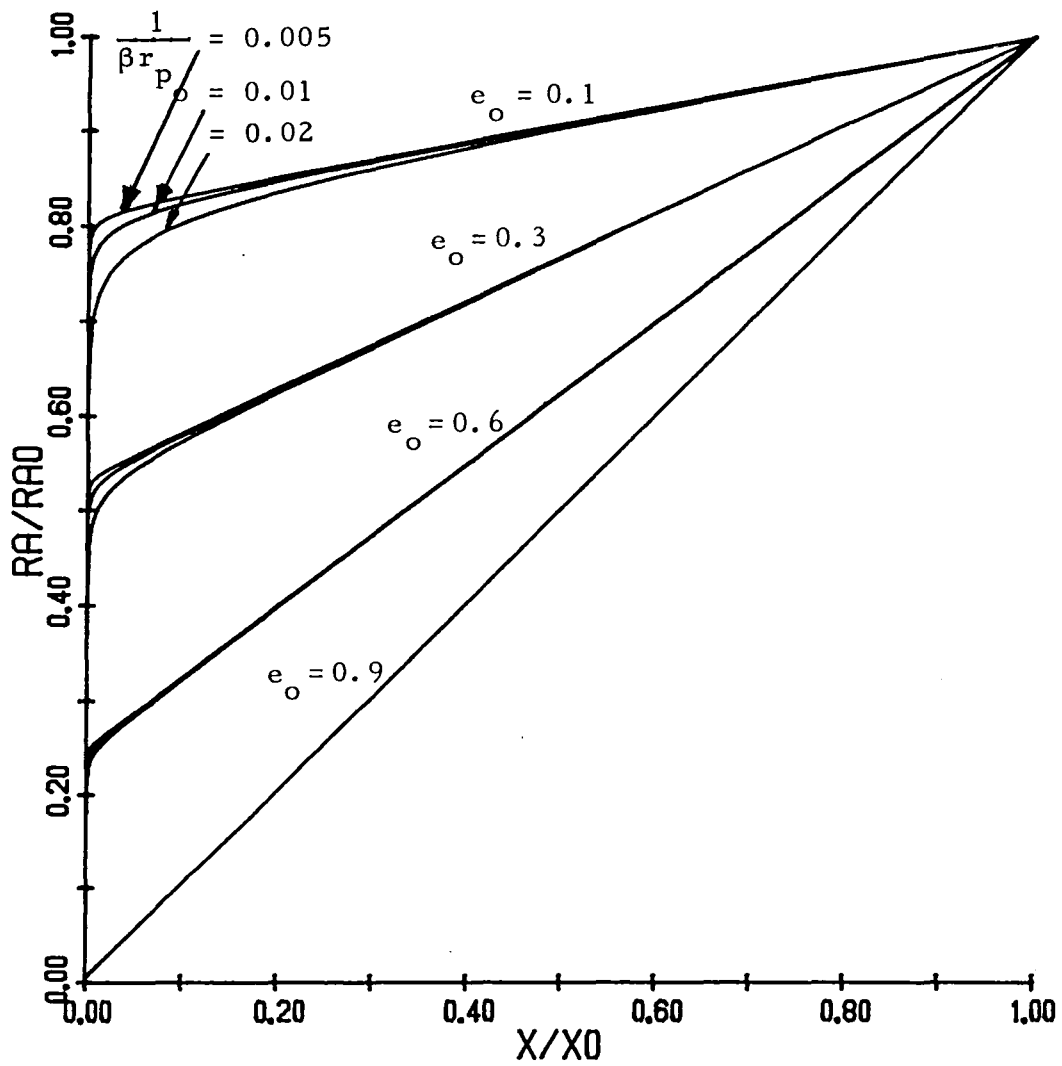


Fig. 4-5. Variations of  $r_a/r_{a_0}$  as Function of  $x/x_0$ .  
 $r_a/r_{a_0}$  = ratio of apoapsis to initial apoapsis,  
 $e_0$  = initial eccentricity and  $x = \beta a e$ . The plot  
 is generated from Eqs. (4-37), (4-32) and (4-31).

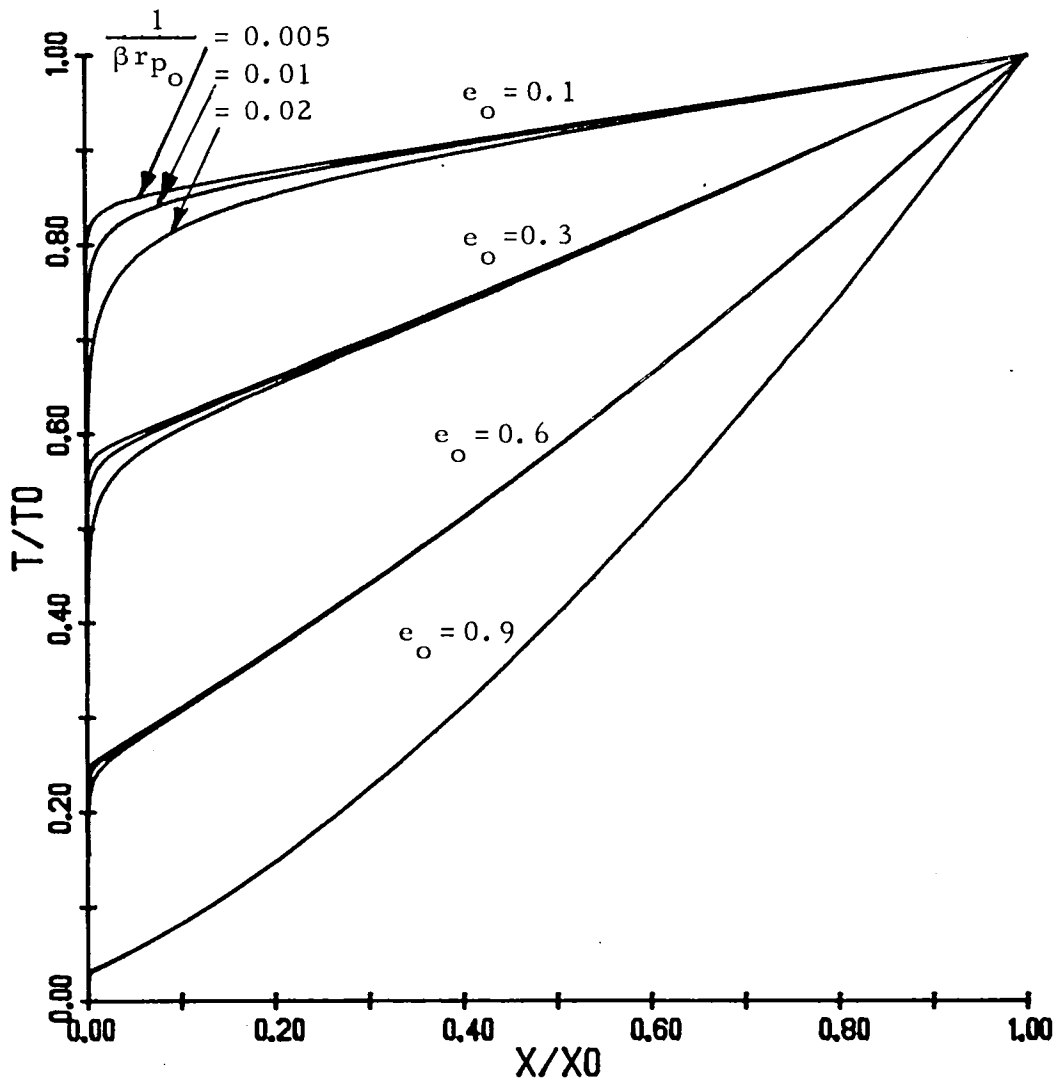


Fig. 4-6. Variations of  $T/T_0$  as Function of  $x/x_0$ .

$T/T_0$  = ratio of orbital period to initial orbital period,  
 $e_0$  = initial eccentricity and  $x = \beta a e$ . The plot is  
 generated from Eqs. (4-38), (4-32) and (4-31).

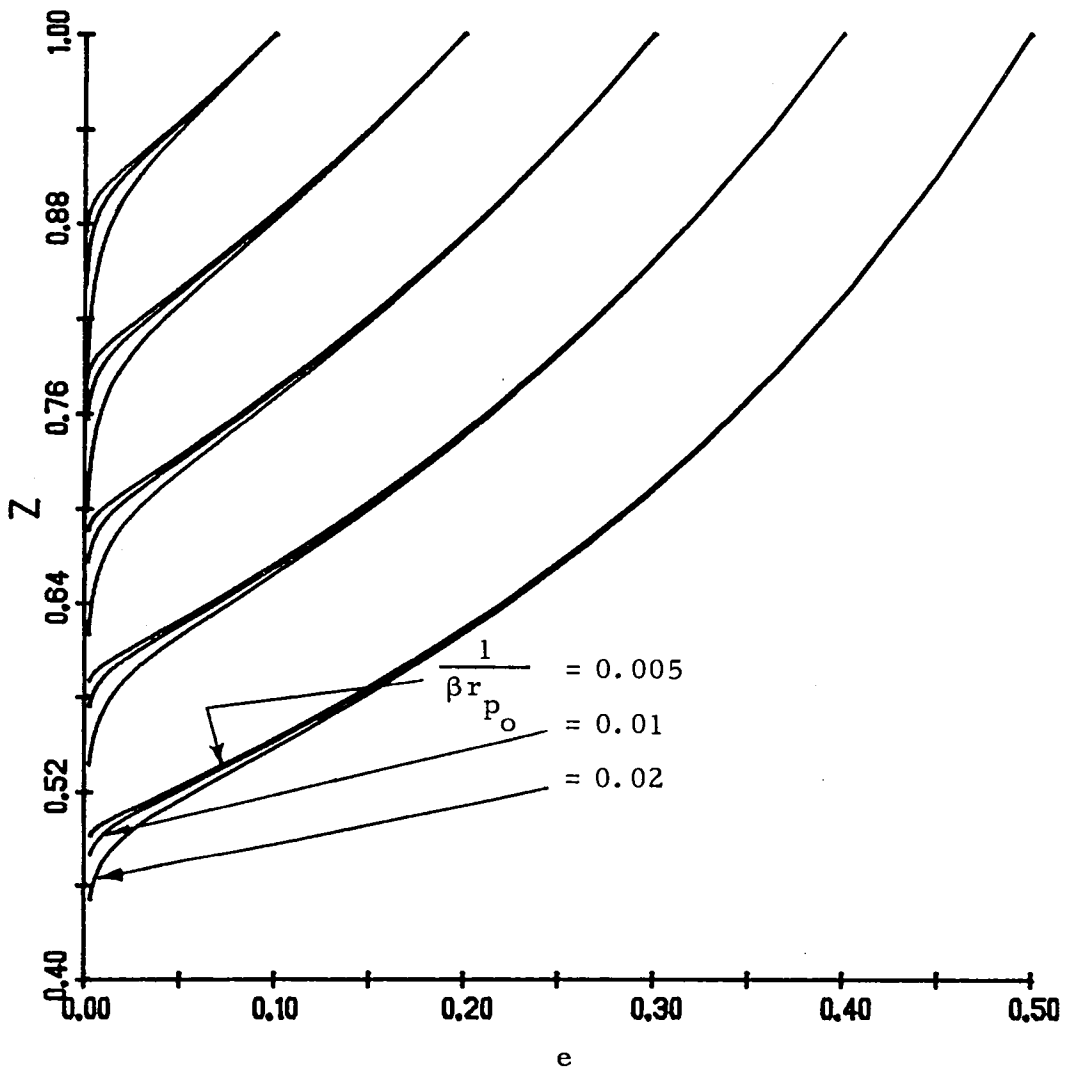


Fig. 4-7. Variations of  $z$  as Function of  $e$ .

$z$  = nondimensional semi-major axis =  $a/a_o$  and  
 $e$  = eccentricity. The explicit solution  $z(e)$  is  
 generated by Eqs. (4-46) and (4-47).

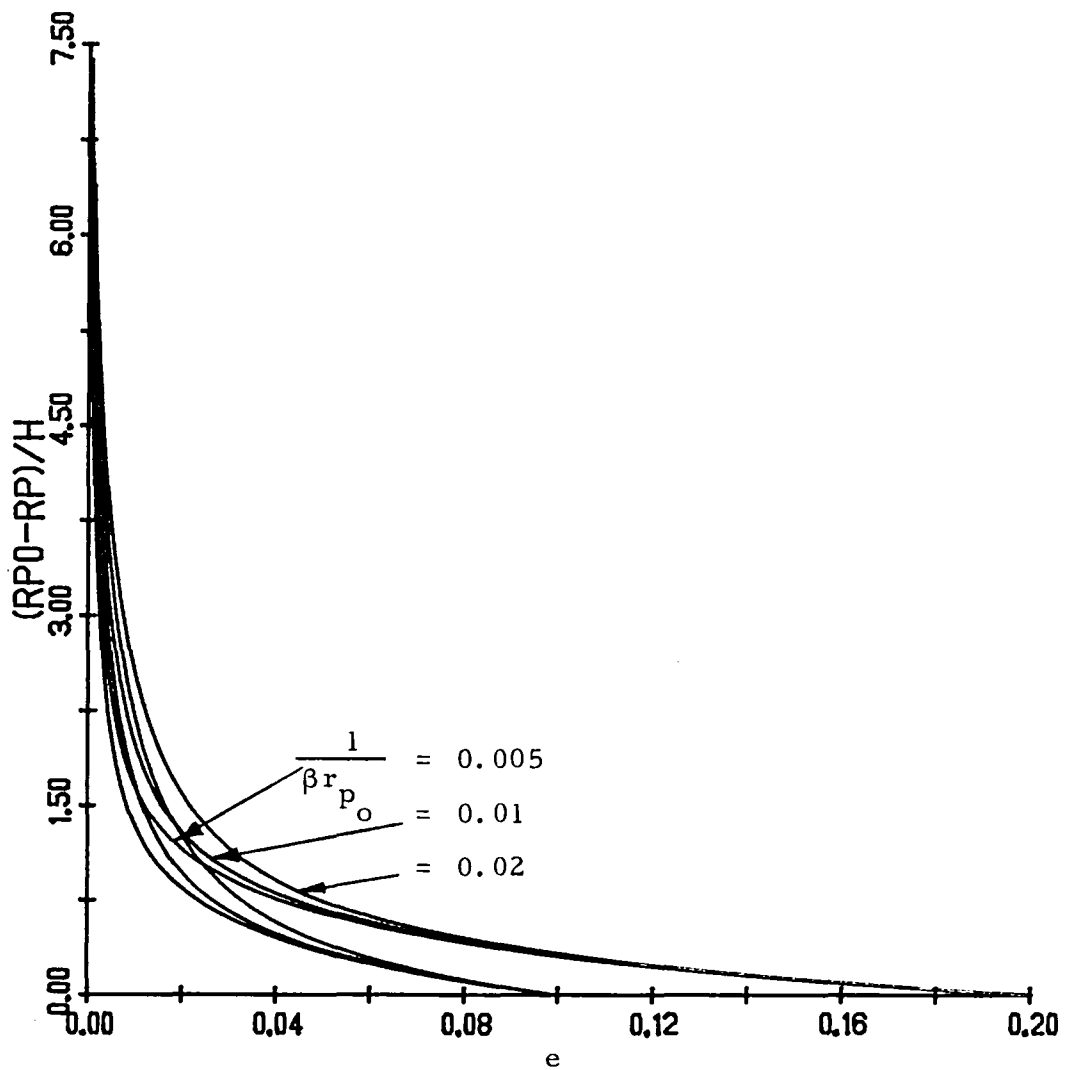


Fig. 4-8. Variations of  $(r_{p_0} - r_p)/H$  as Function of  $e$ .  
 $(r_{p_0} - r_p)/H$  = drop of periapsis in scale heights  
and  $e$  = eccentricity. The plot is generated  
from Eqs. (4-49) and (4-47).

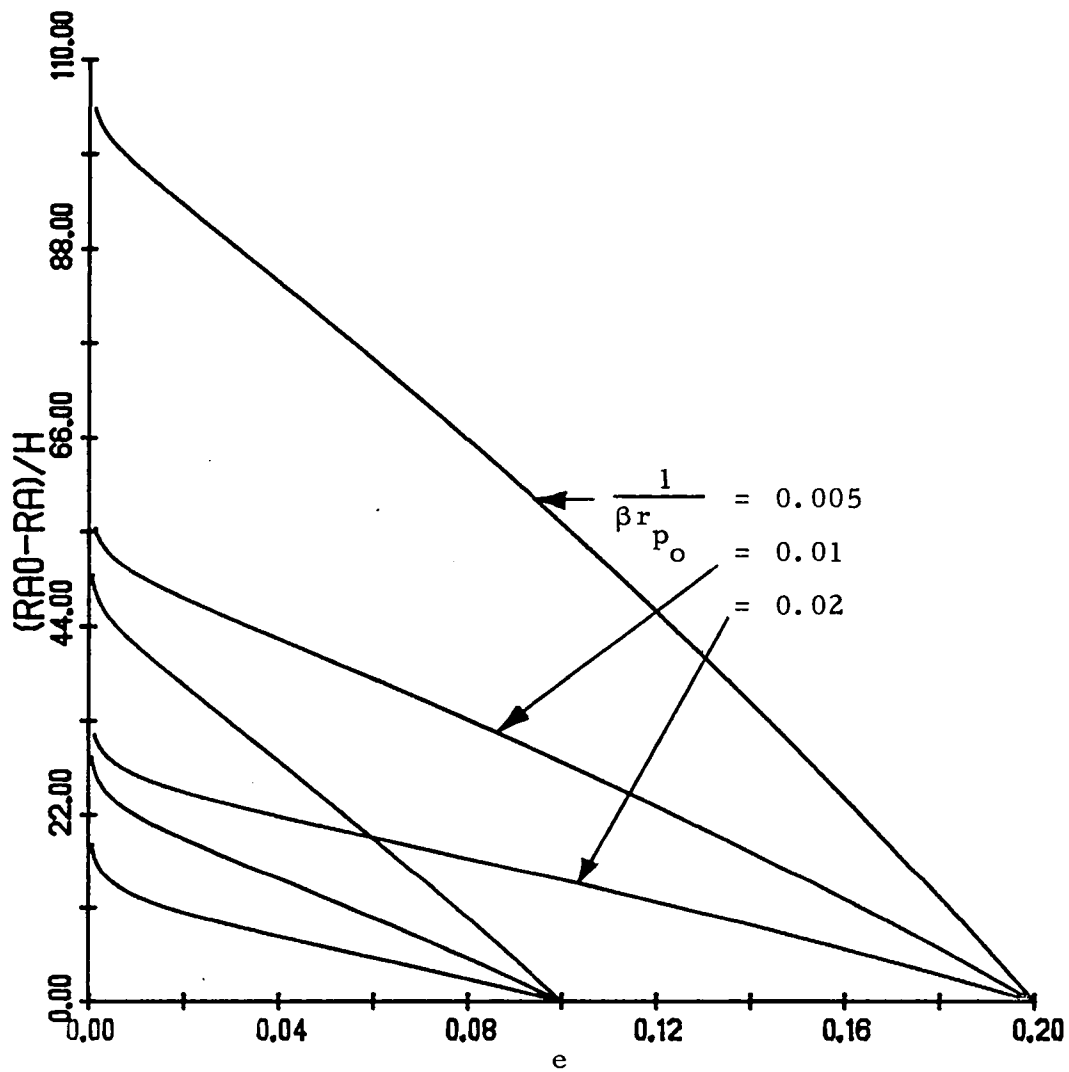


Fig. 4-9. Variations of  $(r_{a_0} - r_a)/H$  as Function of  $e$ .

$(r_{a_0} - r_a)/H$  = drop of apoapsis in scale heights  
and  $e$  = eccentricity. The plot is generated by  
Eqs. (4-50) and (4-47).

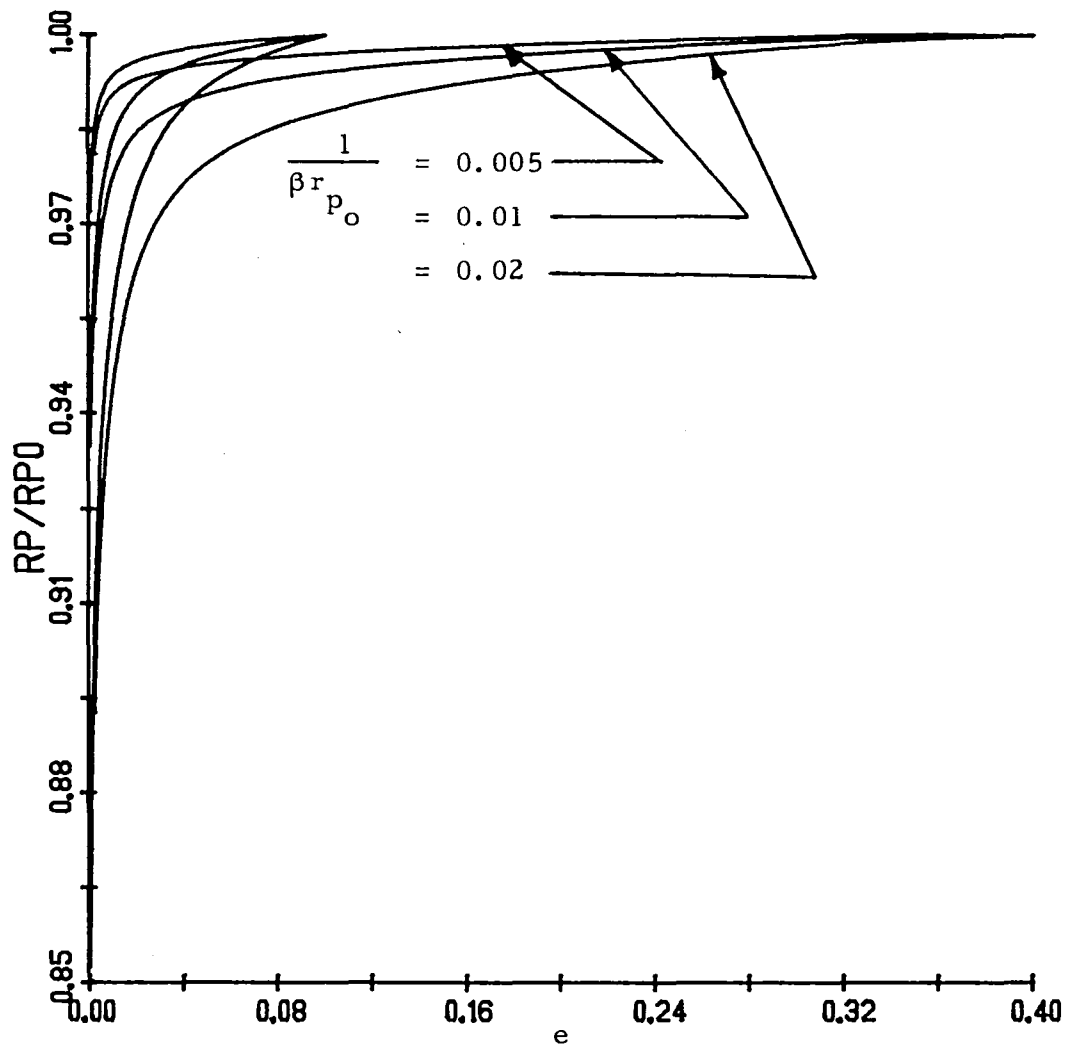


Fig. 4-10. Variations of  $r_p / r_{p_0}$  as Function of  $e$ .

$r_p / r_{p_0}$  = ratio of periapsis to initial periapsis  
and  $e$  = eccentricity. The plot is generated by  
Eqs. (4-51), (4-46) and (4.47).

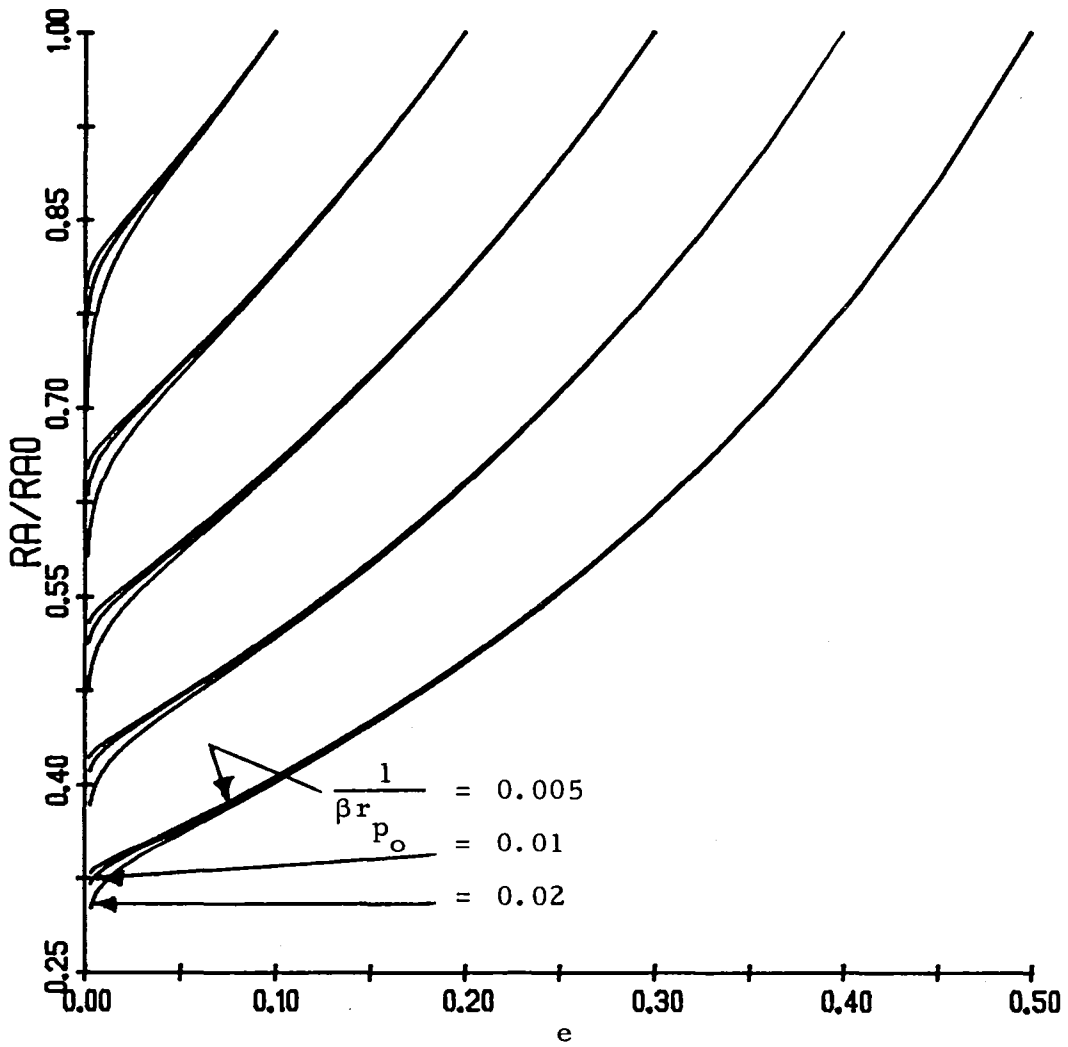


Fig. 4-11. Variations of  $r_a/r_{a_0}$  as Function of  $e$ .

$r_a/r_{a_0}$  = ratio of apoapsis to initial apoapsis  
and  $e$  = eccentricity. The plot is generated by  
Eqs. (4-52), (4-46) and (4-47).

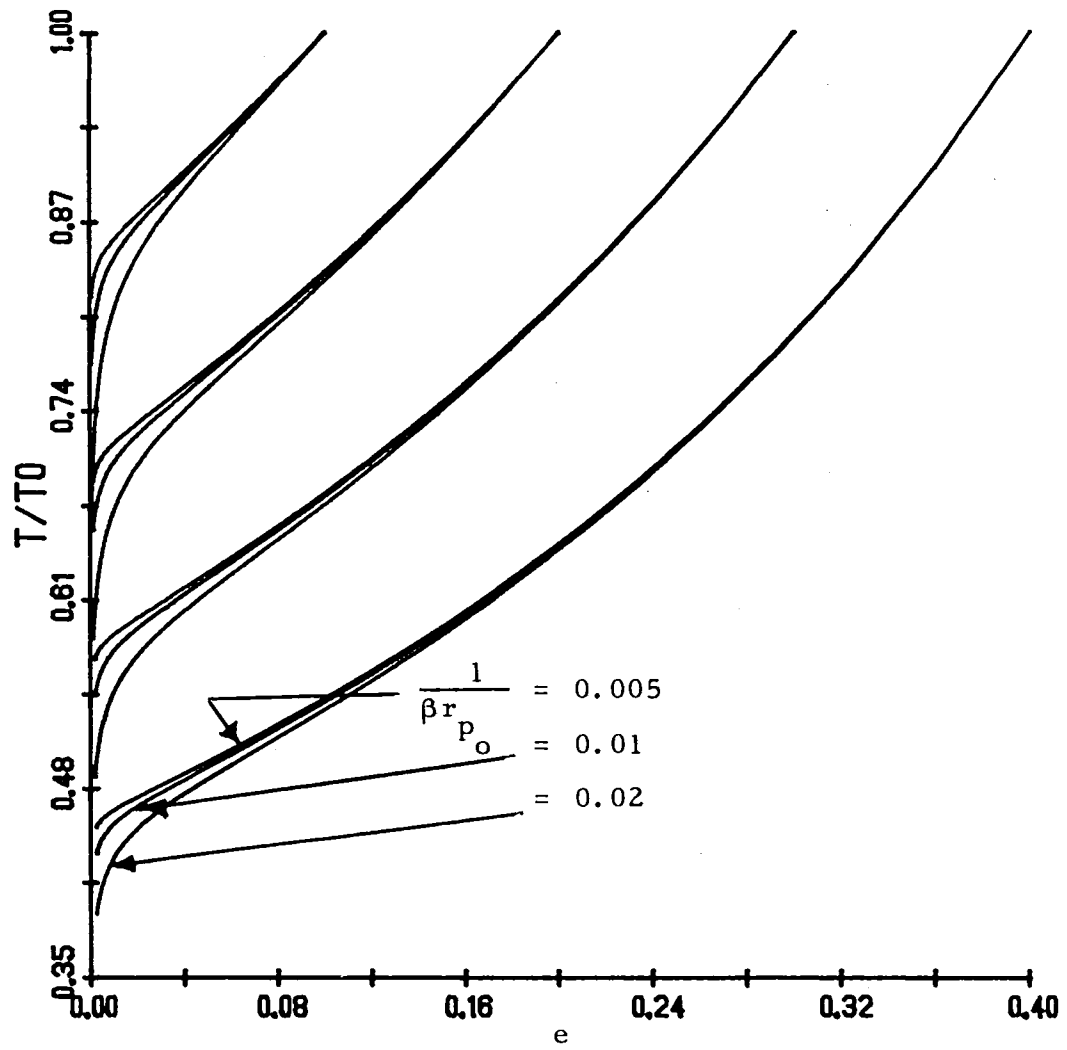


Fig. 4-12. Variations of  $T/T_0$  as Function of  $e$ .

$T/T_0$  = ratio of orbital period to initial orbital period and  $e$  = eccentricity. The plot is generated by Eqs. (4-53), (4-46) and (4-47).

CHAPTER 5  
TIME IN ORBIT

5.1 The Time Equation

The final orbital variable to be determined is the time which is found from Kepler's equation

$$\sqrt{\frac{\mu}{a^3}} t = E - e \sin E \quad (5-1)$$

In its differential form

$$\frac{dt}{dE} = \frac{a^{3/2}}{\sqrt{\mu}} (1 - e \cos E) \quad (5-2)$$

The average equation is simply

$$\frac{dt}{dE} = \frac{a^{3/2}}{\sqrt{\mu}} = \frac{T_o}{2\pi} \left(\frac{a}{a_o}\right)^{3/2} \quad (5-3)$$

where  $T_o$  is the initial orbital period. Since the other elements have been given in parametric form as functions of  $x$ , it would be most convenient to find  $t$  as a function of  $x$  also. Dividing Eq. (5-3) by the average equation for  $x$ , Eq. (4-8), gives the average equation for the time

$$\frac{dt}{dx} = - \frac{T_o r p_o \exp(x_o)}{4\pi \beta a_o^2 z_o} \frac{\exp[\beta a_o (z-1)]}{z^{1/2} \left[ I_1 + \frac{1}{2} e^{(3I_o + I_2)} + \dots \right]} \quad (5-4)$$

The exponential term is found by using the parametric solution for  $z = a/a_o$  from Eq. (4-32).

$$\begin{aligned} \exp[\beta a_o (z-1)] &= \exp[z_1 + \epsilon z_2 + \epsilon^2 z_3 + \dots] \\ &= \exp(z_1) \left[ 1 + \epsilon z_2 + \frac{\epsilon^2}{2} (z_2^2 + 2z_3) + \dots \right] \\ &= \frac{x I_1(x)}{x_o I_1(x_o)} \left[ 1 + \epsilon z_2 + \frac{\epsilon^2}{2} (z_2^2 + 2z_3) + \dots \right] \end{aligned} \quad (5-5)$$

Defining the dimensionless time  $\tau$  as

$$\tau \equiv \frac{2\pi \beta a_o^2 p_o S f C_D}{m T_o} x_o I_1(x_o) \exp(-x_o) t \quad (5-6)$$

the dimensionless time equation takes the form

$$\frac{d\tau}{dx} = - \frac{x \left[ 1 + \epsilon z_2 + \frac{\epsilon^2}{2} (z_2^2 + 2z_3) + \dots \right]}{z^{1/2} \left[ 1 + \frac{\epsilon x}{2z} (3y_o + y_2) + \frac{\epsilon^2 x^2}{8z^2} (11 + y_3) + \dots \right]} \quad (5-7)$$

After substituting for  $z(x)$ , applying the binomial expansion and dividing, Eq. (5-7) becomes

$$\begin{aligned}
\frac{d\tau}{dx} = & -x \left[ 1 - \frac{\epsilon}{2} (z_1 - 2z_2 + 3xy_0 + xy_2) \right. \\
& + \frac{\epsilon^2}{8} (-11x^2 - x^2 y_3 + 18xy_0 z_1 + 6xy_2 z_1 + 18x^2 y_0^2 + 2x^2 y_2^2 \\
& + 12x^2 y_0 y_2 - 12xy_0 z_2 - 4xy_2 z_2 + 3z_1^2 - 4z_2 \\
& \left. - 4z_1 z_2 + 4z_2^2 + 8z_3) \right] \tag{5-8}
\end{aligned}$$

## 5.2 Integration of the Time Equation

It is convenient, but not necessary, to assume the solution of the time equation in the following form

$$\tau = \tau_0 + \epsilon \tau_1 + \epsilon^2 \tau_2 \tag{5-9}$$

Substituting Eq. (5-9) into Eq. (5-8) provides the three differential equations for  $\tau_0$ ,  $\tau_1$  and  $\tau_2$ .

$$\begin{aligned}
\frac{d\tau_0}{dx} &= -x \\
\frac{d\tau_1}{dx} &= (2A_0 - 1)x + \frac{7}{2} xz_1 \\
\frac{d\tau_2}{dx} &= -2x^3 + \frac{1}{2}(7x_0^2 - 8A_0^2 - 11A_0)x + 9x^2 y_0 \\
&\quad - (10 + 7A_0) xz_1 - \frac{63}{8} xz_1^2 \tag{5-10}
\end{aligned}$$

with initial conditions

$$\tau_0(x_0) = \tau_1(x_0) = \tau_2(x_0) = 0 \quad (5-11)$$

Integrating Eqs. (5-10) from  $x_0$  to  $x$ , it is found that

$$\begin{aligned} \tau_0 &= \frac{1}{2} (x_0^2 - x^2) \\ \tau_1 &= \frac{1}{2} (x^2 - x_0^2)(2A_0 - 1) + \frac{7}{4} x^2 z_1 \\ &\quad - \frac{7}{4} \int_{x_0}^x x^2 y_0 dx \\ \tau_2 &= -\frac{1}{2} (x^4 - x_0^4) \\ &\quad + \frac{1}{4} (x^2 - x_0^2)(7x_0^2 - 8A_0^2 - 11A_0) \\ &\quad - \frac{1}{2} x^2 z_1 (10 + 7A_0) - \frac{63}{16} x^2 z_1^2 \\ &\quad + \frac{1}{2} [28 + 7A_0] \int_{x_0}^x x^2 y_0 dx \\ &\quad + \frac{63}{8} \int_{x_0}^x z_1 x^2 y_0 dx \end{aligned} \quad (5-12)$$

Unfortunately, the two integrals  $\int x^2 y_0 dx$  and  $\int z_1 x^2 y_0 dx$  cannot be expressed in terms of known functions. Approximate techniques will be applied in the next section to yield an accurate solution of these integrals.

### 5.3 Approximate Integration of the Unknown Integrals

For the modified Bessel Function  $I_n(x)$  the following series expansion is available for small  $x$  (Beyer, 1976)

$$I_n(x) = \frac{x^n}{2^n n!} \left\{ 1 + \frac{x^2}{2^2 \cdot 1!(n+1)} + \frac{x^4}{2^4 \cdot 2!(n+1)(n+2)} + \frac{x^6}{2^6 \cdot 3!(n+1)(n+2)(n+3)} + \dots \right\} \quad (5-13)$$

For  $n = 0$  and  $n = 1$  this formula becomes

$$I_0(x) = 1 + \left(\frac{x}{2}\right)^2 + \frac{1}{4}\left(\frac{x}{2}\right)^4 + \frac{1}{36}\left(\frac{x}{2}\right)^6 + \frac{1}{576}\left(\frac{x}{2}\right)^8 + \frac{1}{14400}\left(\frac{x}{2}\right)^{10} + \dots$$

$$I_1(x) = \frac{x}{2} + \frac{1}{2}\left(\frac{x}{2}\right)^3 + \frac{1}{12}\left(\frac{x}{2}\right)^5 + \frac{1}{144}\left(\frac{x}{2}\right)^7 + \frac{1}{2880}\left(\frac{x}{2}\right)^9 + \frac{1}{86400}\left(\frac{x}{2}\right)^{11} + \dots \quad (5-14)$$

Dividing the first equation of Eqs. (5-14) by the second gives the series expansion of  $y_{0s}(x)$  for small  $x$  which will be designated  $y_{0s}$ .

$$y_{0s} = \frac{2}{x} + \frac{1}{4}x - \frac{1}{96}x^3 + \frac{1}{1536}x^5 - \frac{1}{23040}x^7 + \frac{13}{4423680}x^9 - \dots \quad (5-15)$$

On the other hand, for large  $x$ , the asymptotic expansion (Abramowitz and Stegun, 1972) is

$$I_n(x) = \frac{e^x}{\sqrt{2\pi x}} \left\{ 1 - \frac{\mu-1}{8x} + \frac{(\mu-1)(\mu-9)}{2!(8x)^2} - \frac{(\mu-1)(\mu-9)(\mu-25)}{3!(8x)^3} + \dots \right\} \quad (5-16)$$

where  $\mu = 4n^2$ . Setting  $n = 0$  and  $n = 1$  gives the asymptotic expansions for  $I_0$  and  $I_1$ .

$$I_0(x) = \frac{e^x}{\sqrt{2\pi x}} \left\{ 1 + \frac{1}{8x} + \frac{9}{128x^2} + \frac{75}{1024x^3} + \frac{3675}{32768x^4} + \frac{59535}{262144x^5} + \dots \right\}$$

$$I_1(x) = \frac{e^x}{\sqrt{2\pi x}} \left\{ 1 - \frac{3}{8x} - \frac{15}{128x^2} - \frac{105}{1024x^3} - \frac{4725}{32768x^4} - \frac{72765}{262144x^5} - \dots \right\} \quad (5-17)$$

After performing the division, the expansion of  $y_0(x)$  for large  $x$  designated by  $y_{0L}$  is

$$y_{0L} = 1 + \frac{1}{2x} + \frac{3}{8x^2} + \frac{3}{8x^3} + \frac{63}{128x^4} + \frac{27}{32x^5} + \dots \quad (5-18)$$

Multiplying Eqs. (5-15) and (5-18) by  $x^2$  and integrating term by term from  $x_0$  to  $x$ , the approximate solution of the first unknown

integral is obtained for small and large values of  $x$ .

$$\int_{x_0}^x x^2 y_{0s} dx = (x^2 - x_0^2) + \frac{1}{16}(x^4 - x_0^4) - \frac{1}{576}(x^6 - x_0^6) \\ + \frac{1}{12288}(x^8 - x_0^8) - \frac{1}{230400}(x^{10} - x_0^{10}) \\ + \frac{13}{53084160}(x^{12} - x_0^{12}) \quad \text{for } x < 3$$

$$\int_{x_0}^x x^2 y_{0L} dx = \frac{1}{3}(x^3 - x_0^3) + \frac{1}{4}(x^2 - x_0^2) + \frac{3}{8}(x - x_0) \\ + \frac{3}{8} \text{Log} \frac{x}{x_0} + \frac{63}{128} \left( \frac{1}{x_0} - \frac{1}{x} \right) + \frac{27}{64} \left( \frac{1}{x_0^2} - \frac{1}{x^2} \right)$$

$$\text{for } x \geq 3 \quad . \quad (5-19)$$

Comparison of the approximate solution (5-19) and the numerical integration of  $x^2 y_0$  indicates a maximum error of 0.3%. Since the integral appears in the  $\epsilon$  term, this is equivalent to an error of 0.003% or less, which is sufficiently accurate.

Next, the second unknown integral which appears in the  $\tau_2$  equation of Eqs. (5-12) must be evaluated.

Integration by parts reveals

$$\int_{x_0}^x z_1 x^2 y_0 dx = z_1 \int x^2 y_0 dx - \int_{x_0}^x \left[ \int x^2 y_0 dx \right] y_0 dx \quad (5-20)$$

The first integral on the right hand side has been solved and the second can be determined easily from the earlier work. By dropping the constants from Eq. (5-19) and then multiplying by Eqs. (5-15) and (5-18) and integrating term by term from  $x_0$  to  $x$ , the integration of Eq. (5-20) can be performed for small and large values of  $x$ .

$$\begin{aligned} \int_{x_0}^x z_1 x^2 y_{0s} dx = z_1 & \left[ x^2 + \frac{1}{16} x^4 - \frac{1}{576} x^6 + \frac{1}{12288} x^8 - \frac{1}{230400} x^{10} + \frac{13}{53084160} x^{12} \right] \\ & - (x^2 - x_0^2) - \frac{3}{32} (x^4 - x_0^4) - \frac{1}{3456} (x^6 - x_0^6) \\ & + \frac{5}{147456} (x^8 - x_0^8) - \frac{299}{110592000} (x^{10} - x_0^{10}) \\ & + \frac{623}{3185049600} (x^{12} - x_0^{12}) \quad \text{for } x < 3 \end{aligned}$$

$$\begin{aligned} \int_{x_0}^x z_1 x^2 y_{0L} dx = z_1 & \left[ \frac{1}{3} x^3 + \frac{1}{4} x^2 + \frac{3}{8} x + \frac{3}{8} \text{Log } x - \frac{63}{128x} - \frac{27}{64x^2} \right] \\ & - \frac{1}{12} (x^4 - x_0^4) - \frac{5}{36} (x^3 - x_0^3) - \frac{5}{16} (x^2 - x_0^2) \\ & - \frac{1}{32} (x - x_0) + \frac{9}{512} \left( \frac{1}{x} - \frac{1}{x_0} \right) + \frac{9}{256} \left( \frac{1}{x^2} - \frac{1}{x_0^2} \right) \\ & + \text{Log } x \left[ -\frac{3}{8} x + \frac{3}{32} - \frac{3}{32} \text{Log } x + \frac{9}{64x} + \frac{9}{128x^2} \right] \end{aligned}$$

$$- \text{Log } x_o \left[ -\frac{3}{8} x_o + \frac{3}{32} - \frac{3}{32} \text{Log } x_o + \frac{9}{64x_o} + \frac{9}{128x_o^2} \right]$$

for  $x \geq 3$  (5-21)

The exact integration of  $z_1 x^2 y_o$  was determined numerically by computer and compared to Eqs. (5-21). The greatest error was found to be less than 1%. Since the integral appears in the  $\epsilon^2$  term the error is of the order 0.0001%. Thus, Eqs. (5-12), (5-19) and (5-21) give the solution of the dimensionless time  $\tau$  as a function of  $x$  to a high degree of accuracy. Now, for any value of the parameter  $x$ , the semi-major axis, eccentricity, periapsis, apoapsis, period and the time can be computed. The solutions are very useful in determining the total lifetime of the satellite as well. For example, the final value of one of the orbital elements such as periapsis or period can be specified for orbit decay and the corresponding  $x_f$  can be put into the time solution to obtain an accurate estimate of the satellite's lifetime.

In order to provide a formula for the maximum lifetime, the limit of  $\tau_o$ ,  $\tau_1$  and  $\tau_2$  will be taken as  $x_f \rightarrow 0$ . This can be done by inspection for most of the terms in Eqs. (5-12). For the remaining terms, L'Hospital's Rule is applied. For example,

$$\begin{aligned}
\lim_{x \rightarrow 0} x^2 z_1 &= \lim_{x \rightarrow 0} \frac{z_1}{\frac{1}{2x}} = \lim_{x \rightarrow 0} \frac{y_0}{-2x^{-3}} \\
&= \lim_{x \rightarrow 0} -\frac{1}{2} x^3 \left( \frac{2}{x} + \frac{1}{4} x - \frac{1}{96} x^3 + \dots \right) \\
&= 0
\end{aligned}
\tag{5-22}$$

Similarly,

$$\lim_{x \rightarrow 0} x^2 z_1^2 = \lim_{x \rightarrow 0} x z_1 \lim_{x \rightarrow 0} x z_1$$

and

$$\begin{aligned}
\lim_{x \rightarrow 0} x z_1 &= \lim_{x \rightarrow 0} \frac{z_1}{\frac{1}{x}} = \lim_{x \rightarrow 0} \frac{y_0}{-x^{-2}} \\
&= \lim_{x \rightarrow 0} -x^2 \left( \frac{2}{x} + \frac{1}{4} x - \dots \right) \\
&= 0
\end{aligned}$$

so that

$$\lim_{x \rightarrow 0} x^2 z_1^2 = 0
\tag{5-23}$$

Thus, the maximum lifetime of the satellite is the finite quantity  $\tau_{L \max}$

$$\begin{aligned}
\tau_{L_{\max}} = & \frac{1}{2} x_o^2 + \epsilon \left[ -\frac{1}{2} (2A_o - 1) x_o^2 - \frac{7}{4} \int_{x_o}^0 x^2 y_o dx \right] \\
& + \epsilon^2 \left[ \frac{1}{2} x_o^4 - \frac{1}{4} (7x_o^2 - 8A_o^2 - 11A_o) x_o^2 \right. \\
& + \frac{1}{2} (28 + 7A_o) \int_{x_o}^0 x^2 y_o dx \\
& \left. + \frac{63}{8} \int_{x_o}^0 z_1 x^2 y_o dx \right] \tag{5-24}
\end{aligned}$$

where the integrals are evaluated by Eqs. (5-19) and (5-21). It should be noted that the lifetime obtained from Eq. (5-24) is the maximum and that it is possible that the entry phase may commence at an earlier time, when  $x_f$  is not yet equal to zero, as mentioned earlier.

The accuracy of Eqs. (5-24) and (5-12) along with Eqs. (5-19) and (5-21) has been tested by comparing the analytic solution to the numerical integration of Eq. (5-8). The greatest error found is in the fourth or fifth digit which is sufficiently accurate when the range of validity is restricted to small eccentricities,  $0 < e < 0.2$ .

Since the maximum lifetime is expressed as a function of  $x_o$  and  $\epsilon$ ,  $\tau_{L_{\max}} = \tau_L(x_o, \epsilon)$ , in Eq. (5-24) the final equation can also be put in terms of  $e_o$  and  $\epsilon$ ,  $\tau_{L_{\max}} = \tau_L(e_o, \epsilon)$ . It is

interesting to note that for very small values of eccentricity, the classical parabolic law is deduced.

$$\epsilon^2 \tau_{L_{\max}} = \frac{1}{2} e_o^2 \quad (5-25)$$

So that, as a rough estimate, the time in orbit is proportional to the square of the eccentricity. The expression for  $\tau_{L_{\max}}$  given by Eqs. (5-24), (5-19) and (5-21) provides a substantial improvement both in accuracy and range of application over the classical parabolic law.

## CHAPTER 6

### BALLISTIC ENTRY

#### 6.1 The Ballistic Entry Equations

Near the final stages of orbit decay the orbit circularizes and the entry phase is imminent. The universal entry equations (2-18) still apply. For  $C_L = 0$  and  $\beta r = \text{constant}$ , the equations become

$$\frac{dZ}{ds} = -\beta r Z \tan \gamma$$

$$\frac{du}{ds} = -\frac{2\sqrt{\beta r}}{\cos \gamma} Zu - u \tan \gamma$$

$$\frac{d\gamma}{ds} = 1 - \frac{\cos^2 \gamma}{u}$$

$$\frac{d\alpha}{ds} = 1$$

$$\frac{d\Omega}{ds} = 0$$

$$\frac{di}{ds} = 0 \tag{6-1}$$

From the last three equations of (6-1) it is apparent that  $s$  is equivalent to  $\alpha$ , the angle between the ascending node and the position vector, and that  $\Omega$  and  $i$  are constants. This reduces the

problem to third order.

$$\begin{aligned}\frac{dZ}{d\alpha} &= -\beta r Z \tan \gamma \\ \frac{du}{d\alpha} &= -\frac{2\sqrt{\beta r}}{\cos \gamma} Z u - u \tan \gamma \\ \frac{d\gamma}{d\alpha} &= 1 - \frac{\cos^2 \gamma}{u}\end{aligned}\tag{6-2}$$

Using the variable

$$v = \frac{v^2}{gr} = \frac{u}{\cos^2 \gamma}\tag{6-3}$$

changes Eqs. (6-2) to

$$\begin{aligned}\frac{dZ}{d\alpha} &= -\beta r Z \tan \gamma \\ \frac{dv}{d\alpha} &= -\frac{2\sqrt{\beta r}}{\cos \gamma} Z v \left[ 1 - \frac{\sin \gamma}{2\sqrt{\beta r} Z} \left( 1 - \frac{2}{v} \right) \right] \\ \frac{d\gamma}{d\alpha} &= 1 - \frac{1}{v}\end{aligned}\tag{6-4}$$

Eqs. (6-4) apply to the motion of any ballistic vehicle in a nonrotating atmosphere from the initial time in orbit to the instant of contact with the surface of the planet. The atmospheric density varies exponentially with altitude and the  $\beta r$  term is assumed to be a constant approximately equal to 900. The dependent variables  $Z$ ,  $v$  and  $\gamma$  are the modified Chapman variable for altitude, the nondimensional velocity squared and the flight path angle. The

significance of the modified Chapman variable  $Z$  is that it allows a single trajectory solution for a given initial velocity and flight path angle to be computed which applies to every possible ballistic satellite, regardless of the mass, surface area or drag coefficient. This means that for particular initial conditions on the velocity and flight path angle, every satellite follows the same trajectory in terms of  $Z$ . The only difference is the particular altitude, which depends directly on the satellite parameters. Thus a single analytic solution has a wide range of application. Furthermore, using the modified Chapman variable the resulting equations are free of the restrictions of the original Chapman formulation, as discussed by Vinh and Brace, 1974, so that the exact tables of  $Z$  functions for entry analyses can now be generated to replace those of Chapman and Kappahn, 1961.

In the next three sections, three distinct analytic theories are developed to cover the cases of ballistic entry from circular orbit, ballistic entry from nearly circular orbit and ballistic entry at moderate and large initial flight path angles. This is due to the fact that singularities arise in the treatment of the problem as a result of dividing either the first or the second of Eqs. (6-4) by the other two and integrating. Unfortunately it does not seem possible

to have a single analytic solution which is uniformly valid for all values of initial flight path angles because of the nature of the problem. In the case of atmospheric entry from circular orbit, the magnitude of the flight path angle, initially zero, rapidly increases, approaching  $90^\circ$  as the velocity becomes small. On the other hand, for steep angle entry, the flight path angle changes very little--of the order of tenths of a degree--as the nondimensional velocity decreases from unity to one tenth the original value (between Mach 2 and 3). The zero order terms of the two theories are totally different, which indicates that separate theories are necessary. The entry theory for large and moderate flight path angles has as its small parameter

$$\bar{\epsilon} = \frac{1}{\beta r \bar{v}_i^2 \tan^2 \gamma_i}$$

where  $\bar{v}_i$  and  $\gamma_i$  are the initial nondimensional velocity squared and the initial flight path angle, respectively. Obviously, when the magnitude of  $\gamma_i$  becomes small a new small parameter must be found. For small initial flight path angles a simple power series solution is found by assuming the magnitude of  $\gamma_i$  is small and  $Z_0$  is zero. The same approach is not available for the zero initial flight path angle analysis, since both initial derivatives are zero and all the terms of the power series would be identically zero. Following the choice of

variables used by Yaroshevskii (1964), the problem is resolved in such a way that the initial point is a singularity, but has the proper behavior as the independent variable approaches zero. The Yaroshevskii solution is found as the zero order term and then a first order term is added, which greatly increases the accuracy.

In the next sections the entry from circular orbit is developed first, since it represents the final stages of the majority of decaying orbits. Next, the small angle theory is presented and finally the moderate and large angle theory, which applies to the case in which entry is usually accomplished on the first orbit from an initially highly eccentric orbit.

## 6.2 Entry from Circular Orbit

The planar entry equations (6-4) will now be considered for entry from circular orbit. Dividing the first and third equation of Eqs. (6-4) by the second gives

$$\frac{dZ}{dv} = \frac{\sqrt{\beta r} \sin \gamma}{2v} \frac{1}{\left[ 1 - \frac{\sin \gamma}{2\sqrt{\beta r} Z} \left( 1 - \frac{2}{v} \right) \right]}$$

$$\frac{d\gamma}{dv} = \frac{(1-v) \cos \gamma}{2\sqrt{\beta r} Z v^2} \frac{1}{\left[ 1 - \frac{\sin \gamma}{2\sqrt{\beta r} Z} \left( 1 - \frac{2}{v} \right) \right]} \quad (6-5)$$

with  $Z$  and  $\gamma$  as the dependent variables which are initially nearly zero and  $v$  as the independent variable, initially one and assumed to decrease to less than one hundredth as the final condition.

Precise initial and final conditions cannot be put on  $Z$  without the knowledge of the satellite parameters. To surmount this difficulty, the final orbit was defined as that orbit in which the initial  $Z$  was such that the satellite's velocity reduced to one tenth the circular velocity, while the longitude reached 360 degrees. In most cases, this definition provides the entire trajectory including or beyond the point of surface contact. Only in the case of very low density entry vehicles, such as balloons, would the definition have to be modified.

The development of the theory is facilitated by the following change of variables:

$$\begin{aligned}
Y &= 2Z \\
\Phi &= -\sqrt{\beta r} \sin \gamma \\
X &= -\text{Log } v \\
\epsilon &= \frac{1}{\beta r}
\end{aligned} \tag{6-6}$$

Note that all the new variables are positive. Rewriting Eqs. (6-5) in terms of these,

$$\begin{aligned}
\frac{dY}{dX} &= \frac{\Phi}{1 + \frac{\epsilon \Phi}{Y} (1 - 2e^X)} \\
\frac{d\Phi}{dX} &= \frac{(1 - \epsilon \Phi^2)(e^X - 1)}{Y \left[ 1 + \frac{\epsilon \Phi}{Y} (1 - 2e^X) \right]}
\end{aligned} \tag{6-7}$$

Expanding Eqs. (6-7) to one term in  $\epsilon$

$$\begin{aligned}
\frac{dY}{dX} &= \Phi \left[ 1 + \frac{\epsilon \Phi}{Y} (2e^X - 1) \right] \\
\frac{d\Phi}{dX} &= \frac{(1 - \epsilon \Phi^2)(e^X - 1)}{Y} \left[ 1 + \frac{\epsilon \Phi}{Y} (2e^X - 1) \right]
\end{aligned} \tag{6-8}$$

Poincaré's method of small parameters for integration of a system of equations can now be demonstrated. Assume to the first order a solution of the form

$$\begin{aligned}
\Phi &= \Phi_0 + \epsilon \Phi_1 \\
Y &= Y_0 + \epsilon Y_1
\end{aligned} \tag{6-9}$$

Substituting Eqs. (6-9) into Eqs. (6-8) results in two systems of two first order differential equations.

$$\frac{dY_o}{dX} = \Phi_o$$

$$\frac{d\Phi_o}{dX} = \frac{e^X - 1}{Y_o} \quad (6-10)$$

$$\frac{dY_1}{dX} = \Phi_1 + \frac{\Phi_o^2}{Y_o} (2e^X - 1)$$

$$\frac{d\Phi_1}{dX} = \frac{(e^X - 1)}{Y_o} \left[ \frac{\Phi_o}{Y_o} (2e^X - 1) - \Phi_o^2 - \frac{Y_1}{Y_o} \right] \quad (6-11)$$

Eqs. (6-10) must be solved first. They can be put in the form of a second order differential equation.

$$\frac{d^2 Y_o}{dX^2} = \frac{e^X - 1}{Y_o} \quad (6-12)$$

with initial conditions

$$Y_o(0) = 0, \quad \Phi_o(0) = 0 \quad (6-13)$$

An attempt to solve Eq. (6-12) by assuming a solution of the form  $Y_o = a_o + a_1 X + a_2 X^2 + \dots$  fails because the initial conditions (6-13) force the  $a_i$  to be identically zero. Apparently, the first

term is neither a constant nor a linear function of X. Yaroshevskii's approach will be employed to find the first term of the series.

For very small values of X,  $\nu \rightarrow 1$  and Eq. (6-12) becomes

$$Y_o \frac{d^2 Y_o}{dX^2} \approx X \quad (6-14)$$

The solution of Eq. (6-14) is easily found by assuming  $Y_o = c X^n$  and solving for c and n to obtain

$$Y_o \approx \frac{2}{\sqrt{3}} X^{3/2}$$

$$\frac{dY_o}{dX} = \Phi_o \approx \frac{3}{\sqrt{3}} X^{1/2} \quad (6-15)$$

which satisfy the initial conditions (6-13) as  $X \rightarrow 0$ .

With the insight gained from the analysis of Eq. (6-14), the solution to Eq. (6-12) will be

$$Y_o = \frac{2}{\sqrt{3}} X^{3/2} y \quad (6-16)$$

with

$$y = 1 + a_1 X + a_2 X^2 + a_3 X^3 + a_4 X^4 + \dots \quad (6-17)$$

Using Eqs. (6-16) and (6-17) in Eq. (6-12) provides

$$Xy + 4X^2 \frac{dy}{dX} + \frac{4}{3} X^3 \frac{d^2 y}{dX^2} = \frac{e^X - 1}{y} \quad (6-18)$$

Expanding the exponential term and substituting for  $y$  and its derivatives allows the  $a_i$  terms to be found after equating coefficients of like powers in  $X$ . Thus,

$$Y_0 = \frac{2}{\sqrt{3}} X^{3/2} \left[ 1 + \frac{1}{3} \left( \frac{X}{4} \right) + \frac{1}{6} \left( \frac{X}{4} \right)^2 + \frac{47}{594} \left( \frac{X}{4} \right)^3 + \frac{20021}{605880} \left( \frac{X}{4} \right)^4 \right] \quad (6-19)$$

$$\Phi_0 = \sqrt{3} X^{1/2} \left[ 1 + \frac{5}{9} \left( \frac{X}{4} \right) + \frac{7}{18} \left( \frac{X}{4} \right)^2 + \frac{47}{198} \left( \frac{X}{4} \right)^3 + \frac{20021}{165240} \left( \frac{X}{4} \right)^4 \right] \quad (6-20)$$

Next, the second system of differential equations, Eqs. (6-11) corresponding to the  $\epsilon$  term will be solved. The resulting second order equation in  $Y_1$  is

$$\frac{d^2 Y_1}{dX^2} + \left( \frac{e^X - 1}{Y_0^2} \right) Y_1 = \frac{\Phi_0}{Y_0} \left\{ (e^X - 1) \left[ \frac{3(2e^X - 1)}{Y_0} - \Phi_0 \right] + 2e^X \Phi_0 - (2e^X - 1) \frac{\Phi_0^2}{Y_0} \right\} \quad (6-21)$$

The correct form for the series solution of  $Y_1$  can be obtained by letting  $Y_1 = c X^n$  and solving Eq. (6-21) for the lowest power of  $X^n$ . From this it is found that the  $Y_1$  series solution must be in

the form

$$Y_1 = \frac{7\sqrt{3}}{3} X^{3/2} y_1$$

$$y_1 = 1 + b_1 X + b_2 X^2 + b_3 X^3 + \dots \quad (6-22)$$

Before substituting Eqs. (6-22) into Eq. (6-21), it is convenient to let

$$C = \frac{e^X - 1}{X}$$

$$D = 2e^X - 1$$

$$Y_o = \frac{2X^{3/2}}{\sqrt{3}} A$$

$$\Phi_o = \sqrt{3} X^{1/2} B \quad (6-23)$$

Now, with Eqs. (6-22) and (6-23) put into Eq. (6-21)

$$A^2 \left( \frac{3}{4} y_1 + 3X \frac{dy_1}{dX} + X^2 \frac{d^2 y_1}{dX^2} \right) + \frac{3}{4} C y_1 =$$

$$\frac{9}{14} \frac{B}{X} \left\{ \frac{3}{2} D(C-B^2) + \frac{X}{2} B A (D+3) \right\} \quad (6-24)$$

Expanding A, B, C and D,

$$A = 1 + \frac{1}{3} \left( \frac{X}{4} \right) + \frac{1}{6} \left( \frac{X}{4} \right)^2 + \frac{47}{594} \left( \frac{X}{4} \right)^3 + \frac{20021}{605880} \left( \frac{X}{4} \right)^4$$

$$B = 1 + \frac{5}{9} \left( \frac{X}{4} \right) + \frac{7}{18} \left( \frac{X}{4} \right)^2 + \frac{47}{198} \left( \frac{X}{4} \right)^3 + \frac{20021}{165240} \left( \frac{X}{4} \right)^4$$

$$C = 1 + 2 \left(\frac{X}{4}\right) + \frac{8}{3} \left(\frac{X}{4}\right)^2 + \frac{8}{3} \left(\frac{X}{4}\right)^3 + \frac{32}{15} \left(\frac{X}{4}\right)^4$$

$$D = 1 + 8 \left(\frac{X}{4}\right) + 16 \left(\frac{X}{4}\right)^2 + \frac{64}{3} \left(\frac{X}{4}\right)^3 + \frac{64}{3} \left(\frac{X}{4}\right)^4 \quad (6-25)$$

After substituting Eqs. (6-25) and (6-22) into Eq. (6-24) and equating coefficients of like powers of X, the  $Y_1$  solution is found.

$$Y_1 = \frac{7\sqrt{3}}{3} X^{3/2} \left[ 1 + \frac{65}{63} \left(\frac{X}{4}\right) + \frac{105047}{79002} \left(\frac{X}{4}\right)^2 + \frac{191876677}{132960366} \left(\frac{X}{4}\right)^3 \right] \quad (6-26)$$

The solution for  $\Phi_1$  is

$$\Phi_1 = \frac{7\sqrt{3} X^{1/2}}{2} \left\{ 1 + \frac{325}{189} \left(\frac{X}{4}\right) + \frac{105047}{33858} \left(\frac{X}{4}\right)^2 + \frac{191876677}{44320122} \left(\frac{X}{4}\right)^3 \right\} - \frac{(2e^X - 1)}{Y_0} \Phi_0^2 \quad (6-27)$$

Thus, the solution for reentry from circular orbit has been found in Eqs. (6-9), (6-19), (6-20), (6-26) and (6-27). It is interesting to note that the Yaroshevskii solution appears as the zero order term. With the first order term included, the accuracy

is greatly improved. The only drawback is that the  $\Phi_1$  expression, Eq. (6-27), has a singularity at  $X = 0$  due to the  $\Phi_0^2 / Y_0$  term. However, the Yaroshevskii solution is not accurate near values of  $X \approx 0$ , and so the defect in the present theory is more than compensated for by the large gain in accuracy.

### 6.3 Entry from Nearly Circular Orbits

If the entry phase initiates before the orbit has completed circularization, then a new theory must be applied which takes into account a small initial flight path angle. An approximate theory can easily be developed assuming

$$\sqrt{\beta r} \ Z \ v \gg \left( \frac{2-v}{2} \right) \left| \sin \gamma \right| \quad (6-28)$$

where the term on the left hand side is the deceleration in g's due to the atmospheric drag. This assumption is valid for a large portion of the entry trajectory. It is violated initially when the deceleration is very small, but this effect is only transient. The only other violation occurs at the final stage of entry when the magnitude of the flight path angle,  $\gamma$ , becomes large and the dimensionless velocity squared,  $v$ , is small. By this time the essential features of the entry dynamics such as peak deceleration and peak heating rate have already occurred. With these consider-

ations, assumption (6-28) is justified and Eqs. (6-4) become

$$\begin{aligned}\frac{dZ}{d\alpha} &= -\beta r Z \tan \gamma \\ \frac{dv}{d\alpha} &= -\frac{2\sqrt{\beta r} Z v}{\cos \gamma} \\ \frac{d\gamma}{d\alpha} &= 1 - \frac{1}{v}\end{aligned}\tag{6-29}$$

Dividing the first and third equations of Eqs. (6-29) by the second equation ,

$$\begin{aligned}\frac{dZ}{dv} &= \frac{\sqrt{\beta r}}{2v} \sin \gamma \\ \frac{d\gamma}{dv} &= \frac{(1-v) \cos \gamma}{2\sqrt{\beta r} Z v^2}\end{aligned}\tag{6-30}$$

Now, Eqs. (6-30) can be transformed by the change of variables

$$\begin{aligned}\bar{Y} &= \frac{2Z}{\sqrt{\beta r}} \\ \bar{\Phi} &= -\sin \gamma \\ X &= -\text{Log } v \\ \epsilon &= \frac{1}{\beta r}\end{aligned}\tag{6-31}$$

to

$$\begin{aligned}\frac{d\bar{Y}}{dX} &= \bar{\Phi} \\ \frac{d\bar{\Phi}}{dX} &= \frac{\epsilon (e^X - 1)(1 - \bar{\Phi}^2)}{\bar{Y}}\end{aligned}\tag{6-32}$$

with the initial conditions

$$\begin{aligned}\bar{Y}(0) &\approx 0 \\ \bar{\Phi}(0) &= \bar{\Phi}_0 = -\sin \gamma_i\end{aligned}\tag{6-33}$$

The equations will be integrated by Poincaré's method of small parameters. Assume

$$\begin{aligned}\bar{Y} &= \bar{Y}_0 + \epsilon \bar{Y}_1 + \epsilon^2 \bar{Y}_2 \\ \bar{\Phi} &= \bar{\Phi}_0 + \epsilon \bar{\Phi}_1 + \epsilon^2 \bar{\Phi}_2\end{aligned}\tag{6-34}$$

Substituting Eqs. (6-34) into Eqs. (6-32) gives the three systems of two first order differential equations.

$$\begin{aligned}\frac{d\bar{Y}_0}{dX} &= \bar{\Phi}_0 \\ \frac{d\bar{\Phi}_0}{dX} &= 0\end{aligned}\tag{6-35}$$

$$\frac{d\bar{Y}_1}{dX} = \bar{\Phi}_1$$

$$\frac{d\bar{\Phi}_1}{dX} = \frac{(e^X - 1)}{\bar{Y}_0} (1 - \bar{\Phi}_0^2) \quad (6-36)$$

$$\frac{d\bar{Y}_2}{dX} = \bar{\Phi}_2$$

$$\frac{d\bar{\Phi}_2}{dX} = \left( \frac{e^X - 1}{\bar{Y}_0} \right) \left( \frac{\bar{Y}_1}{\bar{Y}_0} \bar{\Phi}_0^2 - \frac{\bar{Y}_1}{\bar{Y}_0} - 2\bar{\Phi}_0\bar{\Phi}_1 \right) \quad (6-37)$$

The initial conditions are

$$\bar{\Phi}_0(0) = \bar{\Phi}_0 = -\sin \gamma_i$$

$$\bar{Y}_0(0) = \bar{Y}_1(0) = \bar{Y}_2(0) = 0$$

$$\bar{\Phi}_1(0) = \bar{\Phi}_2(0) = 0 \quad (6-38)$$

The solution of Eqs. (6-35) is simply

$$\bar{\Phi}_0(X) = \bar{\Phi}_0$$

$$\bar{Y}_0(X) = \bar{\Phi}_0 X \quad (6-39)$$

To solve Eqs. (6-36), first expand the exponential term and find  $\bar{\Phi}_1$  .

$$\frac{d\bar{\Phi}_1}{dX} = \left( \frac{1 - \bar{\Phi}_0^2}{\bar{\Phi}_0} \right) \left( 1 + \frac{X}{2!} + \frac{X^2}{3!} + \dots + \frac{X^{n-1}}{n!} + \dots \right) \quad (6-40)$$

So that

$$\begin{aligned} \bar{\Phi}_1 &= \left( \frac{1 - \bar{\Phi}_0^2}{\bar{\Phi}_0} \right) \left( X + \frac{X^2}{2 \cdot 2!} + \dots + \frac{X^n}{n \cdot n!} + \dots \right) \\ \bar{\Phi}_1(X) &= \left( \frac{1 - \bar{\Phi}_0^2}{\bar{\Phi}_0} \right) \sum_{n=1}^{\infty} \frac{X^n}{n \cdot n!} \end{aligned} \quad (6-41)$$

Next,  $\bar{Y}_1$  can be found by integrating Eq. (6-41) .

$$\begin{aligned} \bar{Y}_1(X) &= \left( \frac{1 - \bar{\Phi}_0^2}{\bar{\Phi}_0} \right) \int \sum_{n=1}^{\infty} \frac{X^n}{n \cdot n!} dx \\ &= \left( \frac{1 - \bar{\Phi}_0^2}{\bar{\Phi}_0} \right) \sum_{n=1}^{\infty} \frac{X^{n+1}}{n \cdot (n+1)!} \end{aligned} \quad (6-42)$$

In a similar way the last set of equations (6-37) can be integrated to give

$$\begin{aligned} \bar{\Phi}_2(X) &= - \left( \frac{1 - \bar{\Phi}_0^2}{\bar{\Phi}_0} \right) \left( \sum_{n=1}^{\infty} \frac{X^n}{n \cdot n!} \right)^2 \\ &\quad - \frac{(1 - \bar{\Phi}_0^2)^2}{\bar{\Phi}_0^3} \sum_{m=1}^{\infty} \sum_{n=1}^{\infty} \frac{X^{n+m}}{(n+m)m!n(n+1)!} \end{aligned}$$

$$\begin{aligned}
\bar{Y}_2(X) &= - \left( \frac{1 - \bar{\Phi}_0^2}{\bar{\Phi}_0} \right) \sum_{m=1}^{\infty} \sum_{n=1}^{\infty} \frac{X^{m+n+1}}{(m+n+1)m \cdot m! \cdot n \cdot n!} \\
&\quad - \frac{(1 - \bar{\Phi}_0^2)^2}{\bar{\Phi}_0^3} \sum_{m=1}^{\infty} \sum_{n=1}^{\infty} \frac{X^{n+m+1}}{(n+m+1)(n+m)m! \cdot n(n+1)!}
\end{aligned} \tag{6-43}$$

The particular form of the solutions makes computation by computer very easy. It would be convenient to have the first few terms of the series.

Explicitly,

$$\begin{aligned}
\bar{\Phi}_2(X) &= - \left( \frac{1 - \bar{\Phi}_0^2}{\bar{\Phi}_0} \right) \left( X^2 + \frac{1}{2} X^3 + \frac{25}{144} X^4 + \frac{7}{144} X^5 + \dots \right) \\
&\quad - \frac{(1 - \bar{\Phi}_0^2)^2}{\bar{\Phi}_0^3} \left( \frac{1}{4} X^2 + \frac{1}{9} X^3 + \frac{5}{144} X^4 + \frac{7}{800} X^5 + \dots \right) \\
\bar{Y}_2(X) &= - \left( \frac{1 - \bar{\Phi}_0^2}{\bar{\Phi}_0} \right) \left( \frac{1}{3} X^3 + \frac{1}{8} X^4 + \frac{5}{144} X^5 + \frac{7}{864} X^6 + \dots \right) \\
&\quad - \frac{(1 - \bar{\Phi}_0^2)^2}{\bar{\Phi}_0^3} \left( \frac{1}{12} X^3 + \frac{1}{36} X^4 + \frac{1}{144} X^5 + \frac{7}{4800} X^6 + \dots \right)
\end{aligned} \tag{6-44}$$

Thus, the entry from nearly circular orbit problem has been solved to second order in Eqs. (6-34), (6-39), (6-41), (6-42)

and (6-43). The appearance of the  $(1 - \bar{\Phi}_0^2) / \bar{\Phi}_0$  term indicates the limitation of the theory to small  $\bar{\Phi}_0$ ; very small values and large values of  $\bar{\Phi}_0$  are excluded. For very small  $\bar{\Phi}_0$ , the theory of entry from circular orbit can be used. For large and moderate values, a third analytic theory must be developed. With these considerations in mind, the theory for small initial flight path angles is restricted to the range  $2.5^\circ \leq -\gamma_i \leq 7^\circ$ .

Next, the solution will be used to determine the speed at which the peak deceleration occurs. The deceleration in g's is given by

$$G = \frac{1}{2} \beta r \bar{Y}(X) e^{-X} \quad (6-45)$$

Differentiating Eq. (6-45) with respect to X and setting the result equal to zero gives the equation for X at which maximum deceleration occurs.

$$\frac{d\bar{Y}(X)}{dX} = \bar{Y}(X) \quad (6-46)$$

Putting the expressions for the  $\bar{Y}_i$  into Eq. (6-46) gives the formula for the critical value of X and consequently the speed during maximum deceleration.

$$\begin{aligned}
X = 1 + \frac{\epsilon}{\tan^2 \gamma_i} & \left[ \sum_{n=1}^{\infty} \frac{(n+1-X) X^n}{n \cdot (n+1)!} \right] \\
- \frac{\epsilon^2}{\tan^2 \gamma_i} & \left[ \left( \sum_{n=1}^{\infty} \frac{X^n}{n \cdot n!} \right)^2 - \sum_{m=1}^{\infty} \sum_{n=1}^{\infty} \frac{X^{m+n+1}}{(m+n+1)m \cdot m! \cdot n \cdot n!} \right] \\
- \frac{\epsilon^2}{\tan^4 \gamma_i} & \left[ \sum_{m=1}^{\infty} \sum_{n=1}^{\infty} \frac{(n+m+1-X) X^{n+m}}{(n+m+1)(n+m)m! \cdot n \cdot (n+1)!} \right] \quad (6-47)
\end{aligned}$$

As a crude approximation,  $X = 1$  for maximum deceleration which gives  $v = e^{-1} = 0.36788$  or

$$\frac{v}{\sqrt{gr}} = e^{-1/2} = 0.60653 \quad (6-48)$$

This is the classical solution for steep angle entry in which the flight path angle remains nearly constant and the peak drag force occurs when the speed has reduced to 0.60653 of the circular speed. Using  $X = 1$  in Eq. (6-45) gives a rough estimate of the peak g's.

$$G_{\max} = -\frac{1}{2} \beta r \sin \gamma_i e^{-1} \quad (6-49)$$

Inspection of Eq. (6-47) reveals that for small angle entry the critical value of  $X$  is larger than 1, which corresponds to lower speeds. One method of obtaining the correct value of  $X$  would be

by numerical computation. Since  $X = f(X)$ , the first value of  $X$  must be guessed ( $X = 1$  would be a good start) and a second value is generated from the equation. If  $|f'(X)| < 1$ , which is generally valid here, the sequence  $X_1 = f(X_0)$ ,  $X_2 = f(X_1)$ ,  $\dots$ , converges to the unique root  $X^* = f(X^*)$ .

It would be most convenient to have an accurate explicit solution for the critical value of  $X$ . Fortunately, Lagrange's expansion can be applied (Eq. (4-45)) to Eq. (6-47) up to the first order term to give a good approximate solution.

$$X = 1 + \frac{\epsilon}{\tan^2 \gamma_i} \sum_{n=1}^{\infty} \frac{(n+1-X) X^n}{n(n+1)!} \quad (6-50)$$

So that

$$X = 1 + \frac{\epsilon}{\tan^2 \gamma_i} \left( \frac{1}{2!} + \frac{1}{3!} + \frac{1}{4!} + \frac{1}{5!} + \dots \right)$$

or

$$X = 1 + \frac{\epsilon (e-2)}{\tan^2 \gamma_i} \quad (6-51)$$

This simple formula gives the explicit value of  $X$  and, hence the speed, at which the peak deceleration occurs. For small initial flight path angles, it correctly indicates that the peak drag force occurs at lower velocities. In the range of small initial entry angles,

$2.5^\circ \leq -\gamma_i \leq 7^\circ$ , the expression accurately predicts the critical speed to within 2% of the actual value.

#### 6.4 Ballistic Entry at Moderate and Large Initial Flight Path Angles

Although it is unlikely that a satellite undergoing orbit decay due to atmospheric drag would begin entry phase at a large flight path angle, there are certain cases such as return from the moon and atmospheric capture of probes to other planets in which an analytic theory for large initial flight path angles would be highly desirable and useful. In order to give a complete description of the entry phase for ballistic trajectories, the large and moderate initial flight path angle theory will be developed.

Eqs. (6-4) will once again be used, but this time the first equation will be divided into the other two, providing

$$\begin{aligned} \frac{dv}{dZ} &= \frac{2v}{\sqrt{\beta r} \sin \gamma} \left[ 1 - \frac{\sin \gamma}{2\sqrt{\beta r} Z} \left( 1 - \frac{2}{v} \right) \right] \\ \frac{d\gamma}{dZ} &= \frac{1-v}{\beta r Z v \tan \gamma} \end{aligned} \quad (6-52)$$

Eqs. (6-52) are ideal for analyzing the entry phase at steep entry angles. The dependent variables are the nondimensional velocity squared and the flight path angle  $\gamma$ , while the independent variable is now the modified Chapman variable  $Z$ . When  $v_i = 1$  the flight path angle remains nearly constant throughout most of the entry phase

while  $Z$  rapidly increases and  $v$  decreases. Initially,  $\frac{dy}{dZ} = 0$  and remains small until the very end of the trajectory when  $v$  is small and the flight path angle suddenly decreases to nearly  $-90^\circ$ . The known behavior of Eqs. (6-52) suggests an appropriate change of variables.

Let the variables be transformed according to the following

$$\begin{aligned}\bar{S} &= \frac{\sin \gamma_i}{\sin \gamma} \\ \eta &= -\frac{2Z}{\sqrt{\beta r} \sin \gamma_i} \\ \epsilon &= \frac{1}{\beta r} = \text{constant}\end{aligned}\tag{6-53}$$

so that

$$\begin{aligned}\frac{dv}{d\eta} + v\bar{S}\left(1 + \frac{\epsilon}{S\eta}\right) &= \frac{2\epsilon}{\eta} \\ \frac{d\bar{S}}{d\eta} &= \frac{\epsilon(v-1)\bar{S}}{v\eta} \left[ \frac{\bar{S}^2 - \sin^2 \gamma_i}{\sin^2 \gamma_i} \right]\end{aligned}\tag{6-54}$$

Examination of Eqs. (6-54) reveals that Poincaré's method of small parameters can once again be employed.

Assuming

$$\begin{aligned}v &= v_0 + \epsilon v_1 + \epsilon^2 v_2 + \dots \\ \bar{S} &= S_0 + \epsilon S_1 + \epsilon^2 S_2 + \dots\end{aligned}\tag{6-55}$$

with initial conditions

$$\begin{aligned}
 v_o &= v(\eta_1) = v_i \\
 S_o &= \bar{S}(\eta_1) = S_i = 1 \\
 v_1(\eta_1) &= v_2(\eta_1) = \dots = 0 \\
 S_1(\eta_1) &= S_2(\eta_1) = \dots = 0
 \end{aligned} \tag{6-56}$$

Since  $\frac{dS_o}{d\eta} = 0$ ,  $S_o = 1$  and Eqs. (6-55) become

$$\begin{aligned}
 v &= v_o + \epsilon v_1 + \epsilon^2 v_2 + \dots \\
 \bar{S} &= 1 + \epsilon S_1 + \epsilon^2 S_2 + \dots
 \end{aligned} \tag{6-57}$$

Eqs. (6-57) will now be substituted into Eqs. (6-54) to obtain the three systems

$$\begin{aligned}
 \frac{dv_o}{d\eta} + v_o &= 0 \\
 \frac{dS_o}{d\eta} &= 0
 \end{aligned} \tag{6-58}$$

$$\begin{aligned}
 \frac{dv_1}{d\eta} + v_1 + v_o S_1 + \frac{v_o}{\eta} &= \frac{2}{\eta} \\
 \frac{dS_1}{d\eta} = \frac{1}{\tan^2 \gamma_i} \left( \frac{1}{\eta} - \frac{1}{v_o \eta} \right) &
 \end{aligned} \tag{6-59}$$

$$\frac{dv_2}{d\eta} + v_2 + v_1 S_1 + v_o S_2 + \frac{v_1}{\eta} = 0$$

$$\frac{dS_2}{d\eta} = \frac{2}{\sin^2 \gamma_i} \left(1 - \frac{1}{v_o}\right) \frac{S_1}{\eta} + \frac{1}{\tan^2 \gamma_i} \left(\frac{S_1}{\eta} - \frac{S_1}{v_o \eta} + \frac{v_1}{\eta v_o^2}\right)$$

(6-60)

Note that the solution for  $S_o$  has already been substituted into Eqs.

(6-59) and (6-60). The integration of Eqs. (6-58) is easy

$$v_o = \overline{v}_i e^{-\eta}$$

$$S_o = 1 \tag{6-61}$$

where

$$\overline{v}_i = v_i e^{\eta_i} \tag{6-62}$$

The zero order term is the classical approximate solution of the Chapman entry equation (Chapman, 1959). Note that any initial velocity and altitude are incorporated into the solution.

Substituting the  $v_o$  expression into the flight path angle equation of Eqs. (6-59) provides

$$\frac{dS_1}{d\eta} = \frac{1}{\tan^2 \gamma_i} \left(\frac{1}{\eta} - \frac{1}{\eta \overline{v}_i} e^{\eta}\right) \tag{6-63}$$

Integrating

$$S_1 = \frac{1}{\tan^2 \gamma_i} \text{Log} \frac{\eta}{\eta_i} - \frac{1}{\overline{v_i} \tan^2 \gamma_i} \left[ E_i(\eta) - E_i(\eta_i) \right] \quad (6-64)$$

where  $E_i(\eta)$  is the exponential integral

$$E_i(\eta) = \int \frac{e^{-\eta}}{\eta} d\eta \quad (6-65)$$

which is discussed in Section 4.6.

Now the  $v_1$  equation of Eqs. (6-59) can be solved by variation of parameters.

$$v_1 = C_1(\eta) e^{-\eta} \quad (6-66)$$

Putting Eq. (6-66) into the  $v_1$  equation gives the equation for  $C_1$

$$\begin{aligned} \frac{dC_1}{d\eta} &= e^{\eta} \left[ \frac{2}{\eta} - v_o S_1 - \frac{v_o}{\eta} \right] \\ &= \frac{2e^{\eta}}{\eta} - \frac{\overline{v_i}}{\tan^2 \gamma_i} \text{Log} \frac{\eta}{\eta_i} \\ &\quad + \frac{1}{\tan^2 \gamma_i} \left[ E_i(\eta) - E_i(\eta_i) \right] - \frac{\overline{v_i}}{\eta} \end{aligned} \quad (6-67)$$

Upon integrating

$$\begin{aligned}
C_1(\eta) = \frac{1}{\tan^2 \gamma_i} & \left\{ \left[ E_i(\eta) - E_i(\eta_i) \right] (2 \tan^2 \gamma_i + \eta) \right. \\
& - \bar{v}_i \operatorname{Log} \frac{\eta}{\eta_i} (\eta + \tan^2 \gamma_i) \\
& \left. + \bar{v}_i (\eta - \eta_i) - (e^\eta - e^{\eta_i}) \right\} . \quad (6-68)
\end{aligned}$$

The integrations of Eqs. (6-60) are performed in much the same way, but they are much more laborious. It is convenient to put the final results in the form

$$\begin{aligned}
v &= \bar{v}_i e^{-\eta} \left[ 1 + \bar{\epsilon} f_1(\eta) + \bar{\epsilon}^2 f_2(\eta) + \dots \right] \\
\bar{S} &= 1 + \bar{\epsilon} g_1(\eta) + \bar{\epsilon}^2 g_2(\eta) + \dots \quad (6-69)
\end{aligned}$$

where

$$\begin{aligned}
\bar{\epsilon} &= \frac{1}{\beta r \bar{v}_i \tan^2 \gamma_i} \\
\eta &= - \frac{2Z}{\sqrt{\beta r} \sin \gamma_i} \\
\bar{S} &= \frac{\sin \gamma_i}{\sin \gamma} \\
\bar{v}_i &= v_i e^{\eta_i} \quad (6-70)
\end{aligned}$$

and

$$\begin{aligned}
g_1 &= \bar{v}_i L - E_o \\
g_2 &= \bar{v}_i (e^\eta - e^{\eta_i}) - \bar{v}_i e^\eta L + \frac{\bar{v}_i^2}{v_i} \left( \frac{3}{2} + \tan^2 \gamma_i \right) L^2 \\
&\quad + \left[ \bar{v}_i - \bar{v}_i \eta_i + e^{\eta_i} + e^\eta - 3\bar{v}_i (1 + \tan^2 \gamma_i) L \right] E_o \\
&\quad + \left( \frac{3}{2} + 2 \tan^2 \gamma_i \right) E_o^2 - 2E_o (2\eta) + \bar{v}_i \tan^2 \gamma_i F \\
f_1 &= \bar{v}_i (\eta - \eta_i) - (e^\eta - e^{\eta_i}) - \bar{v}_i (\tan^2 \gamma_i + \eta) L + (2 \tan^2 \gamma_i + \eta) E_o \\
f_2 &= \bar{v}_i \left[ e^{\eta_i} - \bar{v}_i (3 + 2 \tan^2 \gamma_i) \right] (\eta - \eta_i) + \frac{1}{2} \frac{\bar{v}_i^2}{v_i} (\eta - \eta_i)^2 \\
&\quad + \bar{v}_i (3 - \eta) (e^\eta - e^{\eta_i}) - \frac{1}{2} (e^{2\eta} - e^{2\eta_i}) \\
&\quad + \bar{v}_i \left[ \bar{v}_i \eta_i (3 + 2 \tan^2 \gamma_i) - (2 + \tan^2 \gamma_i) e^{\eta_i} \right. \\
&\quad \left. + \bar{v}_i (3 + \tan^2 \gamma_i - \eta) (\eta - \eta_i) + (\eta - 2) (e^\eta - e^{\eta_i}) \right] L \\
&\quad + \frac{1}{2} \frac{\bar{v}_i^2}{v_i} (\tan^4 \gamma_i - 3\eta + \eta^2) L^2 \\
&\quad + \left[ \bar{v}_i (2 + \tan^2 \gamma_i) - 4\bar{v}_i \eta + \bar{v}_i \eta^2 + \bar{v}_i \eta (3 - \eta) L + (2 - \eta) e^\eta \right] E_o \\
&\quad + \frac{1}{2} \eta (\eta - 3) E_o^2 + 2(\eta - 1) E_o (2\eta) - \bar{v}_i \tan^2 \gamma_i (2 \tan^2 \gamma_i + \eta) F
\end{aligned} \tag{6-71}$$

where

$$\begin{aligned}
L &= \text{Log} \frac{\eta}{\eta_i} \\
E_o &= E_i(\eta) - E_i(\eta_i) = \int_{\eta_i}^{\eta} \frac{e^x}{x} dx
\end{aligned}$$

$$E_o(2\eta) = E_i(2\eta) - E_i(2\eta_i)$$

$$F = \int_{\eta_i}^{\eta} \frac{E_i(x) - E_i(x_i)}{x} dx \quad (6-72)$$

During the entry phase the altitude variable,  $\eta$ , is initially zero and generally less than 5 when the velocity of the space vehicle has been reduced to less than Mach 3. Thus, the exponential integrals in Eqs. (6-72) should be evaluated for small  $\eta$ . Expanding the exponential term and integrating term by term, gives for  $E_o$

$$\begin{aligned} E_o &= \int_{\eta_i}^{\eta} \frac{1+x+\frac{x^2}{2!}+\dots}{x} dx \\ &= \text{Log} \left( \frac{\eta}{\eta_i} \right) + (\eta - \eta_i) + \frac{1}{2! \cdot 2} (\eta^2 - \eta_i^2) \\ &\quad + \frac{1}{3 \cdot 3!} (\eta^3 - \eta_i^3) + \dots \\ &= \text{Log} \left( \frac{\eta}{\eta_i} \right) + \sum_{n=1}^{\infty} \frac{\eta^n - \eta_i^n}{n \cdot n!} \end{aligned} \quad (6-73)$$

F is found by substituting Eq. (6-73) into the last of Eqs. (6-72).

$$\begin{aligned} F &= \frac{1}{2} \left( \text{Log} \frac{\eta}{\eta_i} \right)^2 - \text{Log} \frac{\eta}{\eta_i} \sum_{n=1}^{\infty} \frac{\eta_i^n}{n \cdot n!} \\ &\quad + \sum_{n=1}^{\infty} \frac{\eta^n - \eta_i^n}{n^2 n!} \end{aligned} \quad (6-74)$$

The solution for the moderate and large initial flight path angle theory is very accurate and has a wide range of application as discussed in the next section. It should be remarked in passing that the theory is necessarily limited to large and moderate flight path angles simply because the small parameter ,

$$\bar{\epsilon} = \frac{1}{\beta r \bar{v}_i \tan^2 \gamma_i}$$

becomes large for small flight path angles.

Next, the solution will be used to obtain an expression for the value of  $\eta$  at which the maximum deceleration occurs. The deceleration in g's is given by

$$G = \sqrt{\beta r} Z v \tag{6-75}$$

The stationary value of G is found from

$$\frac{dZ}{d\eta} v + Z \frac{dv}{d\eta} = 0 \tag{6-76}$$

With the second of Eqs. (6-53) and the first of Eqs. (6-54),

$$v(1 - \bar{S}\eta) + \epsilon(2 - v) = 0 \tag{6-77}$$

To the zero order,  $\epsilon = 0$ ,  $\bar{S} = S_0 = 1$ , which gives the zero order approximation for the altitude at which the peak deceleration occurs

$$\eta = 1 \tag{6-78}$$

The solution can be improved by using the exact equation (6-77) in the form

$$\eta = 1 + \bar{\epsilon} Q(\eta) \quad (6-79)$$

where

$$Q(\eta) = \frac{\left[ -\bar{v}_i \tan^2 \gamma_i - g_1 + \frac{2e^{\eta} \tan^2 \gamma_i}{(1+\bar{\epsilon}f_1 + \bar{\epsilon}^2 f_2)} - \bar{\epsilon} g_2 \right]}{\left[ 1 + \bar{\epsilon} g_1 + \bar{\epsilon}^2 g_2 \right]} \quad (6-80)$$

The transcendental Eq. (6-79) is in a form suitable for the application of Lagrange's expansion. Using Eq. (4-45) with  $\eta$  replacing  $z$  and  $Q(p)$  replacing  $\phi(p)$ , the equation for  $\eta$  becomes

$$\eta = p + \sum_{n=1}^{\infty} \frac{\bar{\epsilon}^n}{n!} \left( \frac{d}{dp} \right)^{n-1} \left[ Q(p) \right]^n \quad (6-81)$$

for small  $\bar{\epsilon}$ . To the first order in  $\bar{\epsilon}$  the value of  $\eta$  at the peak deceleration is given by

$$\eta = 1 + \bar{\epsilon} \left\{ \left[ E_i(1) - E_i(\eta_i) \right] + (2e - \bar{v}_i) \tan^2 \gamma_i + \bar{v}_i \text{Log } \eta_i \right\} \quad (6-82)$$

Eq. (6-82) indicates that the altitude at which the peak deceleration occurs is sensitive to the initial velocity due to the  $\bar{v}_i \text{Log } \eta_i$  term where  $\eta_i$  is very small. Thus, an improved solution is provided which gives the altitude and velocity at the point of greatest drag force for any initial velocity and for large and moderate entry angles in the range  $5^\circ \leq -\gamma_i < 90^\circ$ .

For entry at circular speeds,  $\overline{v}_i = 1$  and the  $\text{Log } \eta_i$  term cancels with the expansion of  $E_i(\eta_i)$ .

Assuming  $\eta_i \approx 0$ ,

$$\sum_{n=1}^{\infty} \frac{1^n - \eta_i^n}{n \cdot n!} \approx \sum_{n=1}^{\infty} \frac{1^n}{n \cdot n!} = 1.31790$$

the altitude at peak deceleration can be computed from

$$Z = -\frac{1}{2} \sqrt{\beta r} \eta \sin \gamma_i \approx -\frac{1}{2} \sqrt{\beta r} \sin \gamma_i \left[ 1 + \frac{1}{\beta r \tan^2 \gamma_i} \left\{ 1.31790 + (2e - 1) \tan^2 \gamma_i \right\} \right] \quad (6-83)$$

which gives very accurate results for  $5^\circ \leq -\gamma_i < 90^\circ$ . As a crude estimate  $\eta = 1$ , in Eq. (6-78), which gives the classical result for the critical velocity and the maximum deceleration.

$$\frac{V}{\sqrt{gr}} \approx e^{-1/2} = 0.60653$$

$$G_{\max} \approx -\frac{1}{2} \beta r \sin \gamma_i e^{-1} \quad (6-84)$$

## 6.5 Applications of the Ballistic Entry Theories

For convenience, the three analytic theories for ballistic entry of Section 6.2, 6.3 and 6.4 will be referred to as the zero angle theory, the small angle theory and the large angle theory respectively, where the angle is the initial flight path angle. The purpose of this section is to discuss the relative merits, ranges of applications and accuracies of these theories.

Fig. (6-1) plots the aerodynamic deceleration versus  $v$  for zero and small initial flight path angles with  $\beta r = 900$  using the equation

$$G = \sqrt{\beta r} Z v \quad (6-85)$$

The dashed line indicates the exact numerical integration of Eqs. (6-4) while the solid line represents the zero and small angle theories. Inspection of the plot reveals the relative accuracy of the small angle theory. In the case of the zero angle theory, however, the solution is very accurate, giving 4 digits of accuracy at the maximum deceleration of 8.3 g's. Note that the high accuracy of the zero angle theory applies to all values of  $v$  from  $v_i = 1$  down to  $v \approx 0.01$ , which corresponds to a velocity of about Mach 2.5 or less. The small angle theory is limited in range of application. For larger angles,  $\gamma_i = 10^\circ$ , there is an obvious discrepancy

between the analytic and numerical solutions which disappears as the magnitude of the initial flight path angle is reduced. For very small values of  $-\gamma_i$ , the small angle theory suffers from the fact that the higher order terms begin to diverge. This is due to the appearance of  $\epsilon / \sin \gamma_i$  in the first order and  $\epsilon^2 / \sin^3 \gamma_i$  in the second order terms of the analytic solution. Taking just two terms in X from Eq. (6-42) and the two largest terms in X from Eq. (6-44)

$$\epsilon \bar{Y}_1 \approx - \frac{\epsilon \cos^2 \gamma_i}{\sin \gamma_i} \left( \frac{1}{2} X^2 + \frac{1}{12} X^3 \right)$$

$$\epsilon^2 \bar{Y}_2 \approx \frac{\epsilon^2 \cos^4 \gamma_i}{\sin^3 \gamma_i} \left( \frac{1}{12} X^3 + \frac{1}{36} X^4 \right)$$

and then taking the ratio to have a rough convergence test

$$\left| \frac{\epsilon^2 \bar{Y}_2}{\epsilon \bar{Y}_1} \right| = \frac{\epsilon}{\tan^2 \gamma_i} \frac{(X^2 + 3X)}{(3X + 18)} < 1 \quad (6-86)$$

it is evident that for very small values of  $-\gamma_i$  the series is no longer convergent. For example, when  $-\gamma_i = 1^\circ$ , for  $X > 1.385$ , or  $v < 0.25$ , condition (6-86) is violated. In the figure it is apparent that this crude analysis is overly conservative and that actually the small angle theory is limited to the range  $2.5^\circ \leq -\gamma_i \leq 7^\circ$ .

In Fig. (6-2) the flight path angle is plotted versus  $v$  for the

zero and small angle theories. Once again, the zero angle theory is very accurate, but the error in the small angle theory is detectable. From Eqs. (6-41) and (6-44), a rough convergence test can be done for the flight path angle solution of the small angle theory.

$$\left| \frac{\epsilon^2 \bar{\Phi}_2}{\epsilon \bar{\Phi}_1} \right| = \frac{\epsilon}{\tan^2 \gamma_i} \frac{(4X^2 + 9X)}{9(X+4)} < 1 \quad (6-87)$$

For  $-\gamma_i \leq 2^\circ$ , this condition is violated when  $X > 3.254$  or when  $v < 0.0386$ . On the other hand, for  $-\gamma_i \leq 1^\circ$  the series diverges for  $X > 0.954$  or when  $v < 0.385$ .

The errors due to divergence in the higher order terms cause the analytic solution of the flight path angle to be less negative than the numerical value. The plot generation of the small angle theory is stopped when the absolute error exceeds the absolute error obtained if the zero angle theory were used instead. From the figure it is apparent that regardless of initial flight path angle, the final phase behaves in much the same way as the zero angle entry.

Fig. (6-3) plots the  $\text{Log}(Z/Z_0)$  versus  $v$ , which by the definition of

$$Z = \frac{\rho S C_D}{2m} \sqrt{\frac{r}{\beta}} = \frac{\rho S C_D r}{2m \sqrt{\beta r}}$$

is

$$\begin{aligned}
\text{Log } \frac{Z}{Z_o} &= \text{Log} \left( \frac{r}{r_o} e^{\beta (r - r_o)} \right) \\
&= \text{Log } \frac{r}{r_o} - \beta (r - r_o) \\
&\approx \beta (r_o - r)
\end{aligned} \tag{6-88}$$

which is the drop in altitude of the entry vehicle. The error in both theories is quite small. Numerical computation indicates that at maximum deceleration the zero angle theory gives 5 digits of accuracy for  $\text{Log } \frac{Z}{Z_o}$  which amounts to an error of approximately 3 meters for typical earth reentry.

In Figs. (6-4) - (6-6) , plots of aerodynamic deceleration in g's , flight path angle and  $\text{Log} (Z/Z_o)$  have been made as a function of  $v$  for large and moderate flight path angles. The large angle theory is very accurate for large angles and has a wide range of applications for small angles. The plots show ranges of initial flight path angles of  $-60^\circ$  down to  $-1^\circ$  to indicate the range of applicability in  $v$ . The theory actually overlaps the small angle theory, providing a definite improvement in the case of  $\gamma_i = -10^\circ$  . The main defect in the large angle theory is the same as in the others-- the higher order terms eventually diverge. The radius of convergence of the higher order terms depends on the initial flight path angle,  $\gamma_i$  ,

and the initial value of the velocity squared,  $v_i$ . This is evident from the definition of  $\bar{\epsilon} = \epsilon / \overline{v_i} \tan^2 \gamma_i$ , which must be small to insure the convergence of the analytic solution of the nonlinear differential equations by Poincaré's method of small parameters. As a result, when  $-\gamma_i$  is small,  $\bar{\epsilon}$  becomes large, and the range of validity of the solution is restricted to small values of the independent variable  $\eta$ . Furthermore, by the definition  $\eta = -2Z / \sqrt{\beta r} \sin \gamma_i$ , small values of  $-\gamma_i$  will make  $\eta$  larger at any value of  $Z$ . This further restricts the application to high altitudes and correspondingly to large values of the speed. It is interesting to note from the numerical computations that even for very small  $-\gamma_i$ , for example,  $-\gamma_i = 1^\circ$ , the large angle theory gives very accurate results in the highly restricted region, providing 6 digits of accuracy for the peak velocity and 3 digits for the minimum flight path angle. An error analysis reveals that the magnitude of the difference between the analytic solution of  $v(\eta)$  and the numerical integration of the differential equations (6-4) is approximated by  $e/2 (\beta r)^2 \tan^4 \gamma_i$  during maximum deceleration. For  $-60^\circ \leq \gamma_i \leq -5^\circ$  this heuristic formula predicts an error which is generally an order of magnitude greater than the true error. The effect of the initial flight path angle is clearly indicated by the error formula. However,

even when the initial flight path angle is  $-5^\circ$ , the large angle theory gives 3 digits of accuracy at the time of maximum deceleration.

For  $\gamma_i = -60^\circ$ , the theory is extremely accurate, giving 7 digits of accuracy for the  $v(Z)$ .

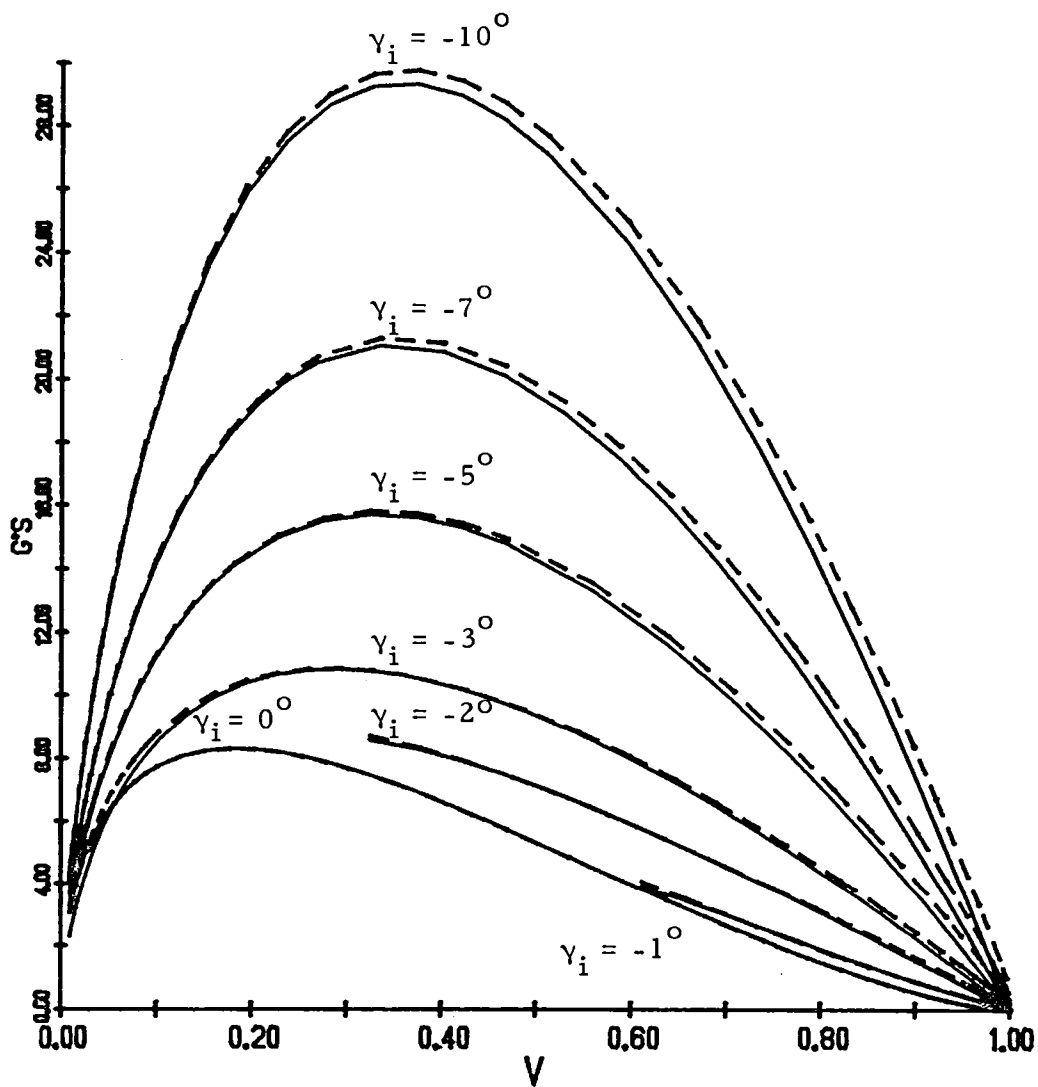


Fig. 6-1. Variations of G's as Function of v.

G's = aerodynamic deceleration,  $v$  = dimensionless velocity squared =  $V^2/gr$  and  $\gamma_i$  = initial flight path angle. The dashed line indicates the exact numerical solution while the solid line represents the analytic solution from Eqs. (6-85), (6-6), (6-9), (6-19), (6-26), (6-31), (6-34), (6-39), (6-42) and (6-43).

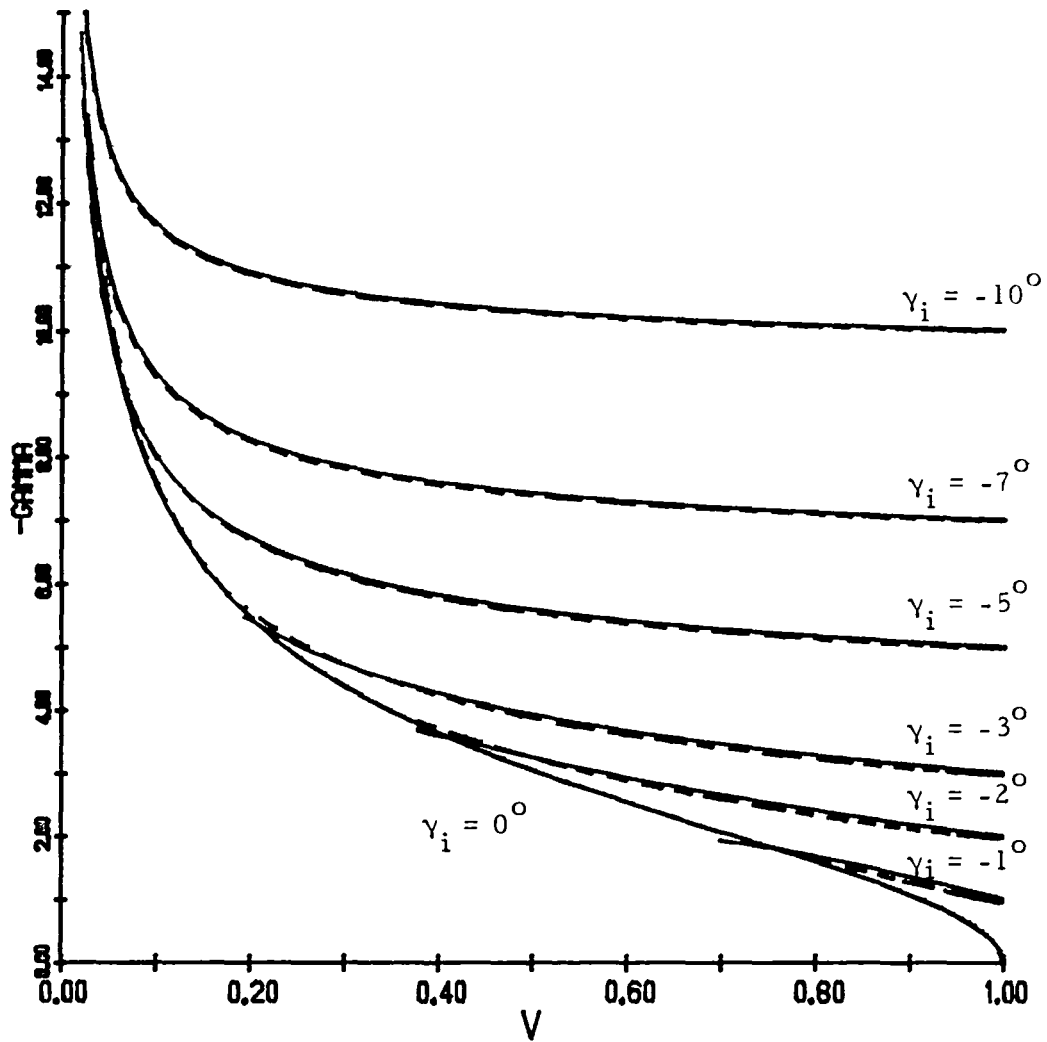


Fig. 6-2. Variations of  $-\gamma$  as Function of  $v$ .

$\gamma$  = flight path angle,  $v$  = dimensionless velocity squared =  $V^2/gr$  and  $\gamma_i$  = initial flight path angle. The dashed line indicates the exact numerical solution while the solid line represents the analytic solution from Eqs. (6-6), (6-9), (6-20), (6-27), (6-31), (6-34), (6-39), (6-41) and (6-43).

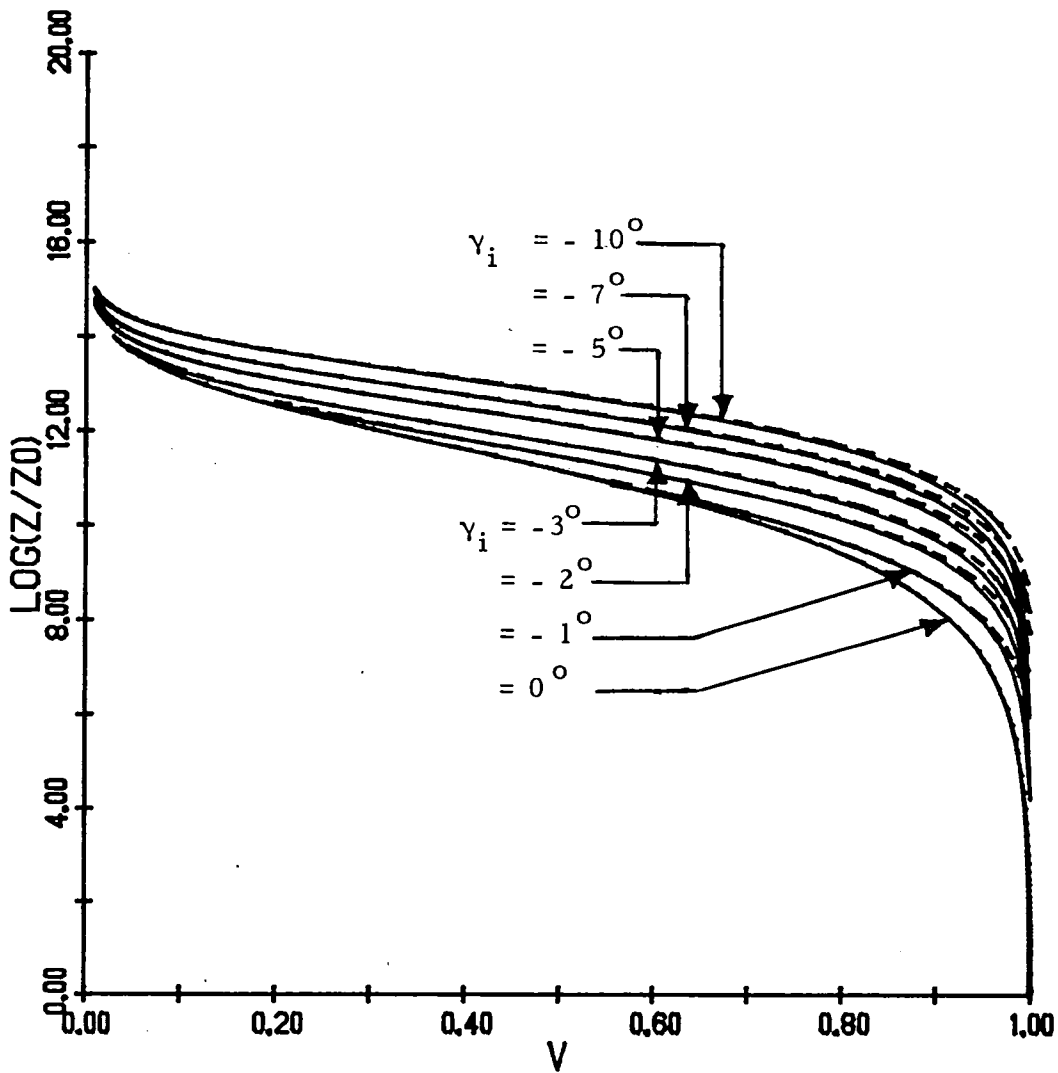


Fig. 6-3. Variations of  $\text{Log}(Z/Z_0)$  as Function of  $v$ .

$\text{Log}(Z/Z_0) \approx (r_0 - r)/H =$  drop in altitude in units of scale height

$v =$  dimensionless velocity squared  $= V^2/gr$  and

$\gamma_i =$  initial flight path angle. The dashed line indicates the exact numerical solution while the solid line represents the analytic solution from Eqs. (6-6), (6-9), (6-19), (6-26), (6-31), (6-34), (6-39), (6-42) and (6-43).

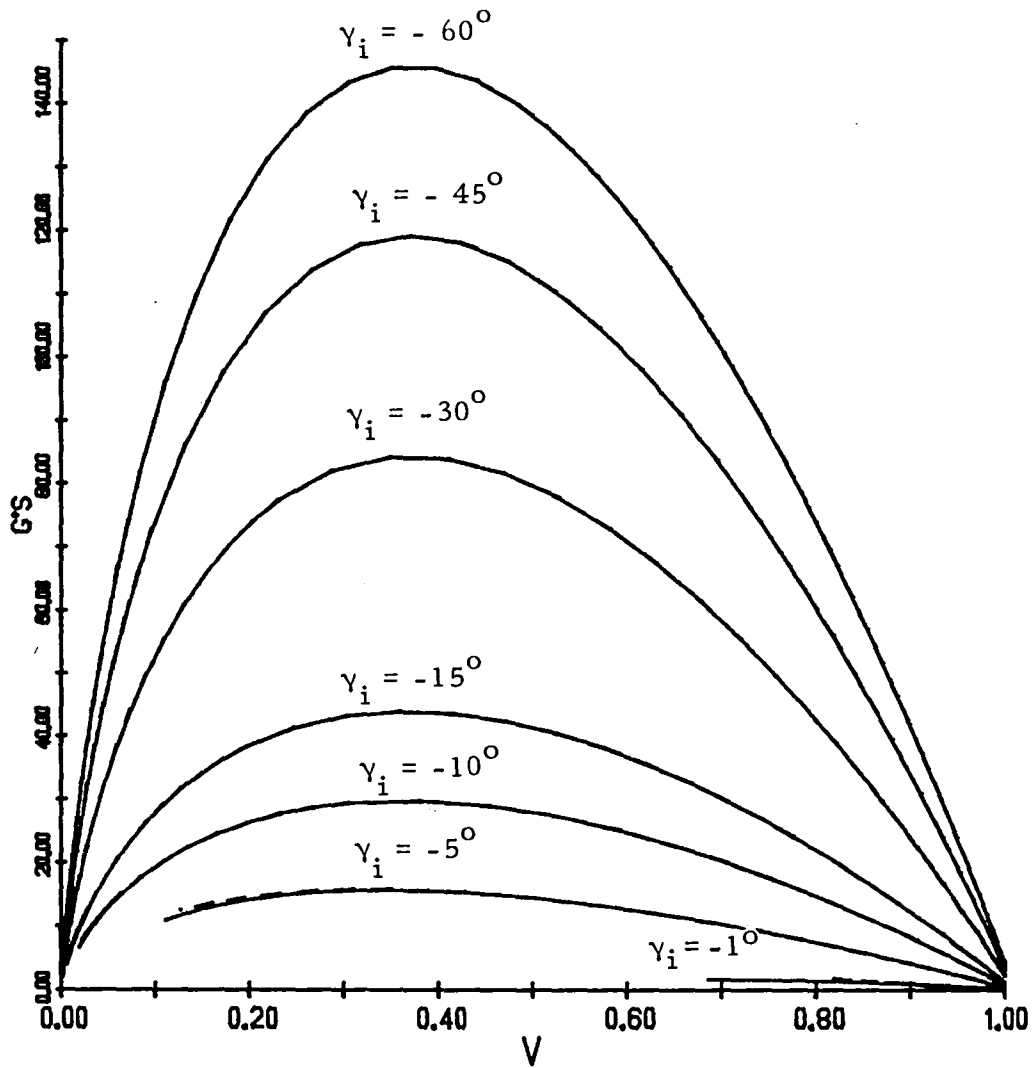


Fig. 6-4. Variations of G's as Function of v.  
 G's = aerodynamic deceleration in g's and  $v =$   
 dimensionless velocity squared =  $V^2 / gr$ .  
 The dashed line indicates the exact numerical  
 solution while the solid line represents the  
 analytic solution from Eqs. (6-85) and (6-69) -  
 (6-72).

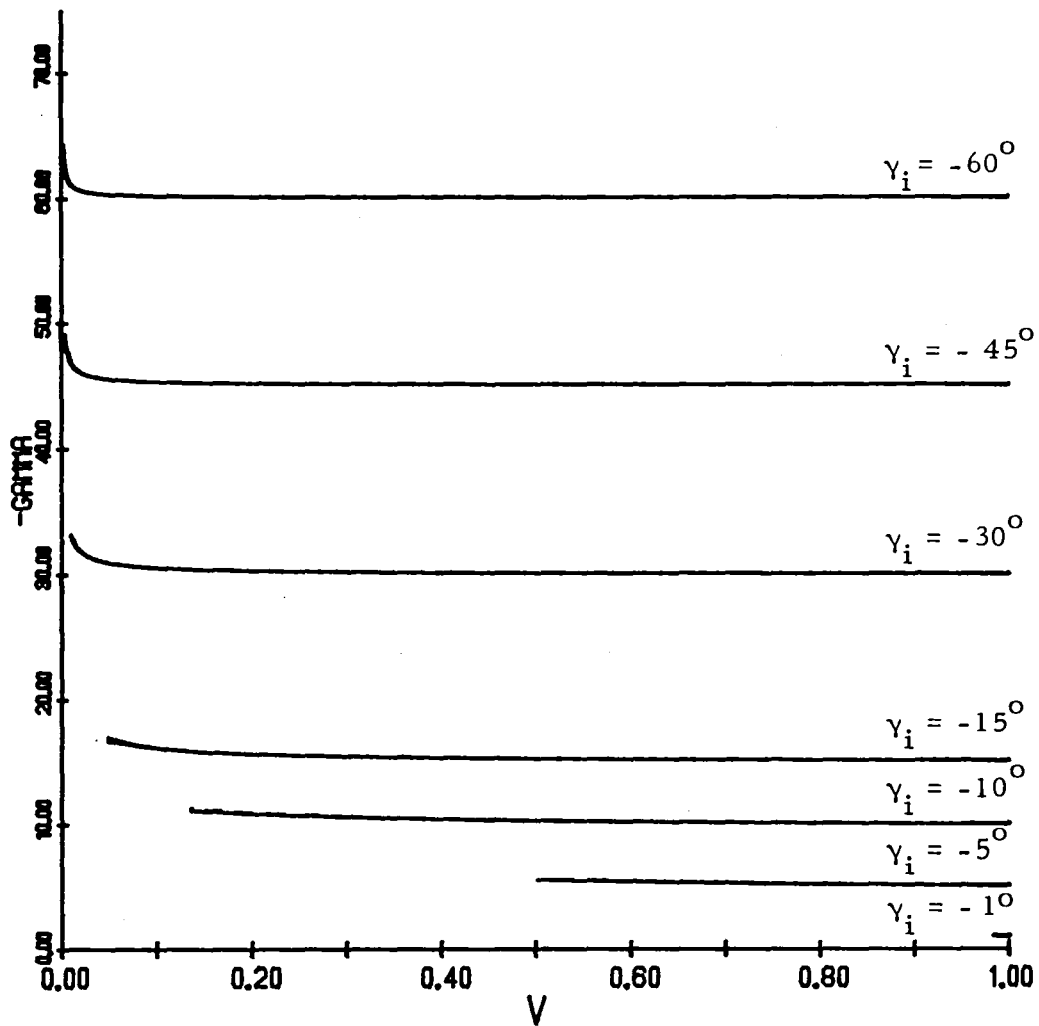


Fig. 6-5. Variations of  $-\gamma$  as Function of  $v$ .

$\gamma$  = flight path angle,  $v$  = dimensionless velocity squared =  $V^2/gr$  and  $\gamma_i$  = initial flight path angle. The dashed line indicates the exact numerical solution while the solid line represents the analytic solution from Eqs. (6-69) - (6-72).

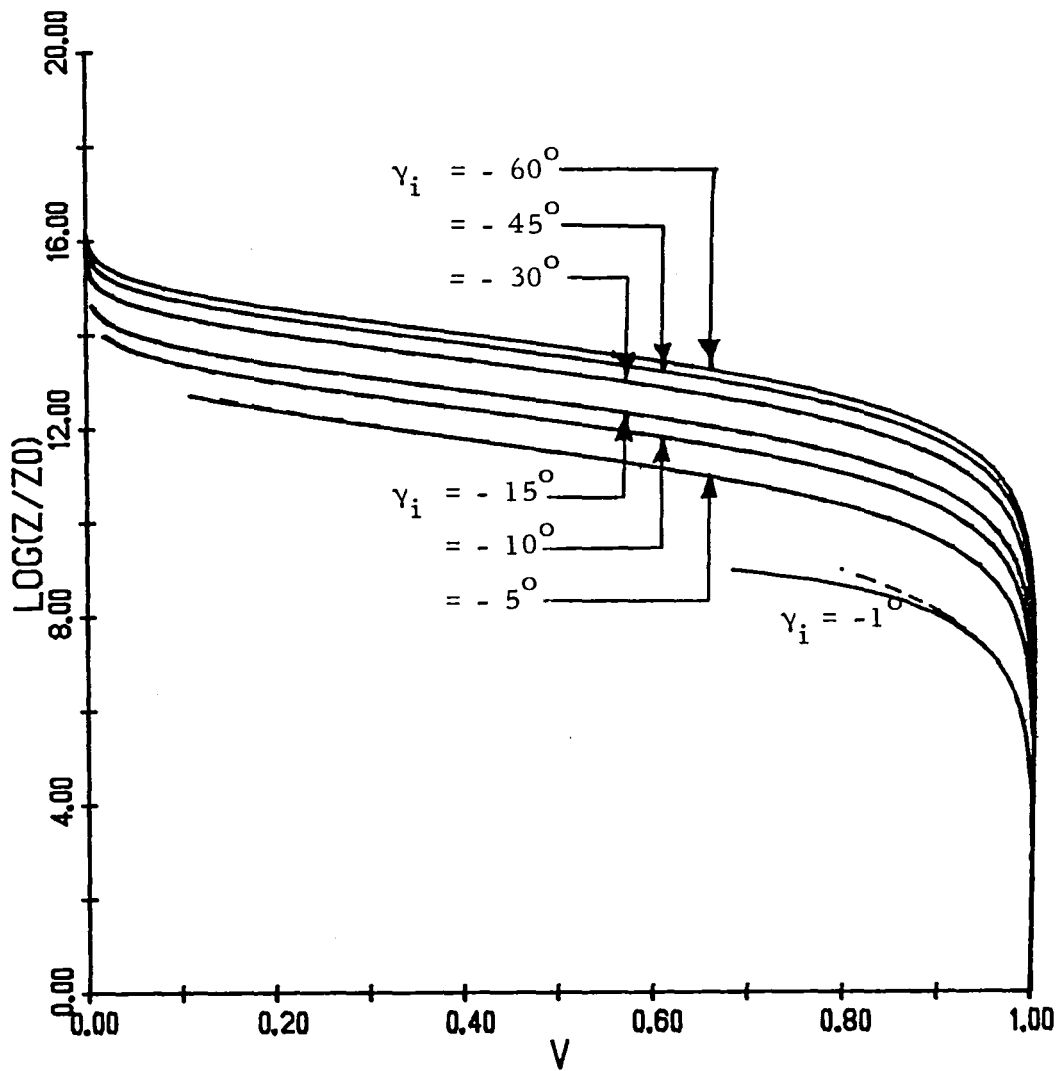


Figure 6-6. Variations of  $\text{Log}(Z/Z_0)$  as Function of  $v$ .

$\text{Log}(Z/Z_0) \approx (r_0 - r)/H =$  drop in altitude in units of scale height,

$v =$  dimensionless velocity squared  $= V^2/gr$  and  $\gamma_i =$  initial flight path angle. The dashed line indicates the exact numerical solution while the solid line represents the analytic solution from Eqs. (6-69) - (6-72).

## CHAPTER 7

### CONCLUSIONS AND RECOMMENDATIONS

A space object traveling through an atmosphere is governed by two forces: aerodynamic and gravitational. On this premise equations of motion were derived in order to provide a set of universal entry equations applicable to all regimes of atmospheric flight from orbital motion under the dissipative force of drag through the dynamic phase of reentry and finally to the point of contact with the planetary surface. The universal entry equations apply to any vehicle whether it is a lifting body or a ballistic missile. They provide a set of variables which can easily be cast in the form of orbital elements or reentry variables so that versatile analytic theories can be formulated. This report clearly demonstrates the flexibility and wide range of applicability of the universal entry equations.

In the case of orbital motion, a complete uniformly valid theory was developed for orbit contraction due to atmospheric drag for all elliptic orbits ( $0 < e < 1$ ). A simple model was chosen in which the atmospheric density was assumed to vary exponentially with altitude, the scale height was assumed constant and the planet

and its atmosphere was assumed to be spherical and rotating. Rigorous mathematical techniques, such as averaging, Poincaré's method of small parameters, and Lagrange's expansion, were applied in order to obtain a highly accurate, purely analytic theory in which the semi-major axis was found as a function of the eccentricity. This represents a major breakthrough in the advancement of analytic theories and should provide ample room for the development of more sophisticated theories which include the variation of scale height with altitude and the effect of an oblate atmosphere and planet. In its present form, the analytic solution can be used to develop a computer algorithm which updates the scale height at frequent intervals and essentially provides the solution for varying  $\beta$ . This method of coupling the theory with numerical computation would have the advantage of very short computer processing time because the method of averaging has removed the need to integrate over every orbit, so that only the orbital elements need to be integrated.

In addition to the orbit contraction, first order solutions were obtained for the orientation of the orbit plane, illustrating once again the aforementioned techniques. Since the argument of the periapsis remains constant and the argument of the ascending longitude and the angle of inclination vary very little, the first

order solution is adequate for small values of eccentricity. Further research work in this area could be done to generate the theory for large values of eccentricity and to include the variation of the argument of the periapsis.

In order to give a complete description of the flight of an object through a planetary atmosphere, the universal entry equations were applied to the problem of ballistic entry. In this case the atmospheric density was assumed to vary exponentially with altitude, as before, but  $\beta r$  was assumed to be a constant in accordance with Chapman's approach and the planet and atmosphere were assumed to be spherical and nonrotating so that the entry is planar. The great advantages of the universal equations are: they are exact; they are free of any restrictive assumptions; and they contain the modified Chapman variable  $Z$ . This variable permits a single trajectory to be solved for specified initial conditions on the velocity and the flight path angle that apply to any ballistic vehicle of arbitrary mass, area and drag coefficient. With this in mind, the complete theory of ballistic entry was developed by analyzing the three typical cases: entry from circular orbit, entry from near circular orbit and entry at moderate and large initial flight path angles.

In the final stages of orbit decay, the orbit circularizes and

the entry phase is imminent. A first order theory was developed which solves for the trajectory of the vehicle during the last orbit. The classical Yaroshevskii solution appears as the zero order term and is easily derived. It is more laborious to obtain the first order term, but its inclusion provides a significant improvement in accuracy. With an error in the fourth or fifth digit, it is not necessary to go to the second order term in order to improve on the final theory.

In some orbit decay problems the entry phase may commence before complete circularization. In other cases, such as those involving recoverable satellites and manned spacecraft, the entry phase may be intentionally initiated. For these, the ballistic entry theory for small initial flight path angles was developed to solve for the modified Chapman Z variable and the flight path angle as functions of the velocity. The second order theory provides adequate numerical results but it is not sophisticated enough to exhibit all the known phenomena which occur during entry from very small initial flight path angles.

There are some cases such as return from the moon, atmospheric capture of planetary probes, atmospheric grazing and ballistic missile entry in which accurate trajectory analysis would be extremely useful. A highly accurate analytic theory for entry at large and moderate flight path angles was developed for these

purposes which provides the velocity and flight path angle as a function of the modified Chapman variable  $Z$ . The second order theory has a wide range of applicability in the initial flight path angle, covering the cases from  $-\gamma_i \geq 5^\circ$  to  $-\gamma_i < 90^\circ$ . Any initial velocity can be used so that the theory applies to all hyperbolic, parabolic and highly elliptic as well as moderately elliptic orbits in the presence of a planetary atmosphere.

In conclusion, a complete theory has been developed for the motion of a ballistic vehicle in a planetary atmosphere. It applies to all regimes of flight from the time in orbit through the entry phase until the instant of touchdown. The solutions of the governing differential equations have been found by mathematically rigorous techniques and provide a firm foundation for the development of more sophisticated theories. The applicability, versatility and generality of the exact universal entry equations have been clearly demonstrated.

## REFERENCES

- Abramowitz, M. and Stegun, I. A. (1972), Handbook of Mathematical Functions, Dover Publications, Inc., New York.
- Beyer, W. H., (1976), Standard Mathematical Tables, CRC Press, Cleveland.
- Bletsos, N. A., (1976), "Performance and Control with Lift Modulation of Hypervelocity Entry Vehicles," Ph. D. Thesis, The University of Michigan.
- Bogoliubov, N.N. and Mitropolsky, Y. A., (1961), Asymptotic Methods in the Theory of Nonlinear Oscillations, Gordon and Breach, New York.
- Brace, F. C., (1974), "An Improved Chapman Theory for Studying Entry into Planetary Atmospheres," Ph. D. Thesis, The University of Michigan.
- Chapman, D. R., (1959), "An Approximate Analytical Method for Studying Entry into Planetary Atmospheres," NASA TR R-11.
- Chapman, D. R. and Kappahn, A. K., (1961), "Tables of Z Functions for Atmospheric Entry Analyses," NASA TR R-106.
- King-Hele, D., (1964), Theory of Satellite Orbits in an Atmosphere, Butterworths, London.
- Moulton, F. R., (1920), Periodic Orbits, Carnegie Foundation XXV No. 162.
- Poincaré, H., (1960), Les Méthodes Nouvelles de la Mécanique Céleste, Vol. 1, Dover Reprint.
- Vinh, N. X. and Brace, F. C., (1974), "Qualitative and Quantitative Analysis of the Exact Atmospheric Entry Equations Using Chapman's Variables," IAF Paper No. 74-010, presented at the XXVth Congress of the International Astronautical Federation, Amsterdam.

Vinh, N. X. , Busemann, A. , and Culp, R. D. , (1975), "Optimum Three-dimensional Atmospheric Entry, " Acta Astronautica, 2, 7/8, pp. 593-611.

Yaroshevskii, V. A. , (1964), "The Approximate Calculation of Trajectories of Entry Into the Atmosphere. I , " translated from Kosmicheskie Issledovaniya, Vol. 2, No. 4.

Yaroshevskii, V. A. , (1964), "The Approximate Calculation of Trajectories of Entry Into the Atmosphere. II, " translated from Kosmicheskie Issledovaniya, Vol. 2, No. 5.

**End of Document**